Cations of Group 14 Organometallics

THOMAS MÜLLER*

Institut für Anorganische und Analytische Chemie, Johann Wolfgang Goethe Universität, Frankfurt, Marie Curie-Str. 11, D 60439 Frankfurt/Main, Germany

Dedicated to the memory of Dr. Uwe Herzog

I
INTRODUCTION

There is a fundamental interest in understanding similarities and differences between carbon and heavier group 14 elements. Many theoretical and experimental studies were carried out in order to ascertain whether the organic compounds of heavier group 14 elements could be demonstrated to exhibit similar chemical properties to their carbon analogues. Such studies have, for example, recently led to the successful isolation of compounds containing formal E≡E triple bonds.[1] One of the most demanding and difficult challenges to chemists was to demonstrate the existence of, and to isolate and characterize, the heavier congeners of carbonium ions R_3E^+ (E = Si, Ge, Sn, Pb). In particular, the silylium ions, R_3Si^+, have received much attention and the debate on their existence was controversial, lively and sometimes overemphasized. Even in 2001, the year of the 100th anniversary of the discovery of the trityl cation,[2,3] no direct structural proof for the existence of analogous three-coordinate, trivalent cationic species R_3E^+ was provided. NMR[4,5] and computational evidence[6,7] for the existence of trimesitylsilylium Mes_3Si^+, **1**, was given, but the only crystallographically characterized tricoordinated cations of the elements silicon[8] and germanium[9] were the cyclic cations **2** and **3**, which are stabilized either by conjugation or homoconjugation.

*Corresponding author. Tel.: +49-69-79829166; fax: +49-69-79829188.
E-mail: dr.thomas.mueller@chemie.uni-frankfurt.de (T. Müller).

ADVANCES IN ORGANOMETALLIC CHEMISTRY
VOLUME 53 ISSN 0065-3055/DOI 10.1016/S0065-3055(05)53005-3

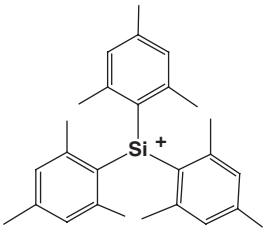

1

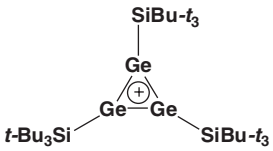

2

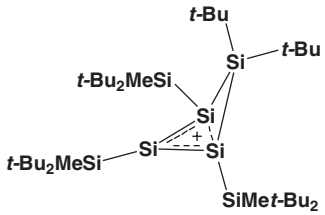

3

The major obstacle for the synthesis of R_3E^+ ions is their inherent high electrophilicity and high reactivity, which leads such species to interact in solution and solid state with solvents and/or counteranions that are found to be innocent in other areas of chemistry. In addition, the tendency of the higher congeners of carbon to extend their coordination sphere, their inherent reluctance towards π-conjugation and to hyperconjugative effects due to less-effective orbital overlap and, finally, the larger size of the electron-deficient center, which is harder to protect sterically, are factors, which complicate the isolation and characterization of organometallic cations of group 14 elements. Since the mid 1990s significant breakthroughs in synthetic methodology have been achieved and at the time this review was finalized (Autumn 2004) for all group 14 elements but lead, examples of strictly three-coordinated, trivalent organometallic R_3E^+ cations have been synthesized, isolated and fully characterized including by crystallography. Moreover, several group 14 element cations having novel bonding features or unusual structures were identified. It is worth mentioning that this progress was facilitated by major advances in computational chemistry, which critically attended the experimental achievements and supported greatly the identification of the synthesized species.

Several reviews appeared on the heavier congeners of the carbenium ions. Clearly, the silylium ion problem has received the most attention, and both theoretical as well as experimental aspects have been reviewed.[10–16] The chemistry of cationic germanium, tin and lead is covered by a recent review by Zharov and Michl.[17] We will concentrate in this review on the description of the progress made during the last 4 years and will try to give an account on the synthesis, the properties and the structure of organosubstituted three-coordinated, trivalent group 14 element cations and closely related species in the condensed phase.

II
SYNTHETIC APPROACHES TO R_3E^+ IONS

A. *Heterolytic Cleavage of E–X Bonds*

The heterolytic cleavage of a C(sp^3)–X bond (X: good leaving group e.g. halide, sulfonates and perchlorate) is the first step in a typical S_N1 reaction and it is the most popular synthetic approach to persistent carbocations.[18] The high bond energy

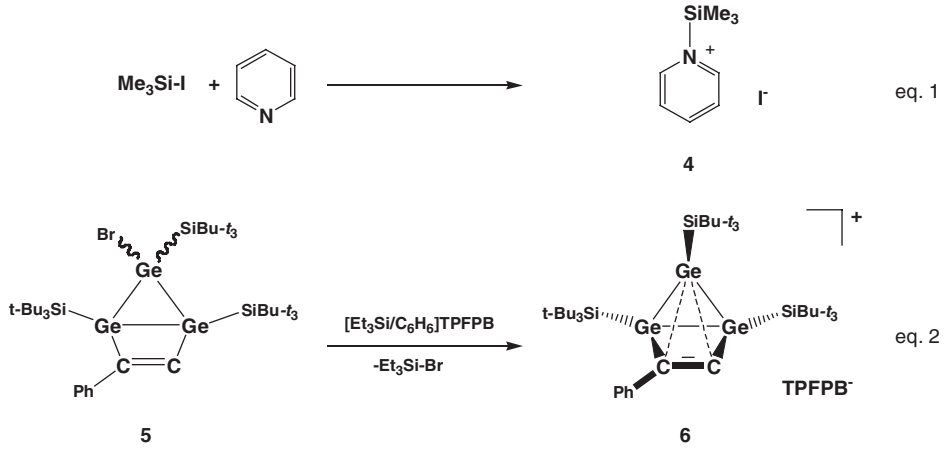

Scheme 1.

of most of the R_3E–X bonds and/or the high reactivity of the incipient element cation toward the leaving group X precludes the use of this synthetically straightforward approach to persistent trivalent organoelement cations. For example, trimethylsilylium Me_3Si^+ cannot be synthesized from the corresponding fluoride in the superacidic HSO_3F/SbF_5 system.[19] Heterolytic E–X bond cleavage can be used, however, if the solvent provides enough stabilization of the transient cation [Scheme 1, Eq. (1)].[20] In this case, solvent complexes of the R_3E^+ cation with the element in a tetrahedral or trigonal–bipyramidal coordination sphere, e.g. the silylated pyridinium cation **4**, are isolated. Similarly, intramolecular interaction can provide enough stabilization of the element cation that it can be generated by dehalogenation, in particular if the halide is efficiently removed from the reaction mixture. A recent example is provided by the dehalogenation of the bicyclic germyl bromide, **5**, to yield the intramolecularly stabilized germyl cation **6**. [Scheme 1, Eq. (2)].[21] As a consequence of the intramolecular interaction of the germyl cation with the remote C=C double bond, the coordination number of the germanium atom in the intramolecularly stabilized element cation is larger than 3.

B. *Hydride Transfer Reaction*

The Bartlett–Condon–Schneider hydride transfer reaction,[22,23] first employed in silicon chemistry by Corey in 1975,[24] developed since then to be the most popular synthetic approach to silylium ions in the condensed phase.[10] Subsequently, it was also used for the generation of germylium[22,56] and stannylium compounds.[4,17,26,29] This method exploits the relative weakness of the E–H bond and involves the transfer of the hydride from the element to a strong Lewis acid, in most cases to trityl cation. The easy access of trityl salts with a wide variety of weakly coordinating counteranions is a clear advantage of this method. The reaction can be applied in polar solvents such as sulfolane, ethers and nitriles but also in chlorinated

or aromatic hydrocarbons. For silicon, careful mechanistic[30] and theoretical[31] studies have shown that the reaction proceeds with the intermediacy of silylium ions and a single electron transfer reaction mechanism that was suggested earlier[32] can be excluded. The hydride transfer method gives access to a wide variety of cationic species of group IV elements, which are either stabilized by intermolecular interaction with solvent molecules and/or with the counterion or by intramolecular interactions. Some recent examples for the application of the hydride transfer reaction in the synthesis of group 14 cationic species are summarized in Scheme 2.[25,33–40] Particularly noteworthy is the synthesis of the silatropylium ion **7** by Komatsu and co-workers from the silepin **8** (see Scheme 3).[33,34]

The major obstacle of the hydride transfer reaction is the steric bulk of the trityl cation as the reagent of choice. Substrates that will allow the isolation of cations R_3E^+, free from intramolecular and/or intermolecular interactions with solvent molecules or anions, need to have bulky substituents and therefore the hydride transfer reaction between the hydride and trityl cation is severely hampered or it is even impossible. Another drawback of this method is the limited availability of the starting hydrido compound, which for example, is not available for lead compounds, due to the high reactivity of lead(IV) hydrides.

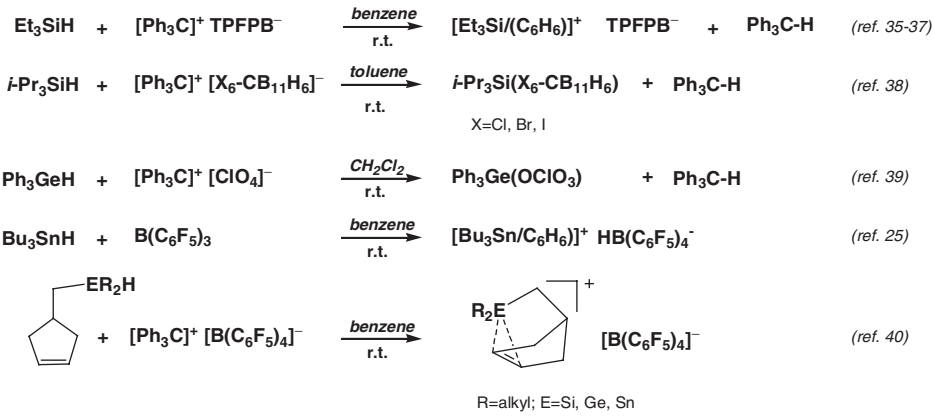

SCHEME 2.

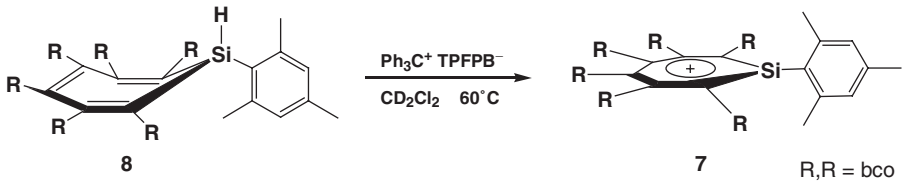

SCHEME 3.

C. *Electrophilic Cleavage of E-Alkyl and E-Silyl Bonds*

The cleavage of an alkyl or silyl group was successfully applied in the synthesis of several R_3E^+ cations. Early attempts were restricted to strongly acidic media. It was shown by Gillespie *et al.*[41,42] and Birchall and co-workers[43–45] that in contrast to silyl or germyl cations, stannyl cations "R_3Sn^+" can be formed by dissolving tetraorganotin compounds in strong acids such as sulfuric acid or fluorosulfonic acid. Similarly, the formation of a Me_3Pb^+ cation in fluorosulfonic acid at low temperatures was reported.[46] Subsequently it was shown by Mössbauer and ^{119}Sn NMR spectroscopy that the generated tin species are five-coordinated complexes of the stannylium ion R_3Sn^+, and two molecules either of the acid or the corresponding anion that adopt the axial positions of the trigonal bipyramidal complete the coordination sphere of tin.[43–45] For the synthesis of R_3E^+ in less nucleophilic organic solvents more moderate reaction conditions and better "leaving groups" had to be found. The use of the allyl moiety as a leaving group was the key for the spectacular synthesis and characterization of silylium, germylium and stannylium ions by Lambert and co-workers.[45,47–49] Reaction of the allyl element compound **9** with the silylated arenium ion $(Et_3Si/C_6H_6)^+$ gives rise to the formation of the β-silyl-substituted carbocation **10,** which undergoes a fragmentation reaction and releases the stable Ar_3E^+ cation (Scheme 4). This allyl fragmentation reaction has some precedence in the reaction of allylsilanes with triflic acid[50] and with trityl cation,[51] and in the fragmentation of β-silyl-substituted vinyl cations, detected in superacidic media at low temperatures.[52]

Similarly, trityl cation in aromatic hydrocarbons initiates the fragmentation of simple tetraalkyl plumbanes and stannanes yielding the plumbyl or stannyl cationic species, e.g. **11**, and alkenes.[40,53,54] The reaction is thought to proceed *via* plumbyl- or stannyl-substituted carbocations **12**, which in a second step eliminate the alkene.[54] This approach was used in the synthesis of norbornyl cations of the elements tin and lead, e.g. **13**, (Scheme 5).[40,53]

The cleavage of a silicon–methyl bond by the silylated benzenium ion $[Et_3Si/C_6H_6]^+$ and formation of the silylium ion **14** is the first step in the unexpected synthesis of the homoaromatic silyl cation **3** from trisilacyclopropene **15** (Scheme 6).[8]

The intermediate formation of the ferrocenyl-substituted silylium ion **16** by protonation of the ansa-ferrocenyl silane **17** can be regarded as a special case of electrophilic cleavage of an activated C–Si bond (see Scheme 7). The driving force for this reaction is the release of a strain by formation of the silyl cation.[55] In a

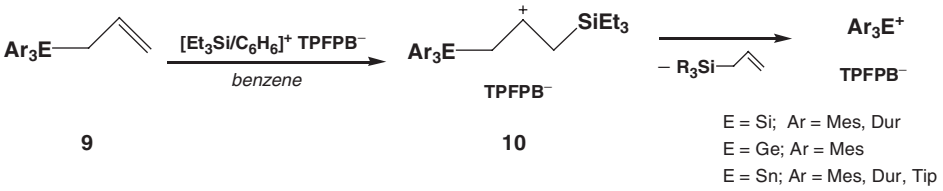

SCHEME 4.

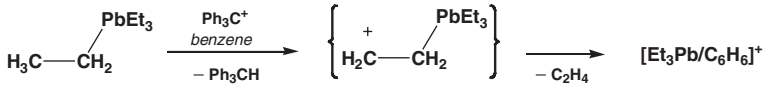

12 11

13

Scheme 5.

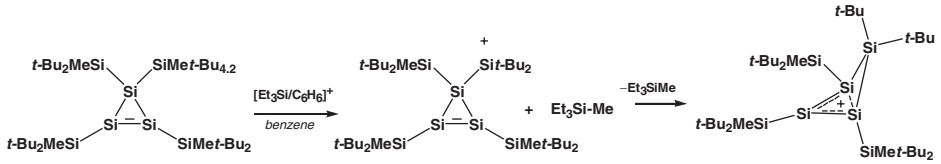

15 14 3

Scheme 6.

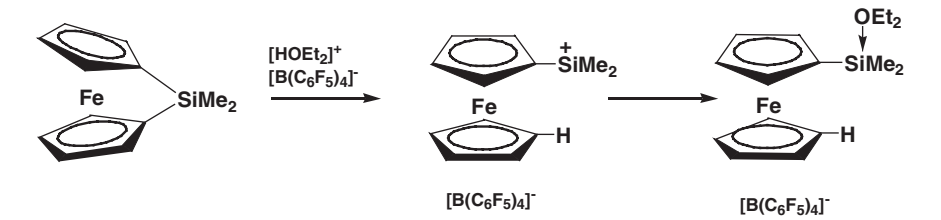

17 16 18

Scheme 7.

spontaneous consecutive reaction the silylium ion **16** forms with ether solvent the oxonium ion **18**.[55]

D. *Oxidative Cleavage of E–E and E–C Bonds*

The early reports on the oxidative generation of R_3E^+ cations are nearly exclusively restricted to the synthesis of R_3Sn^+ cations. Hexamethylditin $Me_3Sn–SnMe_3$ is oxidized in acetonitrile by one-electron oxidants as, for example 10-methacridinium,[56] thianthrene cation radical[57] and $Fe(phen)_3^{3+}$[58] yielding the solvent complexed Me_3Sn^+ cation. Interestingly, the oxidation of the mixed tin element compounds $Me_3Sn–EMe_3$, E = Si, Ge by 10-methacridinium resulted in the

formation of solvated $[Me_3Sn/(N{\equiv}CMe)_n]^+$ and $[Me_3E/(N{\equiv}CMe)_n]^+$ cations ($n = 1, 2$), while the tin-free dielement compounds ($Me_3E–E'Me_3$, E, E′ = Si, Ge) underwent no reaction. This is in line with the lower oxidation potential of the Sn-element bond in tin compounds (see Table I).[56] Mechanistically, these reactions are thought to proceed *via* electron transfer as the rate-determining step. In the case of dielement compounds $R_3E–E'R'_3$ initially the cation radicals $[R_3E–E'R'_3]^{+\bullet}$ are produced, which then decompose by cleavage of the E–E bond to give R_3E^+ and $R_3E^\bullet$. The radical $R_3E^\bullet$ is then further oxidized to the R_3E^+ cation, thus consuming 2 equivalents of the oxidant.[56,57,59,60–62] Oxidation of R_4Sn, Me_3SnR (R = Me, Et, *n*-Bu, Vi, Ph) and Ph_6Sn_2 with thianthrene cation radical was reported to give the solvent complexed stannyl cations.[57] An early communication, reports the preparation of the $[Ph_3Pb/N{\equiv}CMe]^+$ cation by oxidation of the diplumbane Ph_6Pb_2 by $AgNO_3$ in acetonitrile.[63] In all these reactions the need for strongly interacting solvents (in most cases acetonitrile) and the use of chloride or perchlorate as counterion precludes all attempts for the isolation of the generated cationic species. Only with the advent of fluorinated tetraarylborates and carboranes as weakly coordinating anions (WCA^-), did the isolation of the cationic species on a preparative scale become feasible.

The first landmark was the successful synthesis and structural characterization of the cyclotrigermylium cations **2** and **19** by Sekiguchi and co-workers. This was achieved by reaction of trityl cation with the cyclotrigermenes **20** in the presence of weakly coordinating borate anions (Scheme 8). The trityl cation acts here as a one-electron oxidizing reagent and the resulting radical cation of **20** decomposes to the

TABLE I
OXIDATION POTENTIALS (E_P) OF GROUP 14 COMPOUNDS

Compound	E_P(V)
	in MeCN, vs. Ag/AgCl/MeCN
$Me_3Si–SiMe_3$	1.76
$Me_3Ge–GeMe_3$	1.70
$Me_3Sn–SnMe_3$	1.28
$Me_3Si–SnMe_3$	1.60
$Me_3Ge–SnMe_3$	1.44
$Et_3Si–SiEt_3$	1.76
$Et_3Ge–GeEt_3$	1.48
$Et_3Sn–SnEt_3$	1.24
$Et_3Si–GeEt_3$	1.70
$Et_3Si–SnEt_3$	1.56
$Et_3Ge–SnEt_3$	1.40
	in MeCN, vs. Fc/Fc^+
$Ph_3Si–SiMe_3$	1.29
$PhMe_2Si–SiPhMe_2$	1.26
$Me_3Si–SiMe_3$	1.36
$Ph_3Ge–GeMe_3$	1.16
$PhMe_2Ge–GePhMe_2$	1.20
$Me_3Ge–GeMe_3$	1.28

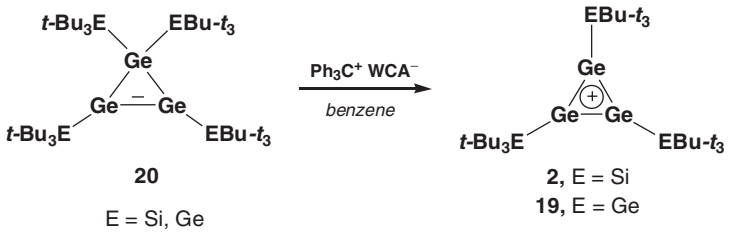

20

E = Si, Ge

2, E = Si
19, E = Ge

$WCA^- = TPB^-, TFPB^-, TPFPB^-, TSFPB^-$

Scheme 8.

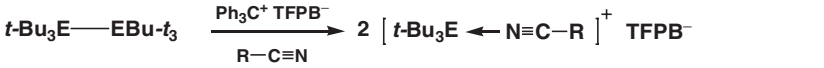

21 E = Si, Ge, Sn, R = *t*-Bu, Me

Scheme 9.

cyclotrigermylium ions, **2**, **19**, by cleavage of a Ge–Si or Ge–Ge bond (Scheme 8).[9,64–66]

Subsequently, the same group demonstrated that the reaction of hexa-*t*-butyldimetallanes *t*-Bu_3E–EBu-t_3; E = Si, Ge, Sn) with two equivalents of trityl $TFPB^-$ in pivaloylnitrile or acetonitrile gave tri-*t*-butylelement cation nitrile complexes, **21**, by oxidative E–E bond cleavage (Scheme 9). The isolated yields of the salts **21** $TFPB^-$ were in the range from 60 to 80%.[67] For silanes, the oxidation only occurs for sterically strongly congested disilanes, having a long central SiSi bond and therefore a low ionization potential. Thus, hexa-*t*-butyl disilane and hexa-iso-propyl disilane gave the corresponding cations, while hexaethyl disilane and hexamethyl disilane are unreactive toward trityl cation in acetonitrile.[67]

A crystalline solvent-free $CB_{11}Me_{12}^-$ salt of the *n*-Bu_3Sn^+ cation with significant anion–cation interaction was prepared by Michl and co-workers by oxidizing *n*-Bu_6Sn_2 with the radical $CB_{11}Me_{12}^{\bullet}$ (Scheme 10).[68] The $CB_{11}Me_{12}^{\bullet}$ radical is a stable and strong one-electron oxidant, comparable in its oxidation power to Ce(IV). It is freely soluble in non-polar solvents as, for example, saturated hydrocarbons and in its reduced form it serves as a WCA^-. Thus, this approach provides the opportunity to generate the group 14 cations in an environment devoid of unsaturated molecules or molecules with lone pairs. This is a clear advantage compared to methods as, for example, the hydride transfer method for which aromatic hydrocarbons as solvents are a prerequisite. Quite recently the solvent-free Me_3E^+ $CB_{11}Me_{12}^-$ salts (E = Ge, Sn, Pb) have been prepared by oxidation of hexamethyldigermane and -distannane and of tetramethyllead, and characterized by NMR and extended X-ray absorption five structure analysis (EXAFS) studies.[69]

The straightforward access to stable radicals[70,71] opened the avenue for the synthesis of the corresponding cations by one-electron oxidations. Thus, the stable radicals $(t\text{-}Bu_2MeSi)_3E^{\bullet}$ (E = Si, Ge, Sn) can be oxidized by trityl cation in benzene, and for germanium and tin the free germylium, **22**, and stannylium ion, **23**, could be

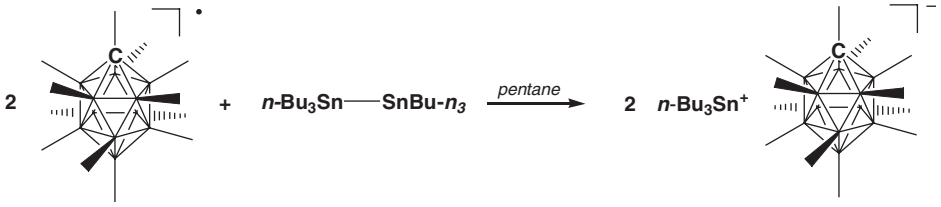

SCHEME 10.

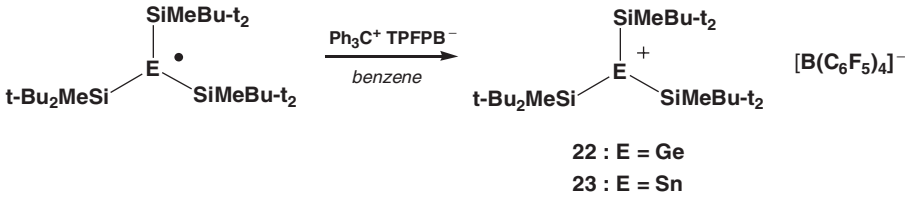

SCHEME 11.

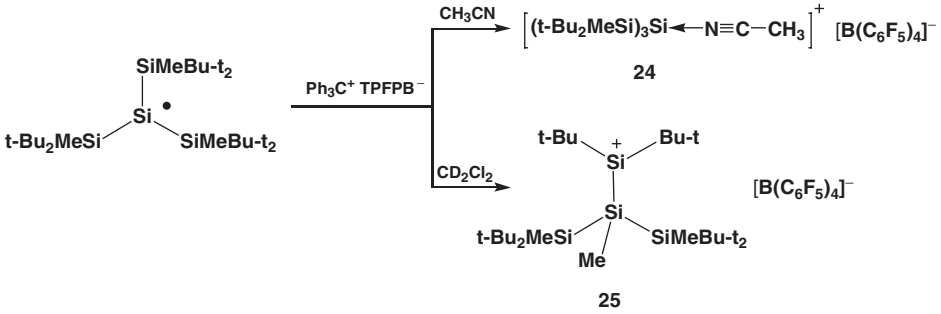

SCHEME 12.

isolated and structurally characterized as tetrakis(pentafluorophenyl)borate ($TPFPB^-$) salts (Scheme 11).[71,72] In the case of the silicon compound the presence of acetonitrile allowed the isolation of the stable nitrilium ion $[(t\text{-}Bu_2MeSi)_3Si/N{\equiv}CMe]^+$, **24**. In the absence of acetonitrile the incipient silylium ion $(t\text{-}Bu_2MeSi)_3Si^+$ undergoes a 1,2-methyl migration yielding the marginally stable silylium ion **25**, which was identified in CD_2Cl_2 solution at low temperatures by NMR spectroscopy (Scheme 12).[73]

In principle, these oxidations are reversible. This was elegantly shown for silenylium ion **3**. Reduction of **3** with *t*-butylsilyl sodium gives the cyclotetrasilenyl radical **26** and one-electron oxidation of **26** by trityl cation results in the back-formation of **3** (Scheme 13).[74] Moreover, **26** can be further reduced giving the corresponding anion **27**. Also the transformation between radical **26** and anion **27** was shown to be reversible. In this case, the silylated benzenium ion $[Et_3Si/C_6H_6]^+$ serves as a one-electron oxidant to give the radical **26** (Scheme 13).[75]

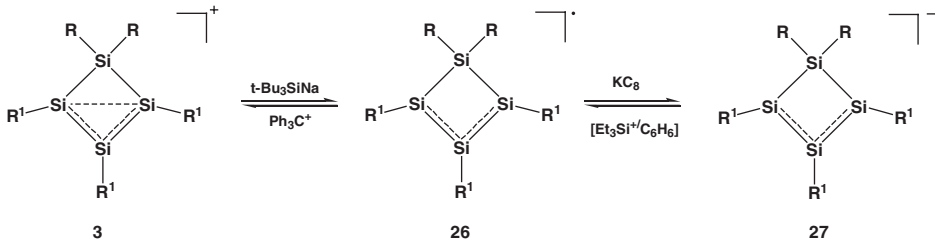

SCHEME 13.

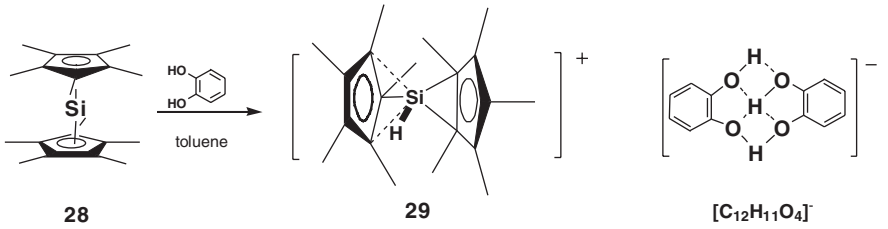

SCHEME 14.

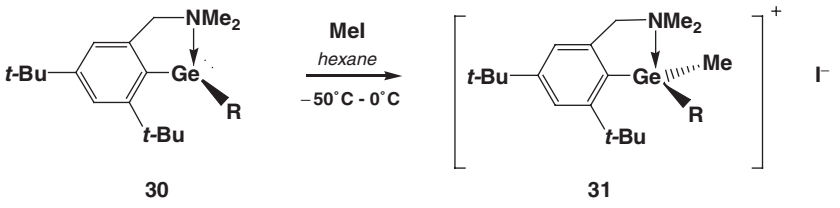

SCHEME 15.

E. *Addition of Electrophiles to Heavy Carbenes*

Alkylation or protonation of neutral, divalent organoelement compounds leads in principle to trivalent cations. There are only a few reports in literature that follow successfully this conceptionally straightforward approach to R_3E^+ cations. In most cases, the resulting cations are strongly stabilized by intramolecular interactions between a remote donor substituent and the electrophilic center. Thus, protonation of decamethylsilicocene **28** by *o*-catechol leads to the unique silyl cation **29** with the unusual hydrogen-bridged bis-catecholate anion, $C_{12}H_{11}O_4^-$ (Scheme 14)[76,77] and the donor-stabilized germylenes **30** reacts with methyliodide to give the four-coordinate germyl cations **31** (Scheme 15) those were isolated as iodide salts.[78,79]

The reaction of the stable germylene **32** with a triarylmethylium ion gave not the expected germylium ion **33**, but in a series of unexpected rearrangements, the germylium ion **34,** which is intramolecularly stabilized by interaction of the electron-deficient germylium center with a remote aryl group (Scheme 16).[80]

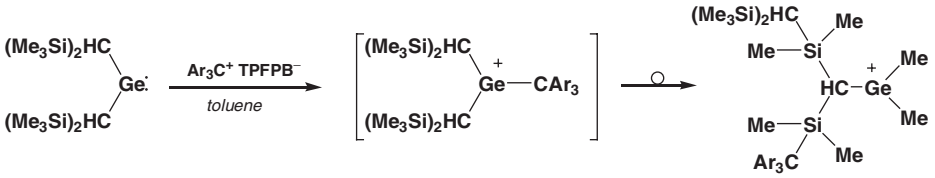

32 33 34

SCHEME 16.

III

STRUCTURE AND PROPERTIES OF R_3E^+ CATIONS

A. *Theoretical Considerations*

1. The EH_3^+ Potential Energy Surface

In agreement with a simple Walsh-type analysis for a AH_3 system with six valence electrons,[81] the planar D_{3h} structure, **35**, is a minimum on the potential energy surface for EH_3^+ cations of all group 14 elements.[82–84] However, a second C_s symmetric minimum, **36**, exists for all cations but the methylium ion CH_3^+.[83,84]

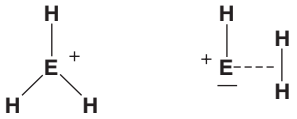

35 **36**

For silylium SiH_3^+ and germylium GeH_3^+ the strongly bonded D_{3h} structures are the global minima, but for Sn and Pb the species **36** are more stable (see Table II). The large preference of the side-on complex **36** for E = Pb by 23.3 kcal mol^{-1} is due to relativistic stabilization of the 6s lone pair in H–Pb$^+$. The EH_3^+-isomers **36** can be described as donor–acceptor complexes between dihydrogen and H–E$^+$, in which the electron density is transferred from the dihydrogen σ-bond to the LUMO of the H–E$^+$ fragment.[83,84] Although the D_{3h} isomers, **35**, of SnH_3^+ and PbH_3^+ are metastable, all D_{3h} EH_3^+ forms should be observable due to the high barriers, which separate **35** from **36** (see Table II). In contrast, the side-on complexes **36** are far less stable toward dissociation into dihydrogen and H–E$^+$. The dissociation energy D_0 for this process is

TABLE II
CALCULATED RELATIVE ENERGIES OF EH_3^+ ISOMERS IN KCAL MOL^{-1} (CALCULATED AT B3LYP/6-311++G(2d,p)(H, C, Si, Ge) SDD (TZ+2p) (Sn, Pb)[83])

Element	E(**35**)	E(**36**)	E(TS(**35**→**36**))	D_0(**36**)
Si	0	27.1	57.8	7.6
Ge	0	10.0	51.3	6.3
Sn	0	–5.2	52.9	2.9
Pb	0	–23.3	54.9	1.1

even for the most strongly bonded complex H_2/SiH^+ merely 7.6 kcal mol^{-1}, this suggests a fast decomposition of the species **36** at elevated temperatures (see Table II).[83]

There is no general theoretical study for trialkyl-substituted cations R_3E^+, which investigates the relationship of the classical planar trigonal structure to isomeric complexes RE^+/R_2 and its relative energy compared to the dissociation products, the singly coordinated four-valence-electron species $R–E^+$ and the hydrocarbon R_2. The only exceptions are 7-norbornadienyl cations **37** for which the germyl and silyl cation has been intensively studied theoretically by Radom and Nicolaides.[85–87] It has been predicted that both cations are unstable toward a facile isomerization to a more stable complex HE^+/C_6H_6, **38**. For the silyl species this was confirmed by fourier transform ion cyclotron resonance (FT-ICR) experiments, which demonstrated that indeed HSi^+/C_6H_6 is formed and not the isomeric trivalent 7-silanorbornadienylium.[88] Similarly, it was shown by our group that the 2,3-benzoannelated 7-silanorbornadienylium **39** undergoes, at ambient temperature in nonpolar solvents, a fast isomerization to the complex $PhSi^+$/tetraphenylnaphthalene (TPN), **40**, which decomposes yielding TPN as the only detectable product.[89]

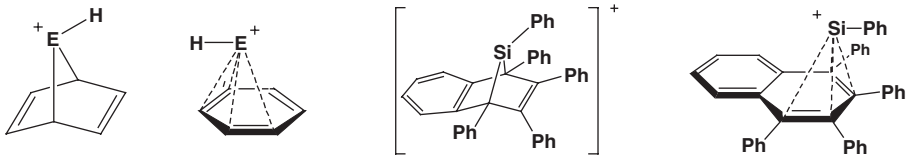

E = Si, Ge

37 **38** **39** **40**

The recent isolation and structural characterization of the toluene complex of the monovalent lead cation **41**[90] in the form of its $[MeB(C_6F_5)_3]^-$ salt is likely to trigger further theoretical work on the intriguing relationship between classical trivalent planar ER_3^+ cations and the monovalent four-valence-electron species ER^+.

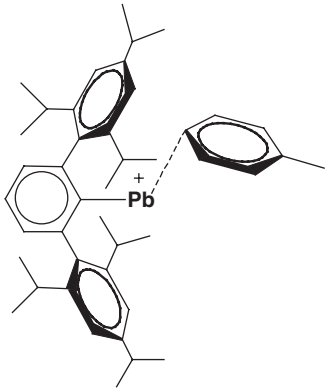

41

2. Thermodynamic Stability of R_3E^+ Cations

The relative thermodynamic stability of R_3E^+ cations as a function of the central element is evaluated by the isodesmic reaction shown in Eq. (3). It increases

TABLE III
STABILIZATION ENERGIES ΔE (KCAL MOL^{-1}) OF R_3E^+, CALCULATED ACCORDING TO ISODESMIC REACTION SHOWN IN EQS. (3) AND (4)

		ΔE, R =							
E	Eq.	H[a]	Me[b]	Ph[c]	SiH_3[d]	F[a]	Cl[a]	Br[a]	I[a]
C	(3)	0.0	0.0	0.0	0.0	0.0	0.0	0.0	0.0
Si	(3)	−58.9	−12.0	2.7	−32.9	−9.1	−9.7	−13.8	−18.4
Ge	(3)	−70.7	−20.6	−2.5	−43.1	−6.1	−9.6	−15.7	−22.4
Sn	(3)	−87.5	−25.6	−3.8	−51.9	−20.8	−15.8	−21.1	−27.4
Pb	(3)	−97.6	−35.2	−10.5	−63.5	−22.1	−19.2	−25.9	−33.6
C	(4)	0.0	−74.8	−111.3	−49.8	−18.8	−42.9	−54.7	−63.1
Si	(4)	0.0	−40.6	−64.5	−26.7	34.9	3.6	−11.5	−25.5
Ge	(4)	0.0	−37.3	−57.4	−28.5	50.8	17.8	0.7	−15.4
Sn	(4)	0.0	−29.9	−45.6	−23.6	50.5	27.1	10.8	−5.1
Pb	(4)	0.0	−29.7	−42.2	−24.9	58.5	35.2	17.6	0.4

[a]From Ref. 93, calculated at MP2/VDZ+P , quasirelativistic ecp for Si, Ge, Sn, Pb, Cl, Br, I.
[b]From Ref. 40, calculated at B3LYP/6-311G(2d,p), SDD for Si, Ge, Sn, Pb // B3LYP/6-31G(d) SDD for Si, Ge, Sn, Pb.
[c]Ref. 92, calculated at B3LYP/6-311G(2d,p), SDD for Si, Ge, Sn, Pb // B3LYP/6-31G(d) SDD for Si, Ge, Sn, Pb.
[d]Ref. 92, calculated at B3LYP/6-31G(d), SDD for Si, Ge, Sn, Pb.

monotonically along the series $R_3C^+ \rightarrow R_3Pb^+$ for most of the substituent listed in Table III, with the exception of the strongly π-donating substituents phenyl, fluorine and chlorine. The increase is most significant for the parent compounds with the plumbylium ion PbH_3^+ being more stable than methylium CH_3^+ by 97.6 kcal mol^{-1}. This marked growth of the thermodynamic stability along the series C→Pb is to be expected on the basis of the known atomic properties of the group 14 elements: the Mulliken electronegativity of the element decreases and the polarizability of the element atom increases steadily for the heavier elements of group 14.[91] The increase of the thermodynamic stability is, however, attenuated for substituted ions. While the electropositive silyl substituent stabilizes the heavier analogues of the trissilyl carbenium ion ($(H_3Si)_3C^+$) still considerably, i.e. the silylium ion ($(H_3Si)_3Si^+$) is more stable than ($(H_3Si)_3C^+$) by −32.9 kcal mol^{-1} and the plumbylium ion ($(H_3Si)_3Pb^+$) by −63.5 kcal mol^{-1}. The effect is, however, markedly smaller for alkyl substituents.[92] In the case of the trimethyl element cations, the plumbylium ion, Me_3Pb^+, is by only 35.2 kcal mol^{-1} more stable than *t*-butyl cation and it diminishes further for the practically very important phenyl substituent. As a consequence Eq. (3) is actually predicted to be slightly endothermic for E = Si, i.e. triphenylsilylium, Ph_3Si^+, is less stable than trityl cation, Ph_3C^+, by 2.7 kcal mol^{-1}. The higher homologues of Ph_3Si^+ are, however, slightly more stable than trityl cation with the plumbylium ion, Ph_3Pb^+, being the most stable cation in this series.[92] For fluorine and chlorine the calculated trend of the thermodynamic stabilization is not so clear, the stabilization of the germylium ions GeF_3^+ and $GeCl_3^+$ being smaller than that of the corresponding silylium ions.[93,94]

$$R_3EH + R_3C^+ \rightarrow R_3E^+ + R_3CH \quad (3)$$

$$R_3EH + H_3E^+ \rightarrow R_3E^+ + EH_4 \quad (4)$$

The substituent effect on the thermodynamic stability of R_3E^+ ion is given by the isodesmic reaction shown in Eq. (4). Carbenium ions are stabilized by each substituent listed in Table III, even by the strongly electronegative fluorine and the effect of many substituents is large, i.e. *t*-butyl cation is more stable than methylium by 74.8 kcal mol^{-1}. The heavier analogues of *t*-butyl cation are also considerably more stable than the hydrogen-substituted cation EH_3^+, the substituent effect is, however, considerably smaller than in the carbon case, i.e. Me_3Si^+ is stabilized by 40.6 kcal mol^{-1} and the plumbylium ion by only 29.7 kcal mol^{-1}.

Similarly, the experimentally important substituents phenyl and silyl are significantly less efficient in stabilizing a silylium or plumbylium ion than a carbenium ion. For example, the stabilization of triphenylsilylium Ph_3Si^+ calculated by using the isodesmic equation (4) is only roughly 58% of that predicted for the trityl cation and it decreases to 38% for the plumbylium ion Ph_3Pb^+. In contrast to the carbon case, plumbylium ions are in general destabilized by halogen substitution, the destabilization increasing with the electronegativity of the halogen atom.[93,94] For a given halogen, there is a constant decrease in their destabilizing effect as E becomes lighter. In consequence, silylium ions are only destabilized by substitution with the most electronegative halogens fluorine and chlorine, while $SiBr_3^+$ and SiI_3^+ are actually more stable than SiH_3^+.[94,95]

The most significant conclusion that can be drawn from the data summarized in Table III is that substituent effects do not exert the same overwhelming importance for the thermodynamic stability of the higher homologues of carbenium ions, thus they do not play the dominant role as in carbocation chemistry. This can be traced back on (i) the inherent higher stability of the trivalent cations of the elements Si→Pb and (ii) the weakness of the stabilizing interaction (in many cases of π-type) of the most common substituents with the central element atom.

One interesting exception is the cyclopentadienyl (Cp) substituent. Density functional calculations at the B3LYP/6-311G(2d,p)//B3LYP/6-31G(d) + ΔZPVE level of theory indicated that the Cp (and likewise the pentamethylcyclopentadienyl (Cp*) substituent) is clearly more efficient in stabilizing a silylium or germylium than a carbenium ion.[77,92] Thus, the isodesmic reaction shown in Eq. (5) is exothermic by −13.8, −18.7 and −25.3 kcal mol^{-1} for E = C, Si, and Ge, respectively. This unusual large substituent effect is explained by the particular bonding situation in the cations **42**–**44**, which is dominated by π-donation to the electron-deficient element atom, which is more efficient for the silylium **43** and in particular for the germylium ion **44**.[77,92]

$$Cp_2EH_2 + Me_3E^+ \rightarrow Cp_2EH^+ + Me_3EH$$

42, E = C

43, E = Si

44, E = Ge (5)

TABLE IV
CALCULATED INTERACTION ENERGIES ΔE_A BETWEEN R_3E^+ CATIONS AND ELECTRON DONORS D[a]

E	C	Si	Ge	Sn	Pb
D = H_2O[a,b]					
R = H	−71.3	−54.7	−44.5	−38.9	−31.4
D = toluene[a,c]					
R = H	−85.1	−53.9	−47.6	−40.3	−44.2
R = Me	−17.8	−28.9	−26.2	−25.7	−30.5
D = RHC=CHR[d,e]					
R = Me	–	−19.5	−17.4	−17.0	−12.5

[a]Calculated as the energy difference between the total energy of the donor acceptor complex $R_3E^+ \leftarrow D$ and the sum of the total energy of D and R_3E^+.
[b]At MP2/VTZ + D + P. Quasi-relativistic pseudopotentials were used for Si, Ge, Sn, Pb, from Ref. 93.
[c]At MP2/CEP. Compact effective core potentials (CEPs) were used for C and Si. Their relativistic counterparts (RCEP) were used for Ge, Sn and Pb. Correction for basis set superposition errors is included, from Ref. 95.
[d]Intramolecular interaction energy calculated for the element norbornyl cations, see Ref. 40.
[e]At B3LYP/6-311G(2d,p), pseudo-relativistic effective core potential and a (31/31/1) valence basis set were used for Si, Ge, Sn, Pb, from Ref. 40.

This particular substituent effect of the Cp ring on the thermodynamic stability gives a rationalization for the exceptionally high stability of protonated decamethyl silicocene **29**, studied by Jutzi and Bunte.[76]

The continuous growth of the thermodynamic stability of the EH_3^+ cations along the series C → Pb is also reflected in the calculated trend of the interaction energies ΔE_A of the EH_3^+ ions with a Lewis base like H_2O (see Table IV).[93] The interaction energy ΔE_A changes from $-71.3\,kcal\,mol^{-1}$ for methylium, H_3C^+, to $-31.4\,kcal\,mol^{-1}$ for plumbylium, H_3Pb^+. A similar trend is computed for the interaction of EH_3^+ ions with the π-electron donating toluene, i.e. the interaction energy for CH_3^+ with toluene is $-85.1\,kcal\,mol^{-1}$, while for silylium H_3Si^+ a significant smaller stabilization energy of $-53.1\,kcal\,mol^{-1}$ is predicted (see Table IV).[95] The trend is reversed for the trimethyl-substituted ions. That is, trimethyl silylium binds much more strongly to toluene than *t*-butyl cation ($-28.9\,kcal\,mol^{-1}$ for Me_3Si^+ compared to $-17.8\,kcal\,mol^{-1}$ for Me_3C^+). This opposite trend in the complexation energies upon substitution at the element reflects a smaller stabilizing interaction between the methyl substituents in Me_3Si^+ compared to Me_3C^+ (see also Table III).[94,95] In the case of the heavier analogues of the norbornyl cations the interaction energy between the remote C=C double bond and the electron-deficient element center decreases steadily from Si → Pb. This indicates less need for additional stabilization in the case of the plumbanorbornyl cation and also suggests that the electrophilicity of the R_3E^+ ions decreases for E = Si → Pb.[40]

B. *NMR Spectroscopic Properties of R_3E^+ Cations*

NMR spectroscopy has, in the last 20 years, become one of the most important analytical tools in the search for R_3E^+ ions in the condensed phases. With only the

exception of germanium, every group 14 element has at least one nucleus of spin 1/2, which is suitable for NMR studies using standard one- and two-dimensional Fourier Transform (FT) NMR techniques. Furthermore, there is a relation between the coordination number of the group 14 element and the NMR chemical shift. The low-frequency limit is defined by compounds with the element in high coordination states. The increasing imbalance of the electron distribution in lower coordination states of the element results in a deshielding of the atom in question. Therefore, cationic species with the charge largely located on the element atom should give a distinctive chemical shift, deshielded with respect to related four-coordinate species, which will allow a straightforward identification of the cationic species and an evaluation of the degree of ionic character indicated by a particular chemical shift. In addition, at least for silicon, reliable NMR chemical shift calculations strongly support the identification and characterization of the cationic species. Therefore, apart from X-ray diffraction, the best criterion for the R_3E^+ species (E = C, Si, Sn, Pb) is the NMR chemical shift of the central element.

1. ^{29}Si NMR Spectroscopic Data of Silylium Ions and Related Species

The presently known silicon chemical shift range is 990 ppm. This includes the D_{5d} form of decamethylsilicocene **28** ($\delta^{29}Si = -423$ (solid state)),[96] which is the most shielded resonance reported to date and the alkyl-substituted silylene **45**, which presently defines the high-frequency end of the spectrum at $\delta^{29}Si = 567$.[97] Most silicon chemical shifts occur, however, in a much smaller range from $\delta^{29}Si = +50$ to -190. This includes hexa-, penta- and tetracoordinated silicon compounds and for trivalent, positively charged silicon a significant low-field shift compared to comparable tetravalent silicon species is expected.

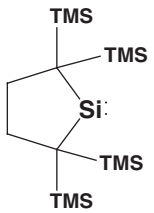

45

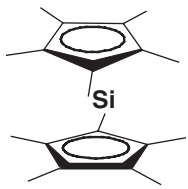

28

a. Si NMR Chemical Shift Calculation for Silylium Ions and Related Species

Early estimates for the ^{29}Si NMR chemical shift of silylium ions were based on an empirical correlation between ^{13}C NMR and ^{29}Si NMR chemical shifts of isostructural silicon and carbon compounds, and predicted for trimethylsilylium a ^{29}Si NMR chemical shift within the range 225–275.[98]

Accurate NMR chemical shift calculations for silicon compounds are available since the early 1990's and these computations played a decisive role in the identification and characterization of silylium ions in the condensed phase. This issue has

been thoroughly reviewed by several authors[10,13,94,99] and we will concentrate here on the pure description of the magnetic properties of silylium ions. Silicon NMR chemical shift calculations for several silylium ions in the gas phase are summarized in Table V. As expected for cationic species with the positive charge mainly localized at the central silicon, all silylium ions are characterized by a distinct chemical shift, significantly deshielded compared to neutral tetravalent compounds. That is, for trialkyl-substituted silylium ions low-field shifts compared to the neutral trialkylsilyl hydride of about 400 ppm are predicted. In addition, the calculations predict also an unusually wide spectral range for the ^{29}Si NMR chemical shift of silylium ions. Silylium ions with π-donating substituents, i.e. amino and phenyl groups have relatively shielded silicon nuclei (app. $\delta^{29}Si = 220$ for Ph_3Si^+ [6] and $\delta^{29}Si = 42$ for $(Me_2N)_3Si^+$),[100] while electropositive trimethylsilyl or dimethylboryl substituents induce a tremendous low-field shift with predicted Si NMR chemical shifts of $\delta^{29}Si = 920$ ($(Me_3Si)_3Si^+$)[101] and $\delta^{29}Si = 572$ ($(Me_2B)_3Si^+$).[102] This huge substituent effect on δ^{29}Si can be easily understood on the basis of the fundamental NMR

TABLE V
CALCULATED ^{29}Si NMR CHEMICAL SHIFTS FOR SILYLIUM IONS USING DIFFERENT METHODS AND BASIS SETS

Compound	Method	δ^{29}Si vs. Me_4Si	Ref.
H_3Si^+	IGLO[a,b]	270.2	106
Me_3Si^+	IGLO[a,b]	355.9	106
	HF/GIAO[c,d]	361.6	6
	B3LYP/GIAO[c,d]	413.0	6
	MP2/GIAO[d,e]	386.2	6
	SOS/DFPT/IGLO[a,b]	382.0	38
Et_3Si^+	IGLO[d,f]	371.3	107
	HF/GIAO[a,b]	371.2	38
	SOS/DFPT/IGLO[a,b]	415.6	38
i-Pr_3Si^+	HF/GIAO[a,b]	342.3	38
	SOS/DFPT/IGLO[a,b]	371.0	38
Ph_3Si^+	HF/GIAO[c,d]	198.8	6
	B3LYP/GIAO[c,d]	205.0	6
Mes_3Si^+	HF/GIAO[c,d]	230.1	6
	B3LYP/GIAO[c,d]	243.9	6
	IGLO	228	7
$(Me_3Si)_3Si^+$	IGLO[b,f]	925.3	108
	IGLO[a,b]	920.4	101
	B3LYP/GIAO[a,d]	1029.1	100
$(Me_2N)_3Si^+$	IGLO[g,h]	42.1	100
$(Me_2B)_3Si^+$	IGLO[a,b]	571.8	102
	B3LYP/GIAO[a,d]	587.3	102

[a]Using Basis II Ref. 109.
[b]Using a HF/6-31G(d) optimized geometry.
[c]Using a 6-311 + G(2df,p) (Si), 6-31G(d) (C,H) basis set.
[d]Using a B3LYP/6-31G(d) optimized geometry.
[e]Using a tz2p (Si), dzp (C,H) basis set.
[f]Using Basis II' Ref. 109.
[g]Using Basis II + sp.
[h]Using a MP2/6-31G(d) optimized geometry.

chemical shift theory. The following discussion can be equally applied for the understanding of the substituent effects on δ^{119}Sn and δ^{207}Pb NMR chemical shifts in stannylium and plumbylium ions. In general, the NMR chemical shift of heteronuclei are dominated by the paramagnetic contributions to the NMR chemical shielding.[101,103–105] This paramagnetic term is, however, directly related to the energy difference ΔE between occupied and unoccupied molecular orbitals with non-vanishing coefficients at the nuclei of interest. The smaller the energy difference ΔE between these magnetically active orbitals the larger is the paramagnetic contribution and in consequence the stronger deshielded is the nuclei. In the case of a trivalent cation R_3E^+ the relevant orbitals are of the R–E σ-bonding type and the formally empty *n*(p) orbital (*n*: principal quantum number) at the central element, the magnetically allowed transition is a $\sigma \leftrightarrow \pi^*$ excitation. Cations R_3E^+ with electropositive substituents in general have high-lying σ-type orbitals and therefore small energy gaps ΔE to the empty *n*(p)-orbital. This results in a strongly deshielding contribution for the nuclei E. On the other hand, electronegative substituents increase ΔE and reduce the paramagnetic contribution. π-Electron-donating substituents R in cations R_3E^+ interact with the p-type orbital at the central element E. This interaction results in destabilization of the *n*(p)E orbital and in a larger energy separation ΔE to the σ-type orbitals. For those cations, R_3E^+, less deshielded nuclei *E* are to be expected. These qualitative arguments give a straightforward interpretation of the computed ^{29}Si NMR data compiled in Table V. The Si NMR chemical shift calculated for the permethylated silaguanidinium ion, $(Me_2N)_3Si^+$,[100] with strongly π-electron-donating dimethylamino substituents marks the high-field end of the expected shift region for trivalent silylium ions, while the substituent effect of the electropositive trimethylsilyl groups of the tris(trimethyl)silylium ion places its predicted Si NMR resonance in the very low-field region. Even more strongly deshielded silicon nuclei are to be expected for germyl and stannyl-substituted silylium ions.

b. Experimental ^{29}Si NMR Data for Silylium Ions and Related Species

The experimental ^{29}Si NMR data on silylium ions are very limited due to the rather small number of examples for truly tricoordinated silylium ions (see Table VI). Trismesityl silylium, **1**, was the first silylium ion to be synthesized in the condensed phase as a long-lived species and it was characterized by its low-field resonance in the ^{29}Si NMR spectra of a solution of the TPFPB salt in benzene at $\delta^{29}Si = 225$.[5] In contrast to all other silyl cationic species previously produced in solution the ^{29}Si NMR chemical shift of **1** was shown to be constant when the solvent was changed from benzene to toluene or other alkylated aromatic hydrocarbons.[4] This indicates negligible interactions between solvent and the cation, characterizing **1** as the first free silylium ion, lacking any coordination to the solvent and the counteranion. NMR chemical shift calculations predict for optimized "gas phase" structures δ^{29}Si between 226 and 230, depending on the method applied.[6,7] Solid state ^{29}Si NMR from the carboranate $[Mes_3Si][HCB_{11}Me_5Br_5]$ obtained by magic angle spinning methods gave an isotropic δ^{29}Si of 226.7.[49] This close congruence suggests that the structure of Mes_3Si^+, **1,** is the same in all phases. The

TABLE VI
^{29}Si NMR CHEMICAL SHIFTS FOR CATIONIC SILICON SPECIES AND RELATED COMPOUNDS

Compound	Solvent	δ^{29}Si vs. Me_4Si	Ref.
1/TPFPB$^-$	C_6D_6	225.5	4, 5
	C_6D_6/C_7H_8 (1/3)	225.7	4, 5
	C_6D_6/*p*-$(D_3C)_2C_6D_4$ (1/1)	225.6	4, 5
	C_6D_6/CH_3CN (1/3)	37.0	4, 5
	C_6D_6/Et_3N (1/1)	47.1	4, 5
1/$HCB_{11}Me_5Br_6^-$	Solid state	226.7	49
46/TPFPB$^-$	C_6D_6	226.8	47
25/TPFPB$^-$	CD_2Cl_2	303.0	73
Me_3Si^+/TPFPB$^-$	C_6D_6	83.6	37
	Solid state	84.8	37
Me_3SiOTf	CD_2Cl_2	43.7	113
$Me_3SiOClO_3$	CD_2Cl_2	46.6	113
Et_3Si^+/TPFPB$^-$	C_6D_6	92.3	37
	C_7D_8	81.8	37
	CD_3CN	36.7	37
	Sulfolane	58.4	37
	Solid state	94.3	37
$Et_3Si^+/[CB_{11}H_6Br_6]^-$	Solid state	111.8/106.2[a]	114
Et_3Si^+/TFPB$^-$	*n*-PrCN	37.0	115
i-Pr_3Si^+/TPFPB$^-$	C_6D_6	107.5	37
	Solid state	107.6	37
i-Bu_3Si^+/TPFPB$^-$	C_6D_6	99.5	37
	Solid state	89.4	37
Me*i*-Pr_2Si^+/TPFPB$^-$	C_6D_6	96.9	37
$Hexyl_3Si^+$/TPFPB$^-$	C_6D_6	90.3	37
$MePh_2Si^+$/TPFPB$^-$	C_6D_6	73.6	37
$(Me_3Si)_3Si^+$/TPFPB$^-$	C_6D_6	111.1	37
55/TPFPB$^-$	C_6D_6	87.2	40
	C_7D_8	87.5	40
	CD_3CN	31.8	40
56/TPFPB$^-$	C_6D_6	82.7	40
57/TPFPB$^-$	C_6D_6	80.2	40
t-Bu_3Si^+/TFPB$^-$	CD_3CN	29.9	67
[*t*-$Bu_3SiOH_2^+$]/$CB_{11}H_6Br_6^-$	Solid state	46.7	116
[(*t*-$Bu_2MeSi)_3SiBu$-t_2]$^+$/TPFPB$^-$	CD_2Cl_2	315.7; 77.3	8
29/$[C_{12}H_{11}O_4]^-$	C_6D_6	−12.1	76
7/TPFPB$^-$	CD_2Cl_2	142.9	33
$(Me_2N)_3Si^+$/TPFPB$^-$	C_6D_6	−30.8	117
	CD_2Cl_2	−39.3	117

[a]Two independent molecules in the unit cell.

determination of the ^{29}Si NMR chemical shift tensor of Mes_3Si^+ provides further important information on the symmetry and electronic situation around the silicon nucleus in **1** (see Table VII).[49] The axially symmetric tensor ($\eta = 0$) is in agreement with a three-fold rotational axis in **1**. The equivalent and strongly deshielded tensor components δ_{11} and δ_{22} lie in the molecular plane and the more shielded δ_{33} component is oriented along the molecular C_3 axis (see Figure 1).

TABLE VII
^{29}Si NMR CHEMICAL SHIFT TENSOR COMPONENTS FOR $Mes_3Si^+/HCB_{11}Me_5Br_6^-$ [49] AND CALCULATED TENSOR COMPONENTS FOR Mes_3Si^+, **1**.[111] THE ORIENTATION OF THE EIGENVECTORS RELATIVE TO THE MOLECULAR FRAME IS GIVEN IN FIG. 1

	Experimental	Theoretical[a]
δ_{11}	319.5	317.6
δ_{22}	319.5	317.6
δ_{33}	41.2	55.3
δ_{iso}	226.7	230.1

[a]At HF/GIAO/Si(6-311 + G(2df,p)//B3LYP/6-31G(d), Ref. 111.

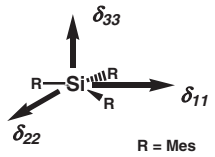

FIG. 1. Orientation of the chemical shift tensor components in trimesityl silylium ion **1**.

The spread of the NMR chemical shift tensor $\Delta\delta$ ($\Delta\delta = \delta_{11} - \delta_{33}$) is 278 ppm, much larger than reported for tetracoordinated silicon compounds ($\Delta\delta = 0-60$)[110]. According to density functional NMR calculations the strong deshielding of the in-plane components δ_{11} and δ_{22} are mainly the result of paramagnetic currents induced by the magnetic field that interrelates the σ-bonding molecular orbitals and the 3(p) Si-type orbital. These currents are very efficient, due the relative small energy gap ΔE between these orbitals in silylium ions.[111]

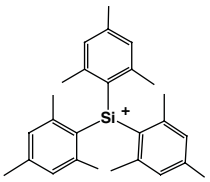

1

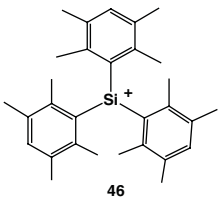

46

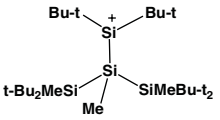

25

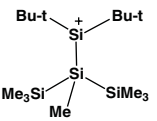

47

There are two other candidates for "free" silylium ions in the condensed phase, the duryl-substituted cation **46**[47] and the silylium ion **25**, which is substituted by two *t*-butyl groups and a bulky silyl group.[73] The situation is clear for the duryl-substituted cation **46**: the ^{29}Si NMR chemical shift of 226.8, very close to that of Mes_3Si^+ and a similar solvent independence of δ^{29}Si strongly suggest that **46** is another example for a silylium ion in the condensed phase.[47] Although for the cation **25** an even more deshielded ^{29}Si NMR resonance is reported ($\delta^{29}Si = 303$),[73] from the theoretical data summarized in Table V, a ^{29}Si resonance at markedly

lower field is expected for silylium ions with the same substitution pattern as **25**. In agreement, silicon NMR chemical shift calculations for **47**,[112] a suitable model for the experimentally investigated silyl cation **25**, predict a ^{29}Si NMR chemical shift of $\delta^{29}Si = 530$, more than 200 ppm to lower field than the signal assigned to the free silylium cation **25**. Thus, some doubts concerning the nature of the observed species in CD_2Cl_2 are warranted.

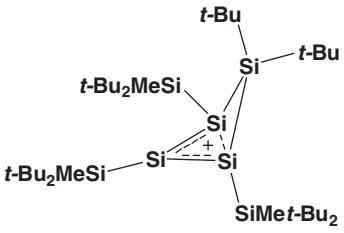

3

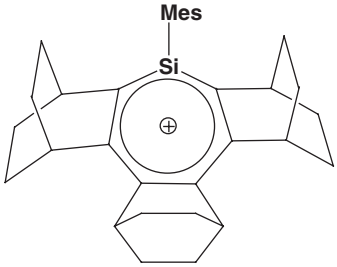

7

Silyl cations like **3** and **7** in which the positively charged silicon is part of a π-conjugated system attracted particular interest. The marginally stable silatropylium ion **7**, is characterized by a ^{29}Si NMR resonance at $\delta^{29}Si = 149$ in CD_2Cl_2 at −50 °C, downfield-shifted by 192 ppm compared to the precursor silane.[33,34] This experimental value is in fair agreement with the calculated silicon NMR chemical shift for the optimized "gas phase" structure of **7** ($\delta^{29}Si = 159.9$, at GIAO/HF/6-311 + G(2df,p)(Si), 6-31G(d) (C,H)).[34] This indicates only small interactions between the cation and dichloromethane, the solvent used for the NMR investigations.[33,34] The reported ^{29}Si NMR data for silyl cation **3** demonstrate its homoaromatic character and characterize **3** as a free silyl cation in solution.[8] The four-membered ring in **3** is identified by three ^{29}Si NMR signals: $\delta^{29}Si = 77.3$ (Si^1, Si^3), 315.7 (Si^2) and 34.3 (Si^2). Remarkably, the most deshielded silicon atom in **3** is the central tricoordinated silicon. This is in agreement with some homoaromatic nature of the cation **3** with charge localization at Si^2 (see Fig. 2a) and it discards the possibility of a classical

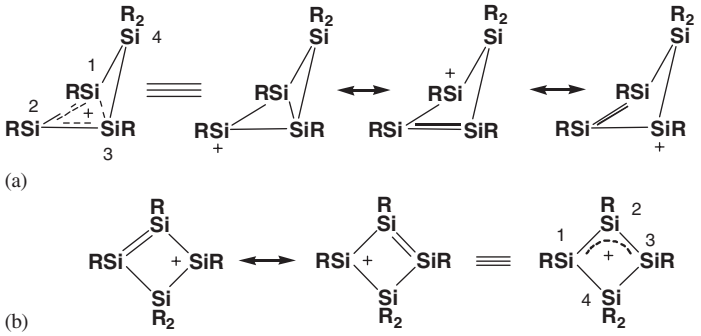

FIG. 2. (a) Homoaromatic conjugation in homocyclotrisilenylium cation **3**. (b) Allylic-type conjugation in a planar tetrasilacyclobutenyl cation.

TABLE VIII
NMR SPECTROSCOPIC DATA FOR SILYL CATIONS HAVING Si–X–Si THREE-CENTER BOND

Compound	X	δ^{29}Si	δX	^{1}J(SiX)	Ref.
48	F	90.6	–	229.2	118
54	F	77.2	−144.2	243.0	119
49	Cl	90.2	–		118
50	Br	90.8	–		118
51	H	99.1	–	26.0	118
52	H	76.7	1.47	39.0	121
53	H	54.4	3.34	45.7	119

allyl-type conjugation in **3**. For a hypothetical trisilaallyl cation the canonical structures imply charge localization at the terminal silicon atoms and therefore strongly deshielded effects for these atoms can be expected (see Fig. 2b). The reported chemical shifts are independent of solvent (dichloromethane, benzene and toluene) implying the lack of any covalent interaction with solvent molecules.[8]

Intramolecular interaction of the positively charged silicon with any remote substituent leads to considerable shielding of the silicon atom. This shielding parallels the extension of the coordination number of silicon from the tricoordinated silylium ion to some intermediate 3 + 1 coordination and, finally, to the regular tetracoordination of neutral silicon(IV) species. Thus, silyl cations stabilized by Si–X–Si three-center bonding with X-groups having lone pair electrons, as for example the halonium ions **48**–**50**, **54** are characterized by ^{29}Si NMR chemical shifts for the positively charged silicon atom between 91 and 77 (see Table VIII).[118,119] The large ^{1}J(SiF) coupling constant found for the fluoronium ions **48** and **54** are in the typical range for the sp^3 silicon–fluorine linkage indicating for the cations **48** and **54** only small silylium ion character.[120]

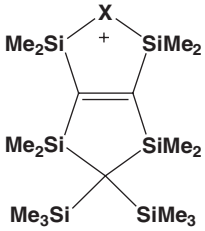

X = F , **48**
X = Cl, **49**
X = Br, **50**
X = H, **51**

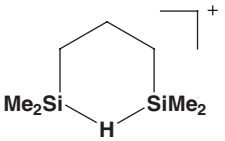

52

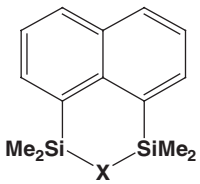

X = H , **53**
X = F, **54**

The situation is different for the silyl cations **51**–**53** having a Si–H–Si 2e-3c-bond.[118,119,121] The ^{29}Si NMR chemical shift of the cationic silicon depends strongly on the system (δ^{29}Si = 99.1, 76.7, 54.4, for **51**, **52**, **53**, respectively) and the ^{1}J(SiH) coupling constant in these cations (^{1}J(SiH) = 26, 39, 46 Hz for **51**, **52**, **53**, respectively) is markedly reduced compared to regular ^{1}J(SiH) coupling constants in

neutral silanes (^{1}J(SiH)~180–200 Hz in R_3SiH).[122] In addition, the central hydrogen of the SiHSi bridge is shielded compared to the precursor silanes. A theoretical analysis of the bonding situation for the silyl cations **52** and **53** suggests that the SiHSi three-center bond results from interaction of orbitals of mostly 3p-character at the silicon atoms with the s-orbital at the hydrogen atom. Due to the mostly complete p-nature of the SiHSi binding orbital at the silicon atoms, the important Fermi contact contribution to the J-coupling is rather small. This explains the very small ^{1}J(SiH) coupling constant in the hydrogen-bridged ions **51**–**53** and suggests that the silylium ion character in these cations is larger than in related halonium ions.[119]

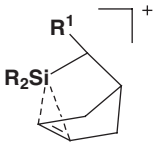

55: R = Me, R^1 = H
56: R = Et, R^1 = H
57: R = n-Bu, R^1 = H
58: R = Me, R^1= C_5H_{11}

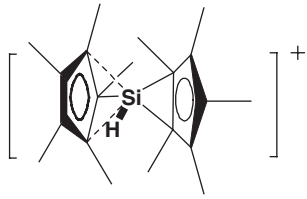

29

The silanorbornyl cations **55**–**58** in which the silicon adopts a formal [3 + 1] coordination, with the extra coordination side occupied by a C═C double bond are characterized by a ^{29}Si resonance between $\delta^{29}Si = 87-80$. The intramolecular interaction between the C═C double bond and the positively charged silicon atom is shown by an appreciable downfield shift of the vinylic carbon atoms by $\Delta\delta^{13}C = 20$ compared to the precursor silanes.[40,123] A quite unusual shielded resonance for a formally three coordinated silyl cation at $\delta^{29}Si = -12.1$ was found for the protonated decamethylsilicocene **29**.[76] The chemical shift reported for **29** is solvent independent, i.e. in benzene the same silicon NMR chemical shift is reported as in THF solution. This high-field resonance clearly mirrors the particular bonding situation in silyl cation **29**. According to a recent computational study silyl cation **29** is a highly fluxional molecule and in the predominant isomer the two Cp* substituents are bonded in an $\eta^2 : \eta^3$-fashion to the positively charged silicon atom.[77]

Silylium ions, which are not protected sterically or are not stabilized either electronically or by intramolecular interaction with a remote substituent do interact strongly with the solvent and/or the counteranion. The reaction of the transient silylium ion with solvents like ethers, nitriles and even aromatic hydrocarbons lead to oxonium, nitrilium and arenium ions with a tetrahedral environment for the silicon atom. These new cationic species can be clearly identified by their characteristic ^{29}Si NMR chemical shifts. That is, the oxonium salt $[Me_3SiOEt_2]^+$ $TFPB^-$ is characterized by $\delta^{29}Si = 66.9$ in CD_2Cl_2 solution at $-70\,^\circ C$.[124] Similar chemical shifts are found for related silylated oxonium ions.[55,116,125,126] Nitrilium ions formed by the reaction of intermediate trialkyl silylium ions with nitriles are identified by Si NMR chemical shifts $\delta^{29}Si = 30-40$[115,127,128–130] (see also Table VI for some examples). Trialkyl-substituted silylium ions generated in benzene solution yield silylated benzenium ions, which can be easily detected by a silicon NMR resonance at $\delta^{29}Si = 90-100$ (see Table VI).[35,36,113,108,131–137] Silyl-substitution

increases the ^{29}Si NMR chemical shift (δ^{29}Si ($[(Me_3Si)_3SiC_6H_6]^+$) = 111), while aryl substitution give smaller δ^{29}Si (δ^{29}Si ($[MePh_2SiC_6H_6]^+$) = 73.6). Therefore, the substituent effects on ^{29}Si NMR chemical shift in silylated arenium ions follows the same pattern as predicted for the free silylium ions (see Table V), however to a less spectacular extent. In general, for toluenium ions ^{29}Si NMR chemical shifts are measured which are by 10 ppm more shielded (see Table VI). More electron-rich arene solvents give an even more shielded ^{29}Si resonance for the silylated arenium ion. That is, the ^{29}Si resonance of the mesitylenium ion $[(cy)_3Si(C_6H_3Me_3)]^+$ ($\delta^{29}Si = 65$), is shifted by 25 ppm to higher field compared to the benzenium ion $[(Cy)_3Si(C_6H_6)]^+$ ($\delta^{29}Si = 90.3$).[37]

The data for *i*-pr_3Si^+ salts, summarized in Table IX, clearly show the influence of the counteranion on the ^{29}Si NMR chemical shift of silyl cationic species. The measured ^{29}Si NMR chemical shift for all *i*-pr_3Si^+ salts deviate considerably from the calculated value ($\delta^{29}Si = 375$, see Table V) being high field shifted by more than 250 ppm. In the absence of solvent/cation interactions, this is a clear indication for ion-pairing in solution and in the solid state. This is further supported by the solid state structure of several trialkylsilylium species with halogenated carborane anions, which show clear indications for interaction between the positively charged silicon center and one of the halogen atoms in the periphery of the carborane anion.[38,114,138] On the other hand, the ^{29}Si NMR chemical shift of the *i*-pr_3Si^+ salts clearly depends on the coordination ability of the counteranion. Therefore, the downfield shift of the ^{29}Si NMR chemical signal of the *i*-pr_3Si^+ X^- species allows a qualitative ranking of WCA^- toward main group Lewis acids.[139,140] By this

TABLE IX
^{29}Si NMR CHEMICAL SHIFTS FOR *i*-Pr_3Si^+/Y^- SALTS AND RELATED SPECIES

Compound	Conditions	δ^{29}Si vs. Me_4Si	Ref.
i-Pr_3SiH	C_7D_8	12	127
i-$Pr_3Si^+/(C_5(CN)_5)^-$	C_7D_8	40	142
i-$Pr_3SiOSO_2CF_3$	C_7D_8	40	143
i-$Pr_3Si(NSO_2CF_3)_2$	C_7D_8	53	144
i-$Pr_3Si^+(AlBr_4)^-$	C_7D_8	56	143
i-Pr_3Si^+(1-H-$CB_{11}H_5I_6)^-$	Solid state	97	143
i-Pr_3Si^+(1-H-$CB_{11}H_5Br_6)^-$	C_6D_6	100	139
	C_7D_8	105	138
	Solid state	110	143
i-Pr_3Si^+(1-H-$CB_{11}H_5Cl_6)^-$	C_6D_6	103	139
	Solid state	115	143
i-Pr_3Si^+(1-H-$CB_{11}Me_5Br_6)^-$	C_6D_6	112	139
i-Pr_3Si^+(1-H-$CB_{11}Me_5Cl_6)^-$	C_6D_6	113	139
i-Pr_3Si^+(1-H-$CB_{11}Cl_5Br_6)^-$	C_6D_6	111	145
i-Pr_3Si^+(1-H-$CB_{11}Br_5Cl_6)^-$	C_6D_6	116	145
i-Pr_3Si^+(1-H-$CB_{11}Cl_{11})^-$	C_6D_6	114	145
i-Pr_3Si^+(1-Me-$CB_{11}F_{11})^-$	C_7D_8	120	141
i-Pr_3Si^+ $TPFPB^-$	C_6D_6	108	37
	C_7D_8	94	127
	Solid state	108	37

criterion, the perfluorinated carborane anion $[1\text{-}MeCB_{11}F_{11}]^-$ is the least coordinating anion, since the salt $[i\text{-}pr_3Si][1\text{-}MeCB_{11}F_{11}]$ has the most deshielded ^{29}Si NMR signal ($\delta^{29}Si = 120$).[141] With anions which have a basicity comparable to that of the arene solvent, competition between solvation and ion-pairing must be considered. For example, according to the ^{29}Si chemical shift criteria in the solid state the interactions between the $TPFPB^-$ anion and the silylium species is stronger than in the case of the chlorinated carborane $[1\text{-}H\text{-}CB_{11}H_5Cl_6]^-$, i.e. the ^{29}Si solid state NMR signal of $[i\text{-}pr_3Si][1\text{-}H\text{-}CB_{11}H_5Cl_6]$ ($\delta^{29}Si = 115$) is at higher frequency than $[i\text{-}pr_3Si][TPFPB]$ ($\delta^{29}Si = 108$, see Table IX). In solution, however the equilibrium shown in Eq. (6) is shifted toward the silylated benzenium ion.[36,37] In the case of the carborane, the ion-pairing prevails also in solution, probably due to the less favored solvation of the anion.[114,140]

$$[R_3Si^+\ X^-] + C_6H_6 \rightarrow [R_3SiC_6H_6]^+ + X^- \qquad (6)$$

c. ^{29}Si NMR Data for Silyl-Substituted Germylium and Stannylium Ions

^{29}Si NMR chemical shifts for several silyl-substituted germylium and stannylium ions were reported. Interestingly, in the case of cyclotrigermylium ions **2** ^{29}Si NMR signals of the α-silicon atom at relatively high frequencies have been found ($\delta^{29}Si = 62-64$).[9,64–66] This is a considerable downfield shift relative to the precursor cyclotrigermene **20** (E = Si) ($\delta^{29}Si = 37.2$ and 50.1). The bishomoaromatic germyl cation **59** is characterized and identified by the two low-field ^{29}Si NMR signals for the SiBu-t_3 groups in the α-position ($\delta^{29}Si = 56.1$ and 67.2).[21] Similarly, for the trissilyl-substituted germylium and stannylium ions **22**, **23** ^{29}Si NMR resonances at $\delta^{29}Si = 50$ and $\delta^{29}Si = 64.9$ were found.[71,72] In the case of the germylium ion, this is about 25 ppm to lower field than in the corresponding germanes ($t\text{-}Bu_2MeSi)_3GeH$.[72] For the germyl cations, this deshielding effect on the silicon atom was rationalized by a significant charge transfer from the positively charged germanium to the more electropositive α-silicon atom.[66,72] It is questionable, however, if arguments based on simple charge delocalization can explain the deshielding effect in the stannylium ion **23**.[71] The influence of energetically high-lying Si–Ge or Si–Sn σ-bonding molecular orbitals on the ^{29}Si NMR chemical shift in the silyl-substituted germyl and stannyl cations should also be taken into account.

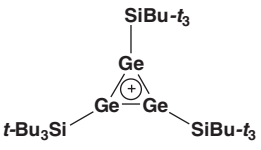

2

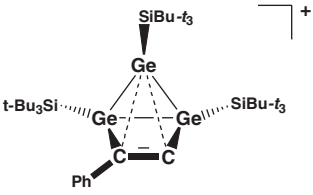

59

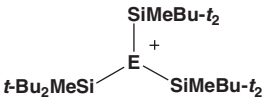

22 : E = Ge
23 : E = Sn

2. ^{119}Sn NMR Spectroscopic Data of Stannylium Ions and Related Species

Sn NMR chemical shifts in organotin compounds cover a range of about 5200 ppm, the current extremes being +2966 ppm in the divalent stannylene

(2,6-$Mes_2C_6H_3$)(GeBu-t_3)Sn:[146] and −2338 ppm in the hypercoordinated (1,3-di(*t*-Bu)C_5H_3)Sn^+ cation.[147] Most tetravalent organotin compounds can be found in a chemical shift range between −200 and +200 ppm and divalent stannylenes are characterized by ^{119}Sn NMR chemical shifts larger than 2000 ppm. These values are the brackets for a rough estimate of ^{119}Sn NMR chemical shift of tricoordinated stannylium ions.

a. Sn NMR Chemical Shift Calculations for Stannylium Ions and Related Species

A number of terms complicate the accurate calculation of Sn NMR chemical shifts, not least the possible importance of spin–orbit coupling and relativistic effects and Sn NMR chemical shift calculations became only feasible quite recently.[48,105,148] Therefore, the early estimates for the ^{119}Sn NMR chemical shift for a trivalent stannylium ion came from empirical correlations between ^{29}Si and ^{119}Sn NMR chemical shift,[46] which has been shown to be a valuable tool for estimating the NMR chemical shifts of structurally related tetravalent silicon and tin compounds.[149,150] Based on these correlations, the ^{119}Sn NMR chemical shift of a trialkylstannylium ion was expected to be around 1770, and for triaryl-substituted cations values around 1250 were predicted.[46] Already early IGLO (individual guage for localized orbitals) calculations of the Sn NMR chemical shift[151] indicated that the empirical correlation between ^{29}Si and ^{119}Sn NMR chemical shift overestimates the deshielding of the tin atom in stannylium ions. That is, for H_3Sn^+ $\delta^{119}Sn = 777$ is calculated and on the basis of methyl increments, the Sn NMR chemical shift for Me_3Sn^+ was estimated to be about 1075,[151] at 700 ppm to higher field of that predicted from the empirical correlation. More recent calculations of ^{119}Sn NMR chemical shift for stannyl cations support this view.[48,105] Computed Sn NMR chemical shifts of various stannylium ions and related species are summarized in Table X. The most striking fact arising from these calculations is the wide spread of the expected ^{119}Sn NMR chemical shift for stannylium ions. That is, for the trisilyl-substituted cation values between $\delta^{119}Sn = 2440$ and 2880 are predicted, depending on the applied method. This is more than 1800 ppm to lower field of that calculated for stannylium ion H_3Sn^+. As already discussed for silylium ions (Section III.B.1.a), this strong deshielding in the silyl-substituted cations is a result from very large paramagnetic (deshielding) contributions to the NMR chemical shift due to the small energy difference ΔE between magnetically active orbitals, here between σ(Sn–Si) bonding orbital and the 5p(Sn) orbital, with large coefficients at the tin atom.

A general comment on the use of the empirical correlation between ^{29}Si and ^{119}Sn NMR (and likewise on ^{13}C/^{29}Si or ^{119}Sn/^{207}Pb NMR) chemical shifts is in order. The basis for this correlation is that the paramagnetic term σ_p dominates the chemical shift. According to Ramsay's theory,[103a,b] σ_p is proportional to the reciprocal energy difference ΔE between the magnetically active orbitals and proportional to the expectation value for the electron radii $\langle r^{-3}\rangle_{np}$. Thus, a linear correlation between the δ^{29}Si and δ^{119}Sn implies that the ratio of *both* determining factors of σ_p is constant for the all compounds of interest. In particular, it is not clear, however, if the ΔE ratio for tetravalent silicon and tin compounds is the same as for trivalent silicon and tin compounds. Therefore, the extension of a correlation based exclusively on the

TABLE X
CALCULATED Sn NMR CHEMICAL SHIFTS FOR CATIONIC TIN SPECIES

Compound	Method	δSn vs. Me_4Sn	Ref.
Mes_3Sn^+, **65**	GIAO/MPW1PW91[a,b]	856	48
Tip_3Sn^+, **68**	GIAO/MPW1PW91[a,c]	763	48
H_3Sn^+	IGLO/HF[d,e]	774	151
	GIAO/HF[a,f]	596	105
	GIAO/MPW1PW91[a,f]	878	105
	GIAO/MP2[a,f]	718	105
Me_3Sn^+	IGLO/HF[d,g,e]	1075	151
	GIAO/HF[a,f]	1166	105
	GIAO/MPW1PW91[a,f]	1466	48, 105
	GIAO/MP2[a,f]	1325	105
$[Me_3Sn/C_6H_6]^+$	GIAO/MPW1PW91[a,f]	482	48
$[Me_3Sn/C_7H_8]^+$	GIAO/MPW1PW91[a,f]	438	48
$Me_3SnOClO_3$	GIAO/MPW1PW91[a,f]	228	48
Me_3SnOTf	GIAO/MPW1PW91[a,f]	229	48
$Me_2Sn^+CH_2C_5H_9$, **62**	GIAO/MPW1PW91[a,h]	406	48
$(H_3Si)_3Sn^+$, **70**	GIAO/MPW1PW91[a,f]	2880	105
	GIAO/HF[a,f]	2440	105
	GIAO/MP2[a,f]	2680	105
	GIAO/B3LYP[i,j]	2841	71
$(Me_3Si)_3Sn^+$, **71**	GIAO/MPW1PW91[a,f]	3450	105

[a]Basis set: 6-31G(d), (Si,C,H,O,S,F) and tzv (19s,15p,9d)[8s,7p,5d] (Sn).
[b]HF/6-31G(d) (Si,C,H,O,S,F) SDD (Sn) optimized geometries has been used.
[c]B3LYP/6-31G(d) (C,H) LACVP** (Sn) optimized geometry has been used.
[d]Basis set: dz(p).
[e]HF/dz(p) optimized geometry has been used.
[f]B3LYP/6-31G(d) (Si,C,H,O,S,F) SDD (Sn) optimized geometries has been used.
[g]Estimated using methyl increments.
[h]MP2/6-311G(d) (Si,C,H,O,S,F) SDD (Sn) optimized geometries has been used.
[i]Basis set: 6-311G(d), (Si,C,H) and [7s,6p,5d] (Sn).
[j]B3LYP/6-31G(d) (Si,C,H) [6s,5p,4d](Sn) optimized geometries has been used.

comparison of tetravalent compounds to trivalent compounds is questionable. Consequently, there are two established correlations between ^{119}Sn and ^{207}Pb NMR chemical shifts, one for divalent[152] and one for tetravalent compounds.[149]

b. Experimental ^{119}Sn NMR Data for Stannylium Ions and Related Species

Early experimental investigations by Birchall and co-workers indicated that tin cations R_3Sn^+ (R = H, Me, Et) are formed from tetracoordinated stannanes $R_{4-n}SnH_n$ ($n = 0-4$) in superacidic media.[43–45] They were identified by ^{119}Sn NMR spectroscopy, and the following shifts in fluorosulfonic acid at low temperatures have been reported: "Me_3Sn^+", $\delta^{119}Sn = 322$ ppm ($T = -60\,^\circ C$), "Et_3Sn^+" $\delta^{119}Sn = 288$ ($T = 20\,^\circ C$) and "H_3Sn^+" $\delta^{119}Sn = -194$.[43] From a careful analysis of the scalar $^1J(SnC)$ coupling and from Mössbauer spectroscopy data, it was concluded that these "R_3Sn^+" cations adopt in fluorosulfonic acid a trigonal-bipyramidal coordination sphere, where the three substituents R form the trigonal basis and two fluorosulfates occupy the apical position.[43,45] The ^{119}Sn NMR

chemical shift depends on the acid and reaction conditions. When 92% sulfuric acid is used for the generation of the "Me_3Sn^+" cation a ^{119}Sn NMR chemical shift of 194 is detected[44] and the ^{119}Sn NMR spectrum of a mixture of Me_4Sn and $SbCl_5$ showed a signal at $\delta^{119}Sn = 208$ attributed to the "Me_3Sn^+" cation.[153]

Various monohalides of triorganotin derivatives have been shown by ^{119}Sn NMR spectroscopy to ionize in polar organic solvents, providing the corresponding coordinated cations.[154–156] The actual ^{119}Sn NMR chemical shift however depends markedly on the solvent, that is for the tin perchlorate, Bu_3SnClO_4, the following ^{119}Sn NMR chemical shifts were reported: $\delta^{119}Sn = 220$ (CH_2Cl_2), 139 (sulfolane), 54 (MeCN), −24 (pyridine), 0 (1,3-dimethyl,2,4,5,6-tetrahydro-2(1 H)-pyrimidone (DMPU)), 12 (dimethyl sulfoxide (DMSO)), −43 (hexamethylphosphoric triamide (HMPA)).[154] This clear dependence of the ^{119}Sn NMR chemical shift on the donicity of the solvent and an analysis of the scalar ^{1}J(SnC) coupling and of the ^{37}Cl NMR linewidths of the perchlorate anion indicate a subtle balance between neutral tetrahedral and cationic trigonal-bipyramidal arrangement of the tin species. Bipyramidal coordination is favored if the solvent donicity is increased. For HMPA as solvent the bipyramidal arrangement is demonstrated by the presence of a ^{119}Sn-^{31}P coupling.[154]

With counteranions of lower nucleophilicity the ^{119}Sn NMR chemical resonance of solutions of tributyl tin salts is further shifted to lower field. Lambert and Kuhlmann reported for the tributylstannyl borate $Bu_3SnB(C_6F_5)_3H$ $\delta^{119}Sn = 360$ in benzene[25] and Kira and co-workers found for the related $Bu_3SnTFPB$ $\delta^{119}Sn = 356$ in CD_2Cl_2.[27] In the latter case, ^{19}F NMR spectroscopy indicates no cation–anion interaction. Finally, for $Bu_3SnTPFPB$ in toluene at −60 °C $\delta^{119}Sn = 434.2$ was reported by Piers *et al.*[28,29] The solvent dependence of the ^{119}Sn NMR chemical shift suggests that in the case of aromatic solvents Wheland-type intermediates are formed.[4,28,29,46] Additional support for the formation of stannylated arenium ions in these experiments[25,28,29] comes from the fair agreement between the calculated ^{119}Sn NMR chemical shift for $[Me_3SnC_6H_6]^+$ ($\delta^{119}Sn = 438$) and $[Me_3SnC_7H_8]^+$ ($\delta^{119}Sn = 482$) compared to the experimental data. The addition of stronger nucleophiles than aromatic hydrocarbons or methylene chloride to the samples has a strong shielding effect on the tin nucleus. That is, addition of excess diethylether to a solution of $Bu_3SnTFPB$ in CD_2Cl_2 yields an oxonium species characterized by a high field shifted ^{119}Sn NMR signal at $\delta^{119}Sn = 165$.[27] Similarly, addition of an equimolar amount of *o*-anisaldehyde to a solution of $Bu_3SnTPFPB$ in C_7D_8 gives a cationic tetracoordinated trialkyltin compound, **60**, identified by a ^{119}Sn NMR chemical shift of $\delta^{119}Sn = 300$. The addition of a second equivalent of anisaldehyde to the reaction mixture leads the formation of the cationic pentacoordinated species, **61**, accompanied by a further decrease of the ^{119}Sn NMR chemical shift ($\delta^{119}Sn = 91$, see Scheme 17).[28]

Recently Michl and co-workers isolated the stannylium ions Bu_3Sn^+ and Me_3Sn^+ with the permethylated carborane anion $[CB_{11}Me_{12}]^-$ as counterion.[68,69] Both cations strongly interact in the solid state with the carborane anion and form infinite one-dimensional columns of alternating R_3Sn^+ and $CB_{11}Me_{12}^-$ ions (see Section III.D.3). In agreement with sizeable cation–anion interactions the solid state NMR chemical shift for both cations ($\delta^{119}Sn = 461$ (Bu_3Sn^+) and $\delta^{119}Sn = 466$ (Me_3Sn^+) are at much higher field than expected for isolated trialkylstannylium ions.[69] Ion aggregation persists in hydrocarbon solution, as the solution ^{119}Sn

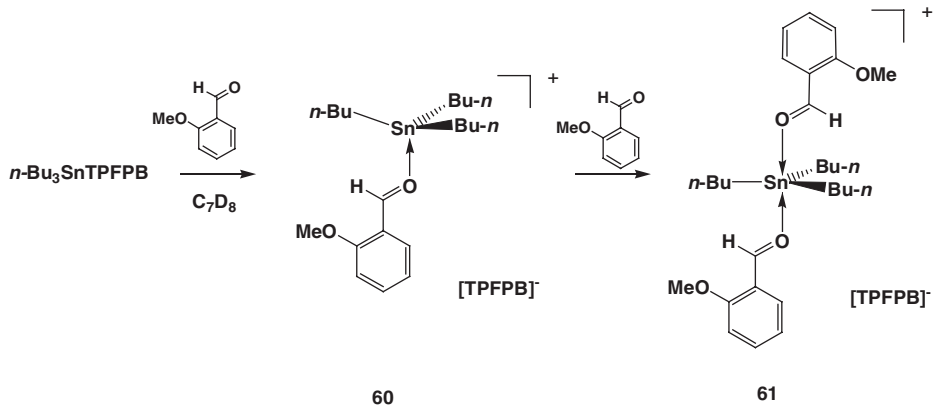

SCHEME 17.

NMR chemical shift in cyclohexane for $[Bu_3Sn^+][CB_{11}Me_{12}^-]$ is only little lower than in the solid state ($\delta^{119}Sn = 454$).[68,69] On the other hand, even in benzene solution, the interaction with the solvent predominates, therefore the ^{119}Sn NMR chemical shift of $[Me_3Sn^+][CB_{11}Me_{12}^-]$ in benzene is 325, indicating formation of stannylated arenium ions. Solutions of these permethylated carborane salts in solvents of higher donicity have ^{119}Sn NMR chemical shifts, which are characteristic for chloronium ions ($\delta^{119}Sn = 336$, $[Me_3Sn^+][CB_{11}Me_{12}^-]$ in CD_2Cl_2), for nitrilium ions ($\delta^{119}Sn = 233$, $[Me_3Sn^+][CB_{11}Me_{12}^-]$ in CDCN) and for oxonium ions ($\delta^{119}Sn = 168$, $[Bu_3Sn^+][CB_{11}Me_{12}^-]$ in Et_2O/CD_2Cl_2).[69]

The intramolecular π-electron donation from the remote double bond to the stannylium ion center in the stannanorbornyl cation, **62** ($\delta^{119}Sn = 336$ in C_6D_6), also leads to a significant shielded tin nucleus compared to what is expected for a free trialkylstannylium ion. As already shown for the sila compounds **55**–**58**, the coordination of the C═C double bond to the electron-deficient tin center in **62** is indicated by a low-field shift of the ^{13}C resonance of the vinylic carbon atoms by 11.1 ppm. Additionally, the small scalar Sn–C coupling constant $^1J(SnC) = 26$ Hz gives clear evidence for the intramolecular π-complexation.[40]

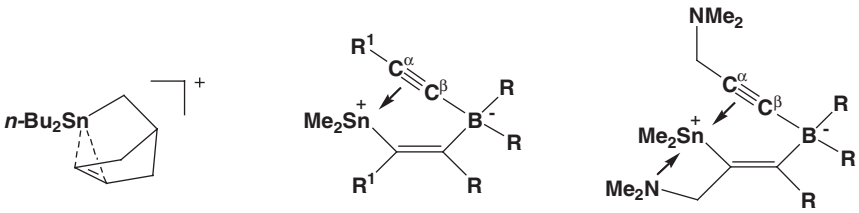

62 **63** **64**

The bonding situation in the stannanorbornyl cation **62** is reminiscent of the intriguing zwitterions of the types **63**[158] and **64**[157] in which triorganotin cations are intramolecularly stabilized by side-on coordination with an alkynyl group. The zwitterions **63** with a [3 + 1] coordination for the tin atom are characterized by a significantly deshielded ^{119}Sn NMR resonance and sizeable ^{1}J(SnC) couplings to the alkynyl carbon atoms (for R^1 = alkyl and R = Et: δ^{119}Sn = 160–215; ^{1}J(SnC^{α}) = 41–48 Hz, ^{1}J(SnC^{β}) = 60–80 Hz).[158] Coordination with the amino group in **64** leads to an additional upfield shift of the ^{119}Sn NMR signal (For R = Et: δ^{119}Sn = 127.7)[157]

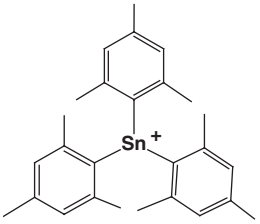

65

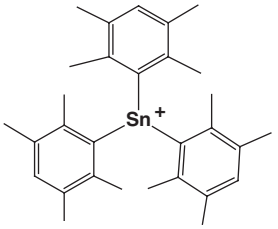

66

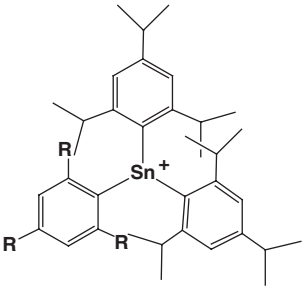

67, R = H
68, R = *i*-Pr

The trimesitylstannylium ion **65**, synthesized in Lambert's group, is characterized by an extremely low-field signal in the ^{119}Sn NMR spectra (δ^{119}Sn = 806 in C_6D_6).[4] This ^{119}Sn NMR chemical shift is unchanged in toluene, mesitylene and *o*-dichlorobenzene, indicating negligible interactions of the cations and aromatic hydrocarbons or their chlorinated derivatives. Similar low-field signals were detected for the tridurylstannylium, **66**, and the di(triisopropylphenyl)-phenylstannylium cation, **67** (δ^{119}Sn (**66**) = 720, δ^{119}Sn (**67**) = 697, see also Table XI).[4,47] These ^{119}Sn NMR chemical shifts are however still at ca 300 ppm at higher field than expected for a *trivalent* triarylstannylium ion based on the empirical correlation between ^{29}Si NMR and ^{119}Sn NMR chemical shifts established for *tetravalent* silicon and tin compounds.[46] For this reason and since cation/anion interaction or intramolecular interactions between the tin center and remote C–H bonds ("agostic interactions") could not be excluded, Lambert and co-workers confined to these cations "only about 75% stannylium ion character".[4,47] The situation changed, however, after the synthesis and structural characterization of the tris(triisopropylphenyl) stannylium ion **68**. Compound **68** was shown to exist as a non-coordinated cation with the TPFPB counteranion (see Section III.D.1). The molecular structure showed no indication for agostic interactions and its δ^{119}Sn NMR chemical shift was 714.[48] Subsequent ^{119}Sn NMR calculations using the MPW1PW91/GIAO density functional method predicted for an optimized structure of cation **68**, a ^{119}Sn NMR chemical shift of 763. A more extensive theoretical study on Sn NMR chemical shift calculations for stannyl cationic species demonstrated that the calculated value (δ^{119}Sn = 763) is fully consistent with the observed value of δ^{119}Sn = 714 (see Tables X and XI).[48,105] On the basis of the experimental results for **68**[24] and

TABLE XI
^{119}Sn NMR CHEMICAL SHIFTS FOR CATIONIC TIN SPECIES

Compound	Solvent	δ^{119}Sn vs. Me_4Sn	Ref.
65/TPFPB$^-$	C_6D_6	806	4
	C_7H_8	806	4
	1,3,5-$(H_3C)_3C_6H_3$	806	4
	1,2-$Cl_2C_6H_4$	806	4
66/TPFPB$^-$	C_6D_6	720	47
67/TPFPB$^-$	C_6D_6	697	4
68/TPFPB$^-$	C_6D_6	714	48
23/TPFPB$^-$	C_6D_6	2653	71
$Me_3Sn^+/CB_{11}Me_{12}^-$	Solid state	466.2	69
	C_6D_6	324.7	69
	CD_2Cl_2	335.9	69
	CD_3CN	233.1	69
Me_3Sn^+/FSO_3^-	FSO_3H	322	43
n-$Bu_3Sn^+/CB_{11}Me_{12}^-$	Solid state	461.2	69
	C_6D_{12}	454.3	68
n-$Bu_3Sn^+/HB(C_6F_5)_3^-$	C_6D_6	360	25
n-Bu_3Sn^+/TFPB$^-$	CD_2Cl_2	356	27
	Et_2O/CD_2Cl_2	165	27
n-Bu_3Sn^+/TPFPB$^-$	C_7D_8	434.2	28
n-$Bu_3SnOClO_3$	CH_2Cl_2	220	154
n-Bu_3SnOTf	CH_2Cl_2	172	154
62/TPFPB$^-$	C_6D_6	334.0	40
	C_7D_8	329.7	40
	CD_3CN	54.4	40
Et_3Sn-O^+(H)-$SnEt_3$/TPFPB$^-$	C_6D_6	250.8	26

supported by the Sn NMR calculations[48,105] it can be concluded that the triarylstannylium ions **65**–**68** all exist as free cations in the condensed phase, unfettered by interaction with solvent, anion or neighboring groups.

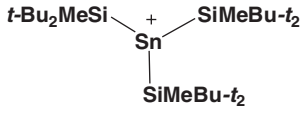

23

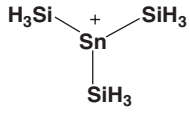

70

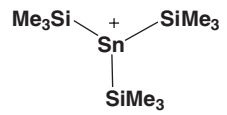

71

The extreme low-field position of the ^{119}Sn resonance of Sekiguchi's trisilyl-substituted stannylium ion **23** ($\delta^{119}Sn = 2653$)[71] is at a first glance surprising, in particular when compared with the ^{119}Sn NMR chemical shifts of the aryl-substituted cations **65**–**68**. The rationalization however, is straightforward on the basis of the discussion in Section III.B.1.a. The occurrence of energetically high-lying SiSn bonding MO's and the relative low-lying p-type orbital at the tin center in stannylium ion **23** leads to large paramagnetic contributions to the Sn NMR chemical shielding and in consequence to the observed absorption at an extraordinarily high frequency.[105] Sn NMR chemical shift calculations at various levels

of theory for stannylium ions **70** and **71**, close models for Sekiguchi's stannylium ion **23**, reproduce qualitatively the tremendous deshielding of the tin nuclei in **23** compared to the triaryl-substituted stannylium ions (see Table X).[71,105]

3. ^{207}Pb NMR Spectroscopic Data of Plumbylium Ions and Related Species

Empirical correlations between δ^{119}Sn and δ^{207}Pb NMR chemical shifts exist for tetravalent[149] and for divalent[152] tin and lead compounds. Keeping in mind the short discussion in Section III.B.2.a, it is clear that both cannot be applied for trivalent cations. Therefore, no empirical estimate for the ^{207}Pb NMR chemical shift of a free plumbylium ion exists. In addition, no reliable NMR chemical shift calculations are available for plumbylium ions.[159] A rough estimate, purely based on the well-established influence of the coordination number on the NMR chemical shift, would place the ^{207}Pb NMR chemical shift for plumbylium ions at higher frequencies than tetravalent organolead compounds ($\delta^{207}\text{Pb} = -1000$ to $+1000$), but shielded compared to divalent diorganoplumbylenes ($\delta^{207}\text{Pb} > 2000$). In agreement with this guideline the formation of triorganoplumbyl cations from tetravalent precursors is always accompanied by a significant low-field shift of the ^{207}Pb NMR chemical signal (see Table XII). The reported ^{207}Pb NMR chemical shift for triorganoplumbyl cationic species depends however, markedly on the actual reaction conditions. That is, while for trimethylplumbyl fluorosulfate in fluorosulfonic acid $\delta^{207}\text{Pb} = 980$ is reported,[48] a solution of the salt $[Me_3Pb^+][CB_{11}Me_{12}^-]$ in C_6D_6 at room temperature is characterized by a ^{207}Pb NMR signal at 1007.[69] In both cases, cation/anion aggregation and/or solvent complexation must be taken into account, since for $[Et_3Pb^+]$TPFPB$^-$ in C_6D_6 a significantly more deshielded lead center is found ($\delta^{207}\text{Pb} = 1432$).[40] The ^{207}Pb NMR chemical shift of $[Et_3Pb^+]$TPFPB$^-$ is relatively insensitive to solvent effects, i.e in toluene solution $\delta^{207}\text{Pb} = 1405$ is found.[160] Therefore, the solvent effect on the ^{207}Pb NMR chemical shift is less than 2%. In the absence of any additional experimental information on the nature of the observed species and in sight of the substantial interaction energy

TABLE XII
^{207}Pb NMR CHEMICAL SHIFTS FOR PLUMBYL CATIONIC COMPOUNDS

Compound	Solvent	δ^{207}Pb vs. Me_4Pb	Ref.
Et_3Pb^+/TPFPB$^-$	C_6D_6	1432	40
	C_7D_8	1405	160
Bu_3Pb^+/TPFPB$^-$	C_6D_6	1309	160
$Me_3Pb^+/CB_{11}Me_{12}^-$	CD_2Cl_2	1007	69
13/TPFPB$^-$	C_6D_6	1049	40
	C_7D_8	1039	40
73/TPFPB$^-$	CH_3CN/C_6D_6	598	40
74/TPFPB$^-$	C_6D_6	807	53
75/TPFPB$^-$	C_6D_6	799	53
72, R = Et		723	161
72, R = *i*-Pr		667	161
Me_3PbOSO_2F		980	46
$Me_3PbOClO_3$		694	46

predicted for Me_3Pb^+ and toluene ($\Delta E_A = 30.5\,kcal\,mol^{-1}$, see Table IV)[94] one cannot exclude the formation and detection of plumbyl arenium ions in these experiments.[40,160]

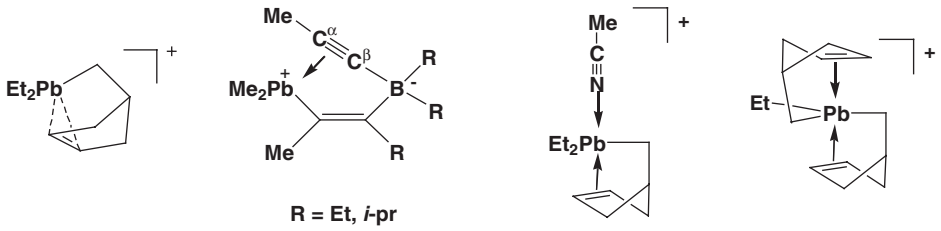

13 72 73 74

Intramolecular π-coordination of the electron-deficient lead center, as for example in the norbornyl cation **13** ($\delta^{207}Pb = 1049$)[40] and in the zwitterions **72** (R = Et : $\delta^{207}Pb = 723$; R = *i*-pr: $\delta^{207}Pb = 667$),[161] leads to a significant high-field shift of the ^{207}Pb NMR resonance when compared to $[Et_3Pb^+]TBFPB^-$. The detection of scalar Pb–C couplings $^1J(CPb)$ between the Pb atom and the vinylic C atoms in **13** or the acetylenic C atoms in **72**, respectively, clearly indicates the intramolecular coordination of the CC multiple bond to the plumbylium ion (**13** : $^1J(CPb) = 16.2$ Hz; **72** : $^1J(CPb) = 11$–30 Hz).[40,161] The significant solvent induced high-field shift detected for **13** when 1 Eq. acetonitrile is added to a benzene solution of [**13** TPFPB] is due to the formation of an acetonitrile complex, **73**, which could also be characterized crystallographically. Similarly, the formation of the bis-alkene complex **74**, in which the Pb atom adopts a trigonal-bipyramidal coordination sphere with the two alkene groups in the apical position, is accompanied by a further decrease of the ^{207}Pb NMR chemical shift ($\delta^{207}Pb = 807$ for **74** in C_6D_6).[53] Nearly the same ^{207}Pb NMR chemical shift as for **74** is measured for the tris-cyclopentenylmethyl-substituted plumbyl cation **75** ($\delta^{207}Pb = 799$ in C_6D_6). ^{13}C NMR data show that all three substituents in the plumbyl cation **75** are equivalent on the NMR time scale at room temperature. This suggests for **75**, a dynamic equilibrium between equivalent bisalkene complexes of trivalent lead, similar to **74** (see Scheme 18).[53]

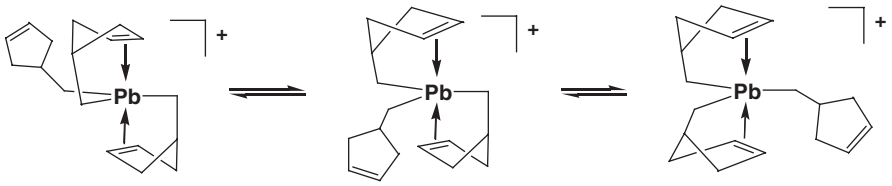

75

SCHEME 18.

4. ^{13}C NMR Spectroscopic Data of Organosubstituted R_3E^+ Cations

^{13}C NMR chemical shifts of organosubstituted R_3E^+ ions are only of small diagnostic value. Several factors such as substitution, charge distribution and small separations of magnetically active molecular orbitals etc. influence the ^{13}C NMR chemical shifts of the C atoms of the organic ligand in R_3E^+ in a not easily predictable manner so that no characteristic pattern is apparent. The only exceptions where ^{13}C NMR chemical shifts are used for the characterization of the R_3E^+ cations are (i) when a series of homologues R_3E^+ cations were investigated and trends in the ^{13}C NMR chemical shifts are discussed and (ii) when intramolecular stabilization of the electron-deficient element atom by CC multiple bonds is important. In these cases, the analysis of ^{13}C NMR chemical shifts played an important role for the characterization of germylium ions, R_3Ge^+, since germanium lacks a sensitive and convenient NMR active nuclide. In the following, examples for both cases are given.

Michl and co-workers recently reported solid state ^{13}C NMR chemical shift of the methyl group in the $Me_3E^+CB_{11}Me_{12}^-$ (E = Ge, Sn, Pb) salts to be 5.6, 10.4 and 31.4 for Me_3Ge^+, Me_3Sn^+ and Me_3Pb^+, respectively.[69] The authors argued that the steady deshielding of the α-carbon atom indicates a continuous increase of positive charge concentration at the central element going from germanium to lead.[69]

Similarly, the cationic character of the germylium ion Mes_3Ge^+, **76**, was estimated by comparison of the low-field shift of the ^{13}C NMR resonances of the aryl carbon atoms upon ionization with those low-field shifts found for the homologous silylium and stannylium ions.[4] The deshielding of the aryl carbon atoms in **76** is comparable to that found for **1** and **65**. This is consistent with charge development on germanium in **76** that is comparable to that on silicon in Mes_3Si^+, **1**, and tin in Mes_3Sn^+, **65**.

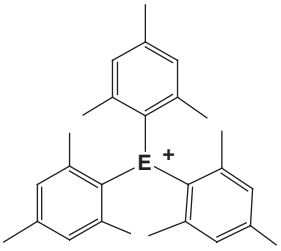

1 E = Si
65 E = Sn
76 E = Ge

55 E = Si, R = Me
56 E = Si, R = Et
57 E = Si, R = *n*-Bu
62 E = Sn, R = *n*-Bu
13 E = Pb, R = Et
77 E = Ge, R = *n*-Bu

The deshielding of the vinylic carbon atoms in the norbornyl cations **13**, **55**–**57**, **62** and **77** compared to the precursor compounds was taken as evidence for the intramolecular coordination of the C=C double bond to the electron-deficient element atom.[40] This high-frequency shift, $\Delta\delta^{13}C$, is largest for the silanorbornyl cations **55**–**57** ($\Delta\delta^{13}C = 20$) and $\Delta\delta^{13}C$ decreases continuously and it reaches for the

plumbanorbornyl cation **13** its minimum value of 8. This implies reduced electron transfer from the C=C double bond to the positively charged element atom in the series C → Pb.[40]

The intramolecular stabilization of germyl cation **34** by a remote aryl substituent was demonstrated by the ^{13}C NMR chemical shifts of the coordinated aryl ring.[80] The chemical shift pattern found for the coordinated arene ring of **34** is characteristic for arenium ions and it closely resembles that found bissilylated arenium ions **78**.[162]

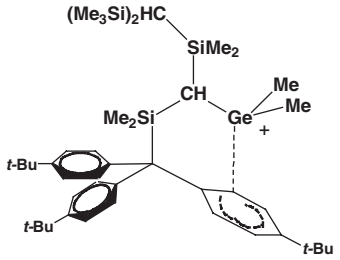

34

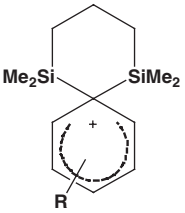

78

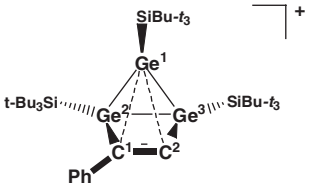

6

One of the most important features of the bicyclic bishomoaromatic germylium ion **6** is the considerably *shielded* ^{13}C NMR chemical shifts of the endocyclic atoms C1 and C2, relative to those of the neutral precursor **5**.[21] Despite the partial delocalization of the positive charge over Ge3, C1 and C2, significant high-field shifts ($\Delta\delta^{13}$C(C1) = −29.8, ($\Delta\delta^{13}$C(C1) = −54.5) are observed and a relatively large ^{1}J(C2H) coupling constant of 165.9 Hz is detected. This counter-intuitive low-frequency shift of the ^{13}C NMR resonance of C1 and C2 as well as the large scalar CH coupling constant was rationalized for similar bishomoaromatic carbon cations like the 7-norbornenyl cation, **79**, by the hypercoordinated nature of the vinylic C atoms and was put forward as spectroscopic evidence for bishomoaromaticity.[163,164]

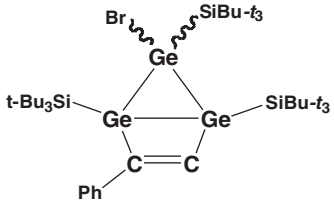

5

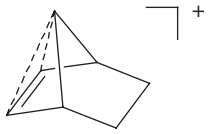

79

C. *Miscellaneous Spectroscopic Data of R_3E^+ Cations*

Spectroscopic information on R_3E^+ other than NMR chemical shifts and coupling constant are hardly available. Some UV data are reported for Mes_3E^+ cations (E = Si, Sn) in benzene solution.[4] The UV absorption in these aryl-substituted

cations was taken as measure for the conjugation between the central element atom and the π-system of the aryl ligand. Two absorptions were observed for the silylium ion Mes_3Si^+, **1**, a maximum at 304 nm and a shoulder at 370 nm. The tailing of the 370 nm absorption into the visible region causes the dark yellow color of the solutions and of the salts of the Mes_3Si^+ cation.[4,49] The silylium cation absorbs at shorter wavelength than triphenylmethylium Ph_3C^+, which exhibits two peaks at 409 and 428 nm in conc. sulfuric acid.[165] The ultraviolet spectrum of trimesitylstannylium TPFPB, (**65**/TPFPB), in benzene showed clear maxima at 286 and 398 nm.[4] The latter is at slightly longer wavelength than the longest wavelength silylium absorption (370 nm). These UV data suggest that the conjugation is slightly more efficient in Mes_3Sn^+ than in Mes_3Si^+ most probably due to the better alignment of the mesityl substituents with the empty π-orbital at the central element in the stannylium ion.[4]

The stannylium ion Tip_3Sn^+, **68**, was investigated by Mössbauer spectroscopy.[166] The resonance spectra consist of a doublet indicating the axial symmetry of the stannylium ion. The quadropole coupling (QS) for **68** of $5.534 \pm 0.011\ mm\ s^{-1}$ is among the largest such values yet reported for an organotin complex and can be compared with the QS values for Me_3Sn^+ in HSO_3F (QS = 4.95) for which a trigonal-bipyramidal coordination is established.[43,45] The isomer shift (IS) is $1.875 \pm 0.011\ mm\ s^{-1}$, at the higher end of the shift range for Sn(IV) compounds [IS(Sn(IV)) = −0.5–2.5 $mm\ s^{-1}$]. This value is consistent with the presence of one 5s electron, expected for a Sn atom with sp^2 hybridization and predominant covalent metal–ligand bonding interaction. The metal atom motion in a temperature range between 90 and 170 K is isotropic within experimental error of the Mössbauer data, which is surprising in regard of the highly anisotropic bonding situation in the trigonal planar coordination environment of the Sn atom in $Tips_3Sn^+$, **68**.[166]

D. *Solid State Structure of R_3E^+ Cations and Related Species*

1. Solid State Structure of R_3E^+ Cations

Until the year 2002 no experimental data existed on the structures of unperturbed R_3E^+ cations, the exact analogues of the carbenium ions. Computational data combined with NMR chemical shift calculations, which could be compared to experiment, were the only source of reliable structural information for silylium ions[6,7,13,77,121] while for germylium, stannylium and plumbylium ions this combined approach was not attractive due to either the non-existence of the experimental data (Ge) or the complexity of the computational problem (Sn, Pb). On the other hand, a series of excellent experimental studies demonstrated, for example, the high coordination tendency of small trialkylsilylium ions either toward the counteranion[38,114,127,138] or toward the solvent.[36,37,67,116,127] The solid state structures of these silyl cation salts showed clear indications either of cation/anion or cation/solvent coordination. Thus, the nature of the observed cation, i.e. the degree of silylium ion character remained disputable.[10,11,13]

One strategy to overcome these problems is to increase the steric bulk around the cationic center in order to minimize intermolecular interactions. However, the

classical hydride transfer reaction also is severely hampered when the steric congestion of the substrate is increased. Therefore, novel synthetic strategies had to be found, which shifts the reactive side from the center of the incipient cation to the periphery of the molecule.

These requirements were perfectly met for the first time by the synthesis of trimesitylsilylium Mes_3Si^+, **1**, by the allyl fragmentation reaction by Lambert and coworkers (see Section II.C).[4,5] Their NMR characterization of the silylium ion and consecutive computational studies indicated that Mes_3Si^+ is the first example for a silylium ion unfettered by any interaction with neighbouring groups solvents or counteranions. In the NMR work the $TPFPB^-$ anion was used, well known for its inertness but also well known for its tendency to form oils intractable to crystallization. In contrast, with the brominated carboranate anion $[HCB_{11}Me_5Br_6]^-$ as counteranion the groups of Reed and Lambert obtained yellow crystals of the benzene solvate of the salt $[Mes_3Si][HCB_{11}Me_5Br_6]$.[49] The crystal structure revealed well separated molecules. No atoms of the carboranate or benzene approach the Si atom closer than 600 pm. The closest approaches to the Mes_3Si^+ cation arise from methyl–methyl group non-bonded interactions rather than from the more electron-rich bromine atoms of the carborane anion or the π-system of benzene. The mesityl groups in Mes_3Si^+ have a propeller-like arrangement around the trigonal planar Si center with twist angles of 51.3, 54.5 and 41.9° relative to the coordinate plane (see Fig. 3). The planar coordination geometry is indicated by summation of the three C–Si–C angles to 359.9°, within experimental error (0.2°) of 360°. As expected, the Si–C bonds (average, 181.7 pm) are significantly shorter than those observed in the neutral tetrahedral trimesitylallylsilane precursor (average, 191 pm).[5] Despite the large twist angles, the aryl rings show a marked dactylic bond length alternation, typical for conjugating interactions between the aryl substituent and the electron-deficient silicon atom (see Fig. 3). The solid state ^{29}Si NMR chemical shift of $[Mes_3Si]$ $[HCB_{11}Me_5Br_6]$ agrees well with the solution value for the TPFPB salt ($\delta^{29}Si = 226.7$ vs $\delta^{29}Si = 225.5$). This demonstrates that in solution as well as in the solid state the structure of Mes_3Si^+ is the same. No structural indication for internal solvation or agostic interaction is found in the experimental geometry of the Mes_3Si^+ cation,[49] in agreement with the conclusions from a previous theoretical study.[6] In general, the previously calculated structures at the density functional level

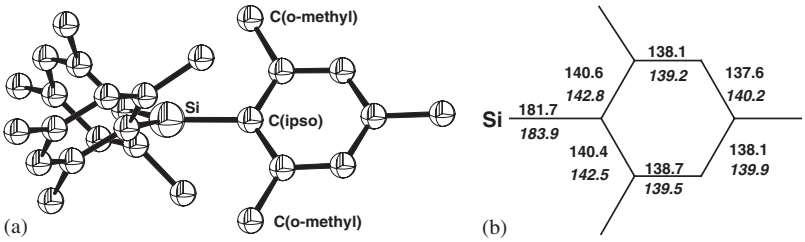

FIG. 3. (a) Perspective view of the Mes_3Si^+ cation. Thermal ellipsoids are drawn at the 50% probability level, for further details see text and Table XIII. (Reprinted with permission from Ref. 49. Copyright 2002, AAAS.) (b) Comparison between experimental and calculated (italic, at the B3LYP/6-31G(d) level of theory) bond lengths [pm] in Mes_3Si^+ (from Refs. 49 and 6).

of theory[6,7] match well the experimental solid state structure of Mes_3Si^+, the differences between the calculated and experimental bond lengths being smaller than 1.2%.[6,7,49] This good agreement between experimental and theoretical structure is reflected also by the correspondence between the ^{29}Si NMR chemical shifts measured in solution and in the solid state and the computed ^{29}Si NMR chemical shift ($\delta^{29}Si = 226-230$).[6,7]

Trismesitylgermanium, **76**, and trismesitylstannylium, **65**, have been prepared as their TPFPB salts however, no experimental structure is reported.[4] For the TPFPB salt of the related stannylium ion Tip_3Sn^+, **68**, suitable crystals for X-ray analysis were obtained and the crystal structure was solved.[48] The stannylium ion and the TPFPB anion are well separated, no atom of the anion approaches the cation to within 400 pm. The molecular structure of the stannylium ion Tip_3Sn^+ parallels in many features closely that of Mes_3Si^+. That is, the aryl groups are twisted in the usual propeller fashion from the plane of the tin atom and its three attached carbon atoms. The twist angle is 61.1°, larger than found for Mes_3Si^+ due to the larger *ortho* substituent in Tip_3Sn^+ (*i*-pr vs. Me) being 61.1°. The sum of the C–Sn–C angles is 359.9(2), which indicates planarity of the central SnC_3 group (Fig. 4). No structural evidence for interaction between the isopropyl-H atoms and the tin center is found.[48] The average Sn–C bond length in Tip_3Sn^+ is 211.1 pm, somewhat shorter than found for the Sn–C bonds in $(o\text{-tol})_4Sn$ (215.2 pm).[167]

The next landmark was the synthesis of the germylium, **22**, and the stannylium ion, **23**, by one-electron oxidations from the corresponding stable radicals with trityl TPFPB by Sekiguchi and co-workers. As in the case of the allyl cleavage to generate the mesityl-substituted cations, the reaction, in this case the oxidation, occurs at the periphery of the molecule and gives the possibility for efficient steric protection of the incipient cation. Both trivalent cations were obtained as their TPFBP salts and the crystal structure show well separated anions and cations.

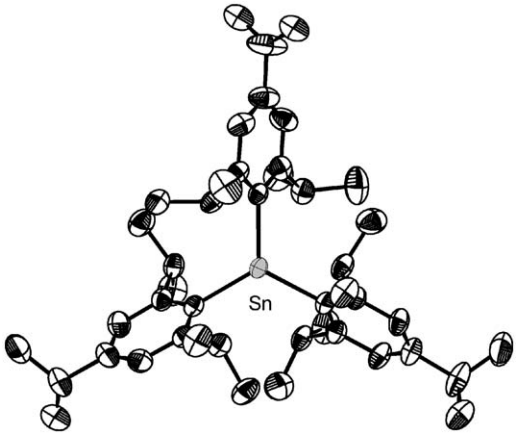

FIG. 4. Molecular structure of Tip_3Sn^+. Thermal ellipsoids are drawn at the 50% probability level, for details see text and Table XIII.[48]

In both structures the element atom has an essentially planar environment, which indicates for the cations **22** and **23** perfect trigonality (see Fig. 5). The average Ge^+–Si bond in **22** is longer [251.95(10) pm] than a regular Ge–Si bond (238.4–246.2)[168] and it is also longer than in the radical $(t\text{-Bu}_2\text{MeSi})_3\text{Ge}^\bullet$ [245.35(4) pm] and the anion $(t\text{-Bu}_2\text{MeSi})_3\text{Ge}^-$ [243.32(10) pm]. This unexpected decrease of the Ge–Si bond length in the cation/radical/anion triple was explained by negative [Ge(4p)→σ*(Si–C)] hyperconjugation in the anion and the radical, which cannot be active in the cation **22**.[72] In contrast, the average Sn^+–Si bond in **23** is in the usual range [268.63(8) pm] for Si–Sn bonds (256.1–278.9 pm)[71,167] although also the Si–Sn bonds in the radical $(t\text{-Bu}_2\text{MeSi})_3\text{Sn}^\bullet$ are shorter [261.76(5) pm].

Historically, the first solid state structure of a truly tricoordinated cation of the heavier group 14 elements (Si–Pb) was that of the cyclotrigermenium cation $[((t\text{-Bu}_3\text{Si})\text{Ge})_3]^+$, **2** published in 1997.[9] Cation **2** was prepared by one-electron oxidation of the cyclotrigermene **20** (E = Si) with trityl cation (see Scheme 8).[9,64–67]

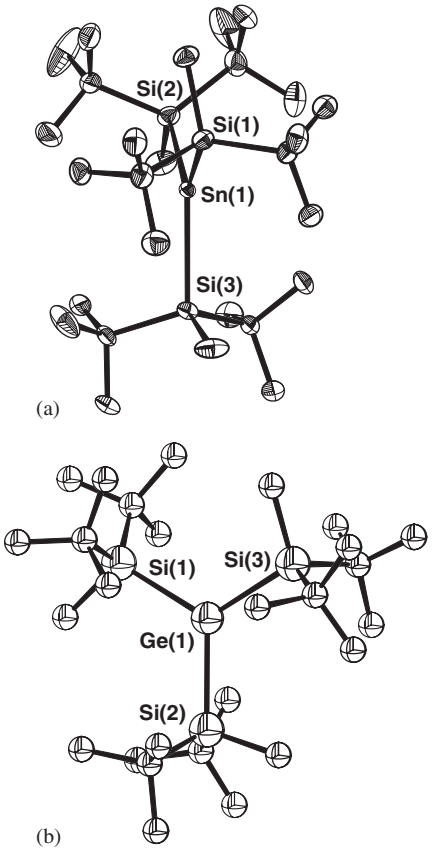

FIG. 5. Molecular structures of (a) $(t\text{-Bu}_2\text{MeSi})_3\text{Sn}^+$, **23**, and (b) of $(t\text{-Bu}_2\text{MeSi})_3\text{Ge}^+$, **22**. Thermal ellipsoids are drawn at the 30% probability level, for details see text and Table XIII. (Reprinted from Ref. 71. Copyright 2003, American Chemical Society and reprinted from Ref. 72. Copyright 2003, Wiley-VCH.)

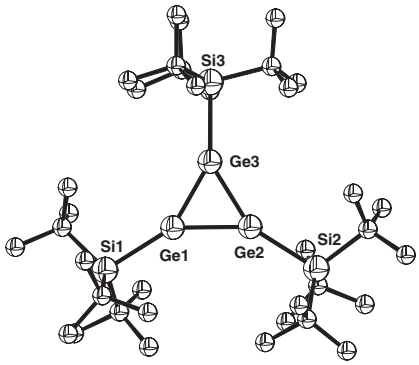

FIG. 6. Molecular structure of tris(tri-*t*-butylsilyl)cyclotrigermenium [*t*-$Bu_3SiGe)_3^+$], **2**. Hydrogen atoms are omitted for clarity. Mean innercyclic bond angle Ge–Ge–Ge: 60.01°, for more data see Table XIII. (Reprinted with permission from Ref. 9. Copyright 1997, AAAS.)

The originally used TPB^- counteranion proved to be unstable in the presence of the cation in methylene chloride solutions at temperatures above −78 °C.[65,66] Therefore, salts with different fluorinated borate counteranions were prepared and crystal structures are reported for the TPB^{-9} (see Fig. 6), $TFPB^{-}$[64–66] and $TSFPB^{-}$[66] salts.

All crystal structures of the cyclotrigermenium cation **2** reveal a free germyl cation with a two π-electron system. The three germanium atoms form an equilateral triangle (mean Ge–Ge distance 233.1 pm, mean innercyclic bond angle GeGeGe : 60.0°). The Ge–Ge bond length observed for **2** is intermediate between the Ge═Ge double bond and the Ge–Ge single bond of the cyclotrigermene **20** (E = Si). The sum of the bond angles around the ring germanium atoms is 359.9°, which indicates planarity of the $(SiGe)_3$ moiety in **2**. These structural features indicate delocalization of the positive charge over the three-membered germanium cycle similar to its carbon analog, the cyclopropenium ion. In agreement, quantum mechanical calculations indicate for the parent cation [$(HGe)_3^+$] a very similar structure [r(GeGe) = 236.1 pm using a B3LYP hybrid density functional and basis sets of triple zeta quality] and a stabilization energy which is ~50% of that of the cyclopropenium ion.[169] Recently, a preliminary communication appeared, which reports the preparation of the analogous cyclotrisilenium cation [((*t*-$Bu_3Si)Si)_2$(*t*-$BuMe_2Si)^+$] which is characterized by an average innercyclic Si–Si bond length of 221.7(3) pm.[170]

The reaction of cyclotrisilene **15** with the silylated benzenium ion $[Et_3Si/C_6H_6]^+$ results in the formation of the cyclotetrasilenylium ion **3** (see Scheme 6). The solid state structure of silyl cation **3** indicates its homoconjugative nature (see Fig. 7 and Table XIII).[8]

The central four-membered ring of cation **3** is folded and the dihedral angle between the Si1–Si2–Si3 and Si1–Si4–Si3 planes is 46.6°. The bond angles at the silicon atoms in the four-membered ring suggest that the silicon atoms Si1, Si2 and Si3 (mean Σ°Si = 359.8, see Table XIII) have a completely planar trigonal geometry and Si4 has a distorted tetrahedral environment. The Si–Si bonds of the cationic

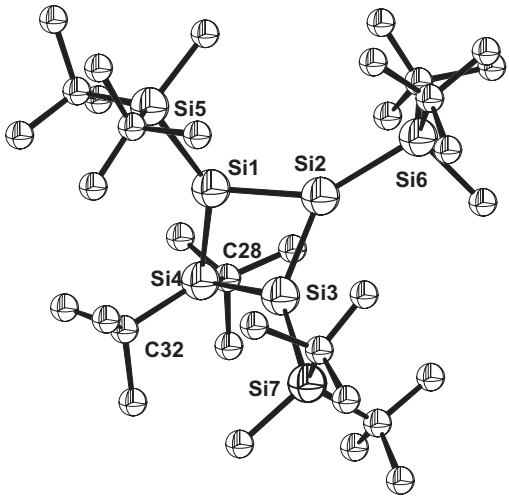

FIG. 7. ORTEP drawing of cyclotetrasilenium **3**. Hydrogen atoms are omitted for clarity. Selected bond lengths (pm) (see also text and Table XIII): Si1–Si4 = 2.336 (2), Si3–Si4 = 2.325 (2). (Reprinted with permission from Ref. 8. Copyright 2000, American Chemical Society.)

TABLE XIII
STRUCTURAL DATA FOR R_3E^+ CATIONS[a]

Compound	d(R–E) (pm)	$\Sigma\alpha$(RER)[b] (deg)	Coordination number	Ref.
$[Mes_3Si^+][HCMe_5Br_6^-]$	181.7	359.9	3	49
$[Tip_3Sn^+][TPFPB^-]$	211.1(4)	359.9(2)	3	48
$[(t\text{-}Bu_2MeSi)_3Ge^+][TPFPB^-]$	251.95(10)	359.9	3	72
$[(t\text{-}Bu_2MeSi)_3Sn^+][TPFPB^-]$	268.63(8)	360.0	3	71
$[(t\text{-}Bu_3SiGe)_3^+][TBP^-]$	232.6(4)[c] 244.3(9)[d]	359.8(2)	3	9
$[(t\text{-}Bu_3SiGe)_3^+][TFPB^-]$	233.5(2)[c] 243.8(3)[d]	358.9(1)	3	64–66
$[(t\text{-}Bu_3SiGe)_3^+][TSFPB^-]$	233.25(8)[c] 243.7(1)[d]	359.94(4)	3	66
$[(t\text{-}Bu_2MeSi)_3^+SiBu\text{-}t_2]$ $[TPFPB^-]$	224.2, 233.1	359.72(8)	3	8

[a]Structural data from X-ray analysis.
[b]Sum of the three bond angles of the element and its three nearest substituents, tetrahedral: $\Sigma = 328.5^\circ$ trigonal planar: $\Sigma = 360^\circ$.
[c]Innercyclic Ge–Ge distance.
[d]Exocyclic Ge–Si distance.

part [Si1–Si2 = 224.0(2) pm and Si2–Si3 = 224.4(2) pm] are intermediate between the Si═Si double bond [213.8(2) pm] and the Si–Si single bond [236.4(3) and 235.2(3) pm] of the precursor **15**.[171] The interatomic distance between Si1 and Si3 is relatively short, 269.2(2) pm, only 15% longer than a normal Si–Si single bond (236 pm).[172] This indicates a possible 1,3-orbital interaction in cation **3**, which is

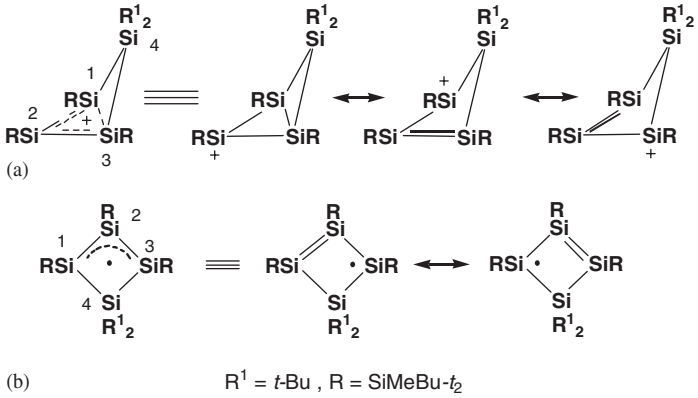

FIG. 8. (a) Homoaromatic 2π-electron conjugation in silyl cation **3**. (b) Allyl-type resonance in 3π-electron radical **26**.[8,74]

supported by the ^{29}Si NMR spectroscopic data (see Section III.B.1.b). Upon reduction of cation **3** to the cyclotetrasilenyl radical **26**, the central Si1/Si3 distance increases (Si1/Si3 322.5(2) pm) and the four-membered ring becomes almost planar with a folding angle of 4.7°.[74] This comparison indicates that homoconjugative effects determine the structure of the 2π-electron cation **3**, while allylic conjugation is important for the 3π-electron radical **26** (see Fig. 8).

2. Solid State Structure of Intramolecularly Stabilized R_3E^+ Cations

The high electrophilicity of the positively charged element can be modified by intramolecular donation from remote donor substituents. This interaction leads to solvent-free cations with coordination numbers for the positively charged element >3 and to a considerable electron transfer from the donor group to the element. Frequently used donor substituents utilize heteroatoms with lone pairs (e.g. amino, hydrazino, methoxy, carboxy, phosphino, etc.), in many cases in combination with pincer-type topology of the ligand, for the stabilization of the cationic center.[173] These strongly stabilized cations are beyond the scope of this review and instead we will concentrate on few examples where we have weak donors such as CC multiple bonds, which stabilize the electron-deficient element atom.

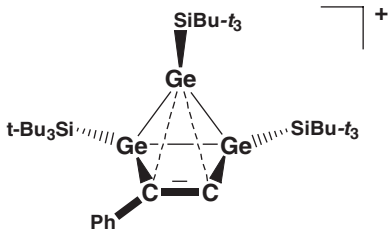

6

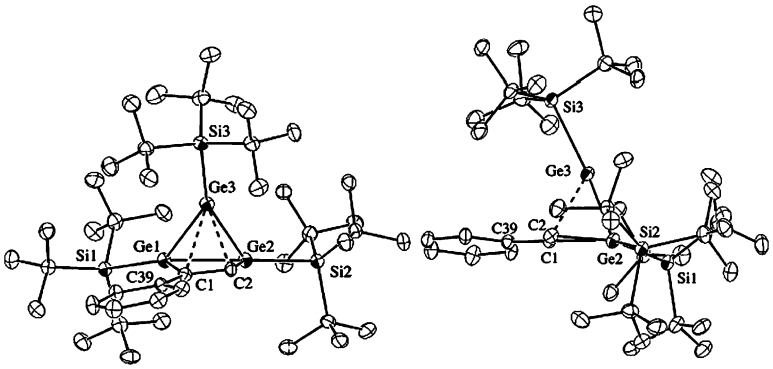

FIG. 9. ORTEP drawing of **6**, left front view on the Ge_3 cycle, right side view. Hydrogen atoms are omitted for clarity. Selected bond lengths (Å): Ge1–Ge2 = 247.65(10), Ge1–Ge3 = 246.71(10), Ge2–Ge3 = 247.40(10), Ge3–C1 = 241.5(7), Ge3–C2 = 225.4(7), C1–C2 = 141.1(9). Selected bond angles (deg): Ge1–Ge2–Ge3 = 59.78(3), Ge2–Ge3–Ge1 = 60.16(3), Ge3–Ge1–Ge2 = 60.06(3). (Reprinted with permission from Ref. 21. Copyright 2003, American Chemical Society.)

A intriguing example for the intramolecular interaction between an germylium ion and a remote C═C double bond was recently provided by Sekiguchi and coworkers.[21] The bishomocyclopropenylium-type cation **6** was synthesized by halogen abstraction from the corresponding germyl bromide **5** (see Scheme 1) and the crystal structure of the TPFPB salt of **6** was determined by X-ray crystallographic analysis (Fig. 9). The germyl cation **6** has a highly strained "housene"-type skeleton, which consists of a Ge_3 equilateral triangle and a Ge_2C_2 four-membered ring. The ridge Ge3 atom is strongly bended towards the C1═C2 double bond with a folding angle between the Ge_3 plane and the mean Ge_2C_2 plane of 67°. This folding results in short Ge3–C1 [241.5(7) pm] and Ge3–C2 [225.4(7) pm] interatomic distances, clearly below the sum of the van der Waals radii of Ge and C(sp^2). In addition, the C1═C2 bond [141.1(9) pm] is considerably longer than a regular C═C double bond in related compounds (135.7 pm[174]). These structural particularities of cation **6** indicate the effective interaction between the empty 4p-orbital on the Ge atom and the π-orbital of the C═C double bond. A natural bond analysis based on a structure of the silyl-substituted model compound for cation **6**, which was optimized at the density functional B3LYP/dzp level of theory, indicates appreciable electron transfer from the C1═C2 double bond to the formally empty 4p orbital at Ge3 (occupancy 0.42 electrons) and predict Wiberg bond orders for the Ge3–C1, Ge3–C2 and C1–C2 bonds of 0.37, 0.46 and 1.39, respectively. In addition, nucleus independent chemical shift calculations [NICS(1)] for the silyl-substituted model compound indicate a diatropic ring current in **6**. Thus, structural as well as theoretical evidence is provided for the 2π-bishomoconjugative nature of cation **6**. Additional support comes from the ^{13}C NMR spectroscopic data (see Section III.B.4).

The stannyl cation in zwitterion **80** is only stabilized by side-on coordination with the remote C≡C triple bond. The crystal structure of **80** revealed a pyramidalized tin center with the sum of valence angles of 351.1° (see Table XIV). The coordination of the tin atom to the C≡C triple bond is unsymmetrical and the SnC distances

TABLE XIV
STRUCTURAL DATA OF INTRAMOLECULAR COORDINATED R_3E^{+} [a]

Compound	d(R–E) (pm)	Σα(RER)[b] (deg)	d(E–X)[c] (pm)	Coordination number	Ref.
74[TPFPB]	221.1(15), 227(2) 231.0(19)	360.0	293.4(14), 285.5(14) 288.9(17), 287.5(15)	3 + 2	53
73[TPFPB]	221.4(4), 221.9(5) 222.3(4)	359.97(16)	296.9(5),298.9(4) 250.6(5)	3 + 2	40
81	220.3(3), 222.2(7) 220.6(7)	355.7(3)	264.8(6), 246.7(6)	3 + 1	161
80	211.6(4), 212.8(5) 213.6(5)	351.1	233.9(4), 252.3(5)	3 + 1	158
6[TPFPB][e]	247.65(10), 247.40(10)[d], 247.2(2)[f]	359.2(5)	225.4(7), 241.5(7)	3 + 1	21
	246.81(10), 247.54(10)[d], 247.1(2)[f]	359.2(5)	225.0(7), 239.6(6)	3 + 1	21

[a]Structural data from X-ray analysis.
[b]Sum of the three bond angles of the element and its three nearest substituents, tetrahedral: $\Sigma = 328.5^{\circ}$, trigonal planar: $\Sigma = 360^{\circ}$.
[c]Distances to the fourth and fifth substituent, in the case of multiple bonds both centers are given.
[d]Innercyclic Ge–Ge distance.
[e]Two independent molecules in the unit cell.
[f]Exocyclic Ge–Si distance.

(264.8, 246.7 pm) are too long for a regular SnC bond [210 pm for SnC(sp)], but are well below the sum of the van der Waals radii of Sn and C(sp). The direct bonding relation between the cationic tin and the C≡C triple bond is also apparent from the sizeable ^{1}J(SnC) couplings detected by NMR spectroscopy.[158]

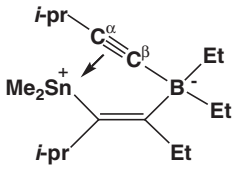

80

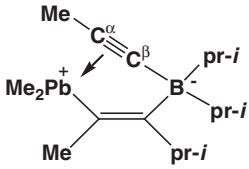

81

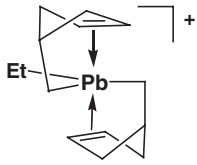

74

The closely related lead analogue **81** shows essentially the same structural features, but the lead atom in **81** is less pyramidalized (355.7°, see Table XIV), which indicates weaker coordination. The NMR spectroscopic parameters for **81**, such as ^{207}Pb NMR chemical shift and scalar Pb–C(sp) coupling constants (see Section III.B.3) clearly demonstrate however the side-on complexation of the plumbyl cation by the C≡C triple bond in zwitterions **81**.[161]

The ''spironorbornyl cation'' **74** is best described as an intramolecular bisalkene complex of a plumbylium ion (see Fig. 10 and Table XIV).[53] The Pb atom in cation **74** has a distorted trigonal–bipyramidal coordination geometry (Fig. 10b). The planarity of the trigonal base is indicated by summation of the three C–Pb–C angles

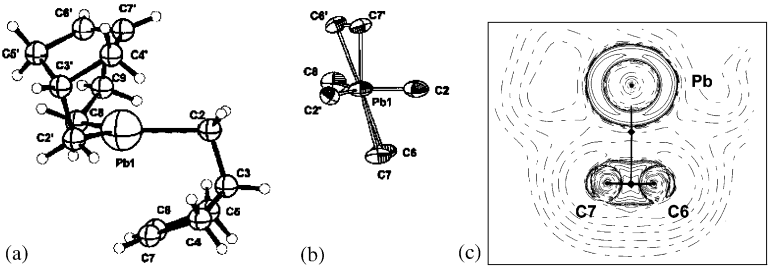

FIG. 10. Molecular and electronic structure of cation **74**. (a) Perspective view on the cation **74**. (b) Coordination sphere of the Pb atom, selected interatomic distances (pm) and angles (deg): Pb–(center C6′, C7), 281.7; Pb–(center C6; C7′), 280.7; Pb1–C2, 227(2); Pb1–C2; 221.1(15); Pb1–C8, 231.0(19); C6–C7, 133(2); C6′–C7′; 132(2); (center C6, C7)–Pb–(center C6′, C7′), 163.6. (c) Contour plots of the Laplacian distribution $[\nabla^2\rho(r)]$ in the plane containing the atoms Pb, C6 and C7. Solid and dotted lines designate regions of local charge concentration and depletion, respectively. The bond paths are indicated by the solid back lines, bond critical points are marked with a black square. (Reprinted with permission from Ref. 53. Copyright 2003, Wiely-VCH.)

to 360.0°. The coordination sphere of lead is completed by the C═C double bonds of the two cyclopentenemethyl substituents, which take up the apical positions. The steric requirements of this intramolecular interaction enforce the deviations from the ideal trigonal–bipyramidal coordination. This spatial arrangement places seven carbon atoms at distances less than 290 pm around the positively charged Pb atom. A topological "atoms in molecules" analysis of the electron density for cation **74** (see Fig. 10c) reveals a T-shaped electron density distribution between the Pb atom and the C═C double bond, typical for π-type complexes between strong Lewis acids and C═C multiple bonds.[53]

The related intramolecular monoalkene complexes of R_3E^+ cations, the norbornyl cations of group 14 elements (Si → Pb), have been synthesized with TPFPB as counteranion and characterized by NMR spectroscopy in solution supported by quantum mechanical calculations.[40] Only the acetonitrile complex, **73**, of the plumbanorbornyl cation **13** could be characterized by X-ray crystallography. Similar to the structure of the plumbyl cation **74**, the Pb atom in the acetonitrile complex **73** adopts a trigonal–bipyramidal coordination sphere with the C═C double bond and the acetonitrile in the apical positions and the Pb atom in the center of the trigonal plane (see Fig. 11 and Table XIV, for details).[40]

3. Solid State Structure of Cation/Anion Aggregates of R_3E^+ Cations

The solid state structure of most carborane salts deriving from hydrocarbon solutions is dominated by cation/anion interactions. For example the *n*-Bu_3Sn^+ salt of the permethylated carborane $[CB_{11}Me_{12}]^-$ forms infinite columns of alternating *n*-Bu_3Sn^+ and $[CB_{11}Me_{12}]^-$ ions,[68] similar to those of covalent R_3SnX compounds. This alignment which results in a trigonal–bipyramidal coordination sphere for the Sn atom with two apical positions occupied by methyl groups of the anion (see Fig. 12 and Table XV). In contrast to the neutral tin(IV) compounds where strong covalent interactions give short SnX bonds, the average axial distance between the

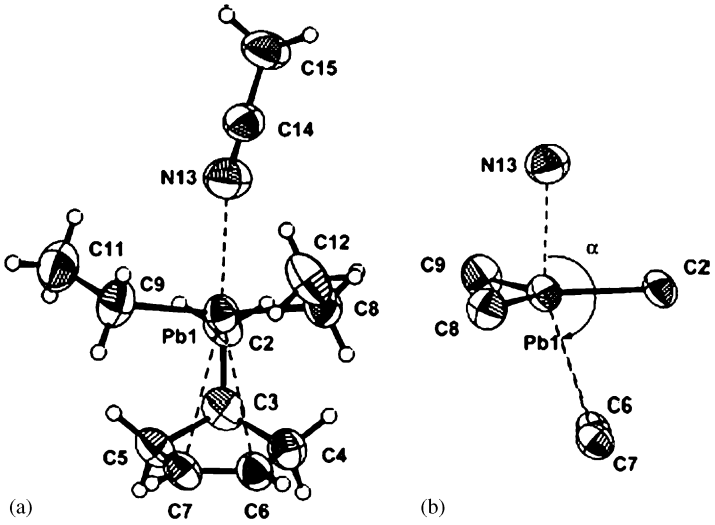

FIG. 11. (a) Molecular structure of cation **73** in the crystal. (b) Coordination sphere of the Pb atom in cation **73**. Selected bond lengths (pm) and bond angles (deg): Pb1–C2, 222.3(4); Pb1–C8, 221.9(5); Pb1–C9, 221.4(4); Pb–(center C6, C7), 290.4; Pb1–N13, 250.6(5); C6–C7, 132.7(5); (center C6, C7)–Pb–N13, 159.0; N13–Pb–C2, 86.80(14). (Reprinted with permission from Ref. 40. Copyright 2003, American Chemical Society.)

Sn atom and the methyl carbon atoms of the anion are large (281 pm), clearly longer than a covalent Sn–C bond (214 pm) but much shorter than the sum (417 pm) of the van der Waals radii of a methyl (200 pm) and tin (217 pm).[175]

The tin atom in $[n\text{-}Bu_3Sn^+][CB_{11}Me_{12}^-]$ is displaced from the center of the trigonal plane toward one of the anions by 3.2 pm, which results in a pyramidalization of the $n\text{-}Bu_3Sn^+$ cation. This is also indicated by the sum of the C–Sn–C angles, which is clearly smaller than the 360° expected for planarity of the $n\text{-}Bu_3Sn^+$ cation.[68] Similar structures have been recently found for the $[CB_{11}Me_{12}^-]$ salts of the most simple organometallic cations of germanium, tin and lead, Me_3E^+ (E = Ge, Sn, Pb). The cations were synthesized from the hexamethyldielement compounds (Ge, Sn) or from Me_4Pb by reaction with the one-electron oxidant $[CB_{11}Me_{12}]^\bullet$ in pentane.[69] The obtained amorphous white solids, insoluble in hydrocarbons, were investigated by trapping experiments and by NMR spectroscopy. Significant structural information was obtained from an EXAFS study. Two sets of E–C distances, a short one and a long one, were found by EXAFS of the salts $[Me_3E^+][CB_{11}Me_{12}^-]$ (E = Ge, Sn, Pb). The first-shell peak is assigned to the methyl carbon directly attached to the metal. As expected, it moves progressively to longer distance on going from Ge to Sn and to Pb (194, 212 and 217 pm, respectively; see Fig. 13 and Table XV). This M–C^α-(sp^3) distance is for Sn and in particular for Pb shorter than a normal M–C^α-(sp^3) bond (194.5 (Ge–C), 214 (Sn–C) and 225 pm (Pb–C)[151]). The precision of EXAFS is typically 0.4 pm,[176] therefore this small difference is significant. For all three cations, the longer E–C distances (250–300 pm) can only be interpreted as the distance between the Me_3E^+ cation and the carbon atom of a

FIG. 12. Part of an infinite column of alternating cations and anions as a detail of the crystal structure of [*n*-Bu_3Sn^+][$CB_{11}Me_{12}$]. Thermal ellipsoids are drawn at 50% probability level. Hydrogen atoms and one component of the disordered butyl groups are omitted for clarity, Sn and B atoms are gray and C atoms are black. (Reprinted with permission from Ref. 68. Copyright 2000, American Chemical Society.)

methyl group of the $CB_{11}Me_{12}^-$ anion with which the cation interacts. These distances are longer than the normal M–C bond lengths but are much shorter than the sum of van der Waals radii of Ge (200 pm), Sn (217 pm) or Pb (220 pm) and of a methyl group (200 pm).[175] The cation/anion interaction energy decreases from Ge to Pb and as a consequence different structures are adopted. In Fig. 13 possible structures on the basis of the EXAFS analysis for all three salts are shown.

For [Me_3Pb^+] [$CB_{11}Me_{12}^-$] a nearly symmetric, trigonal–bipyramidal arrangement for the Me_3Pb^+ cation with rather weak coordination to the two axial methyl groups provided by the $CB_{11}Me_{12}^-$ anions is suggested. In contrast, for the tin compound a clearly unsymmetrical coordination sphere with the Sn atom displaced from the center of the trigonal plane along the central axis, which leads to two different Sn–Me(anion) distances is proposed. The EXAFS analysis for the germanium compound indicates the formation of discrete anion/cation aggregates and the most likely coordination sphere for the germanium is a distorted tetrahedral environment (see Fig. 13).

In a series of papers Reed and colleagues present the solid state structures of a series of simple trialkyl-substituted silyl cations with halogenated carborane anions

TABLE XV
STRUCTURAL DATA FOR COMPOUNDS OF THE TYPE $[R_3E^+]$ [ANION] AND OF $Ph_3SiOClO_3$ FOR COMPARISON[a]

Compound	D(R–E) (pm)	Σα(RER)[b] (deg)	d(E/3R)[c] (pm)	d(E–X)[d] (pm)	Coordination number	Ref.
$[Me_3Ge][CB_{11}Me_{12}]$[e]	194			249	4	69
$[Me_3Sn][CB_{11}Me_{12}]$[e]	212			277, 302	3+2	69
$[Me_3Pb][CB_{11}Me_{12}]$[e]	217			290	3+2	69
$[Bu_3Sn][CB_{11}Me_{12}]$[f]	207	353	3.2	281	3+2	68
$[Bu_3Sn][CB_{11}Me_{12}]$[e]	216			276	3+2	69
$[(i\text{-}pr_3Si)][Cl_6CB_{11}H_6]$	184.8(9)	351.8(4)	3.07	232.3(3)	4	38
$[(i\text{-}pr_3Si)][Br_6CB_{11}H_6]$	186(2)	351.0(13)	3.00	247.9(9)	4	114, 138
$[(i\text{-}pr_3Si)][I_6CB_{11}H_6]$	188.3(21)	346.8(9)	4.00	266.1(6)	4	38
$[Et_3Si][Br_6CB_{11}H_6]$[g]	183(2)	345.0(10)	4.19	244.4(7)	4	114
	184(2)	349.0(9)	3.48	243.0(6)	4	114
$[(t\text{-}Bu_3Si)][Br_6CB_{11}H_6]$	189(2)	348.7(7)	3.71	246.5(5)	4	114
$[(t\text{-}Bu_2MeSi)][Br_6CB_{11}H_6]$	186(4)	345.8(7)	4.08	246.6(12)	4	114
$[i\text{-}pr_3Si][Br_5CB_9H_5]$	347.4(20)		4.0	182(2)	4	127
$Ph_3SiOClO_3$	184.6(5)	340.5(2)	4.79	174.5(5)	4	177

[a]Structural data from X-ray analysis if not indicated otherwise.
[b]Sum of the three bond angles of the element and its three nearest substituents, tetrahedral: $\Sigma = 328.5^\circ$, trigonal planar: $\Sigma = 360^\circ$.
[c]Distance of the element and the plane spanned by the atoms in α-position.
[d]Distance to the fourth substituent.
[e]EXAFS data.
[f]X-ray data, disordered crystal.
[g]Two independent molecules in the unit cell.

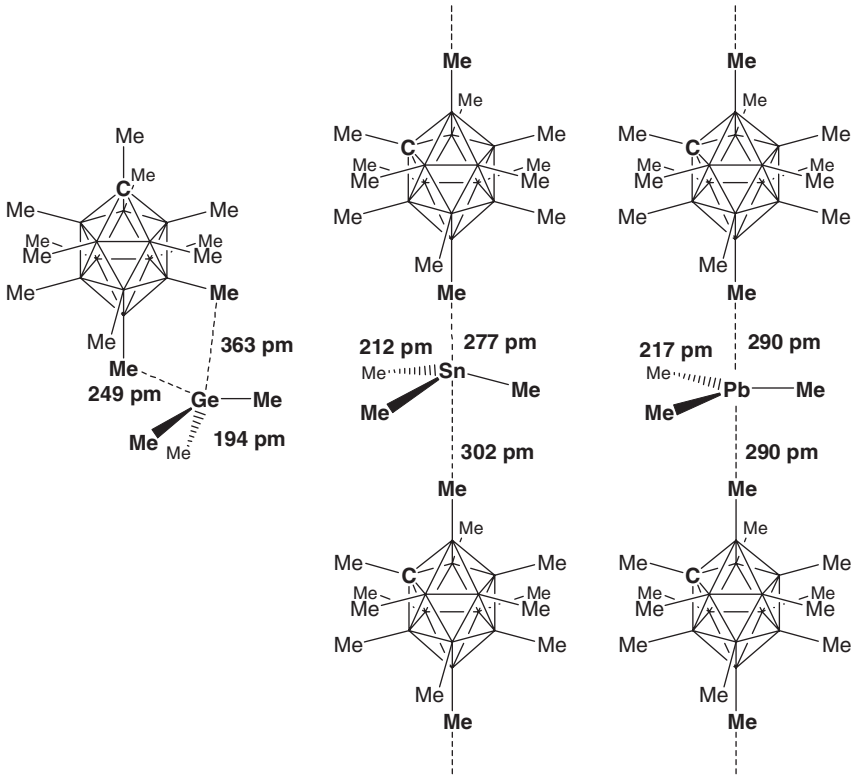

FIG. 13. Possible structures of $[Me_3E]$ $[CB_{11}Me_{12}]$ proposed on the basis of EXAFS results. (a) $[Me_3Ge]$ $[CB_{11}Me_{12}]$, (b) $[Me_3Sn]$ $[CB_{11}Me_{12}]$, (c) $[Me_3Pb]$ $[CB_{11}Me_{12}]$.[69]

(see Table XV and Fig. 14).[11,38,114,127,138] All structures show clear indications of cation/anion interactions, which result in discernible distortions of the R_3Si^+ group from planarity and an effective $3+1$ coordination for the silicon atom. The sum of the bond angles around the silicon atom $\Sigma\alpha$(RSiR) was used to estimate the degree of interaction between silyl cation and the carborane anion. According to this measure, the closest approach to a silylium ion devoid of any distortions was achieved for the *i*-pr_3Si^+ cation and the $[CB_{11}H_6Cl_6^-]$ anion, see Table XV.[38]

4. Solid State Structure of Cation/Solvent Complexes of R_3E^+ Cations

Several solid state structures of R_3E^+(solvent) complexes are known and structural data of significant examples are given in Table XVI. Considerable attention was paid to the structure of the TPFPB salt of the silylated toluenium ion **82** and its interpretation.[36,37,108,126,131,133,135,136] The molecular structure of cation **82** is characterized by a significantly pyramidalized Et_3Si group (sum of the bond angles around Si, $\Sigma\alpha$(Si): 341–342°) and the fourth-coordination side of the silicon atom is occupied by a toluene molecule. The Si–C^{ipso} (toluene) is 217–219 pm, clearly longer

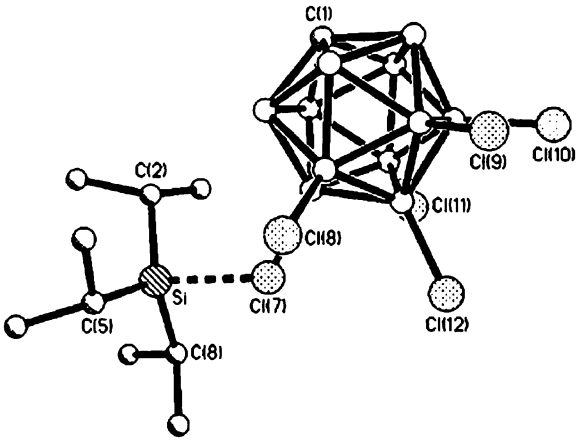

FIG. 14. Perspective view of $[ipr_3Si][CB_{11}H_6Cl_6]$. (Reprinted with permission from Ref. 38. Copyright 1996, American Chemical Society.)

than regular Si–C(aryl bonds (187.9 pm[172]), but also significant smaller than the sum of the van der Waals radii.[36,37]

These features of **82** are typical for many cation/solvent complexes of silylium and germylium ions and they change gradually with the nature of the coordinating solvent and with the cationic group. Hensen's silylated pyridinium iodide **4** with a strongly pyriamidalized trimethylsilyl group and a relatively short Si–N separation marks the strongly coordinating end of this spectrum[20] and the germylated acetonitrilium ion **83**, is, according to the structural data, an example for a more loosely bonded complex.[72] In the nitrilium ion **83**, synthesized by reaction of germylium ion **22** with acetonitrile, the germanium atom is only slightly pyramidalized [$\Sigma\alpha$(Ge): 358.3°] and the Ge/N separation is comparatively large (see Table XVI and Fig. 15).

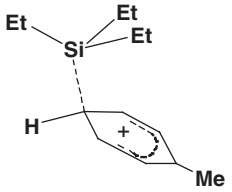

82

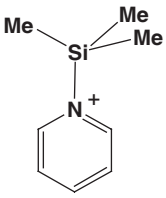

4

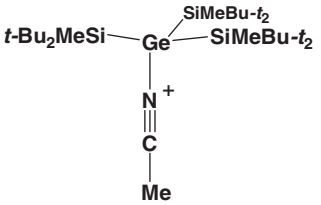

83

While for silyl and germyl cation complexes tetracoordination of the element prevails, stannyl cations favor pentacoordination. That is, the trigonal–bipyramidal environment of the Sn atom in the diwater complex of the stannylium ion Me_3Sn^+ $[Me_3Sn(H_2O)_2]^+$ **84**[178] has its counterpart in the tetrahedral structure of the protonated silanol **85**.[116] The structure of the bis(acetonitrile)tricyclohexyltin hexafluoroantimonate **86** SbF_6[179] reveals pentacoordination for the tin atom,[180] while all

TABLE XVI
STRUCTURAL DATA FOR COMPOUNDS OF THE TYPE $[R_3E^+(\text{solvent})][\text{anion}]$[a]

Compound	d(R–E) (pm)	$\Sigma\alpha$(RER)[b] (deg)	D(E–X)[c] (pm)	Coordination number	Ref.
82 [$TPFPB^-$][d]	185(1)	341.4(5)	219(1)	4	36, 37
	185(1)	342.5(6)	217(1)	4	36, 37
83 [$TPFPB^-$]	252.70(6); 252.10(6)	358.3	201.99(17)	4	72
	256.14(6)				
[(*t*-Bu_3Si)(*t*-BuCN)][$TFPB^-$]	190.1(6)	347.7	182.2(5)	4	67
[(*t*-Bu_3Ge)(*t*-BuCN)][$TFPB^-$]		350.7	197.5(7)	4	67
[(*i*-pr_3Si)(MeCN)][$Br_5CB_9H_5^-$]		346.7(13)	182(2)	4	127
85 [$Br_6CB_{11}H_6^-$]	189.2(15)	348.0(6)	177.9(9)	4	116
[Me_3SiOEt_2][$TFPB^-$]	183.6(5)		177.7(3)	4	126
4 [I^-]	186.7(9)	340.4(5)	185.8(9)	4	20
86 [SbF_6^-]	215.9(3)	359.7(1)	237.4(3), 247.2(3)	5	179
84 [$C_5(CO_2Me)_5^-$]	217.8(12)		229.5(4), 232.6(5)	5	178

[a]Structural data from X-ray analysis.
[b]Sum of the three bond angles of the element and its three nearest substituents, tetrahedral: $\Sigma = 328.5^\circ$, trigonal planar: $\Sigma = 360^\circ$.
[c]Distances to the fourth and fifth substituent.
[d]Two independent molecules in the unit cell.

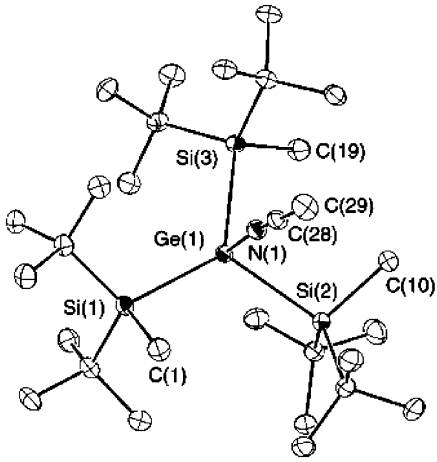

FIG. 15. Molecular structure of nitrilium ion **83** (ORTEP plot, thermal ellipsoids set at 30% probability; hydrogen atoms omitted for clarity). Selected bond lengths (pm) and angles (deg): Ge(1)–N(1), 201.99(17); C(28)–C(29), 144.7(3); Si(3)–Ge(1)–Si(1), 128.682(19); Si(3)–Ge(1)–Si(2) 110.562(19); Si(1)–Ge(1)–Si(2), 119.11(2); N(1)–Ge(1)–Si(1), 92.14(5); N(1)–Ge(1)–Si(2), 92.20(5); N(1)–Ge(1)–Si(3), 98.27(5). (Reprinted with permission from Ref. 72. Copyright 2003, Wiley-VCH.)

structurally characterized germyl and silyl cation complexes with nitriles indicate a tetrahedral coordination of the germanium and silicon atom.

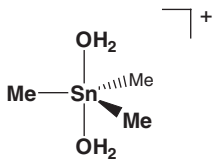

84

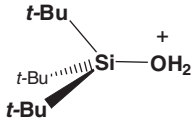

85

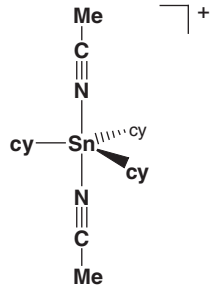

86

IV
A CHEMISTRY OF R_3E^+ CATIONS

The isolation and characterization of stable trivalent cations of the group 14 elements Si, Ge, Sn, which are free of any interaction with solvent, counteranion or neighboring groups, are milestones in organoelement chemistry. These results finally answer the question for the pure existence of these species in the condensed phase. The quest for a chemistry of these highly reactive cations, however remains. Clearly to explore the chemistry of organometallic group 14 cations it is necessary

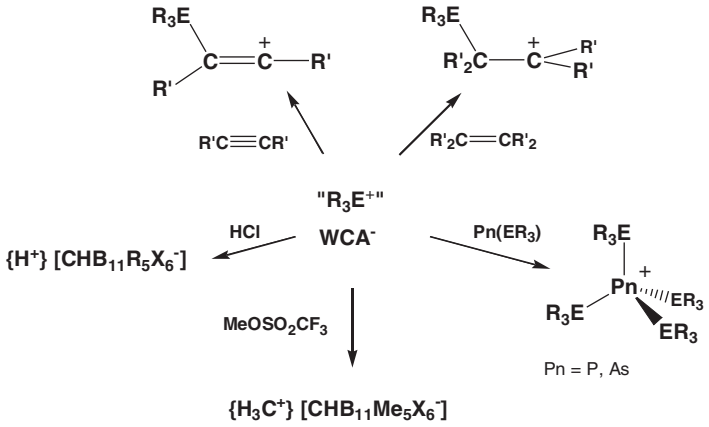

SCHEME 19. Some recent application of organometallic group 14 cations.

to reduce the steric bulk, which was an indispensable prerequisite for the kinetic stabilization and finally isolation of tricoordinated group 14 cations. Consequently, intra- or intermolecular interactions of the cations with electron-donating groups or molecules will be important and a chemistry of cationic R_3E^+ species of group 14 elements will be dominated by either intra- or intermolecular stabilized cations. The electron-donating group or molecule modifies the electron deficiency of the cationic element center and lowers the reactivity. The synthetic challenge is, to find suitable sytems, which allow to control and to exploit the enormous electrophilicity of these cations. Although this chemistry is at its infancy there are already quite spectacular results in various fields. For example, it has been shown that trialkylsilyl arenium ions [R_3Si^+/arene] may react as a synthetic equivalent of trialkylsilylium ions and can be used as highly active silylating agents (Scheme 19). The trialkylsilylium ion adds instantaneously to CC multiple bonds to yield silylated carbenium ions **87**[181] and vinyl cations **88**.[182] Similarly, persilylated onium ions of phosphorus and arsenic **89** are formed by transfer of the trimethylsilyl group from trimethylsilyl arenium to the corresponding phosphanes and arsanes, a reaction which is not possible using conventional trimethylsilylating agents.[126,183] The synthesis of the stable secondary β-trimethyltin-substituted carbocation **90** is thought to proceed by addition of transient trimethylstannylium to the C═C double bond of the propene $(Me_3Si)CH{=}CHCH(SiMe_3)SnMe_3$.[184]

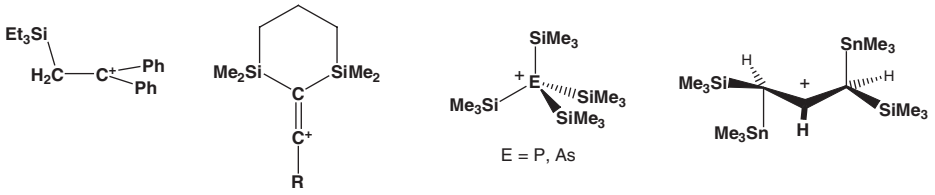

87 88 89 90

Reed and co-workers utilized the silylium carboranate salts to generate novel Brønstedt superacids based on carborane anions as conjugate bases by reaction of the salts with liquid HCl [Eq. (7)].[185] These carborane superacids are able to cleanly protonate C_{60} and benzene at room temperature to yield HC_{60}^{+}[185] and benzenium $C_6H_7^{+}$[186] and are the strongest isolable Brønstedt acids presently known.[187] Similarly, the same group developed the most potent electrophilic methyl transfer agent by reaction of the silyl cation salt $[ipr_3Si^{+}][HCB_{11}Me_5Br_6^{-}]$ with methyltriflate [Eq. (8)].[188] The product $H_3C(HCB_{11}Me_5Br_6)$ abstracts hydride from simple branched alkanes and forms at room temperature the corresponding tertiary carbocations as isolable carborane salts.[189]

$$[Et_3Si]CHB_{11}R_5X_6](s) + HCl(1) \rightarrow Et_3SiCl(g) + H(CHB_{11}R_5X_6)(s) \qquad R = H,\ Me;\ X = Cl,\ Br,\ I \tag{7}$$

$$[i\text{-}pr_3Si][CHB_{11}Me_5Br_6](s) + H_3COSO_2CF_3 \rightarrow i\text{-}pr_3SiOSO_2CF_3 + H_3C(CHB_{11}Me_5Br_6) \tag{8}$$

Owing to the high Lewis acidity the group 14 organometallic cations are polymerization catalysts par excellence.[184,190] Silanorbonyl cations[191] and triethylsilyl arenium[181] have been shown to be efficient catalysts for metal-free hydrosilylation reactions. Chiral silyl cation complexes with acetonitrile have been applied as cata - lysts in Diels Alder-type cyclization reactions[130,192] and intramolecularly stabilized tetracoordinated silyl cations have been successfully used as efficient catalysts in Mukaiyama-type aldol reactions.[193]

The reactions quoted in the last paragraph and partly summarized in Scheme 19, all exploit the high electrophilicity of organometallic group 14 cations, and the reactivity follows conventional routes. Quite recently, however, a novel-type of chemistry for R_3E^{+} cations came into attention. The decisive step in Jutzi's synthesis of η^5-Cp*Si^{+}, **91**, by protonation of decamethylsilicocene, Cp^*_2Si, **28**,[194] is most likely the fragmentation of the intermediate $Cp^*_2Si^{+}$-H cation **29** into the neutral Me_5C_5H and the cation η^5-Cp*Si^{+} (see Scheme 20). The cation **91** can be regarded as synthetic equivalent for the singly coordinated silylidynium η^1-Cp*Si, **92**.

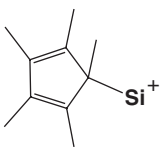

92

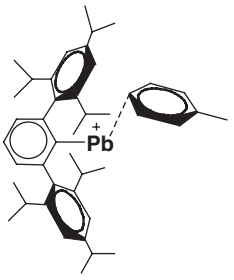

41

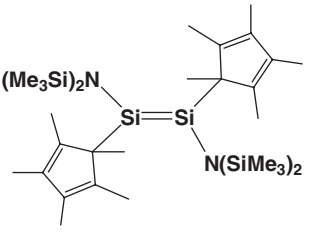

93

This type of α-elimination with the generation of a singly coordinated four-valence-electron compound is rather unusual in silylium ion chemistry, only two

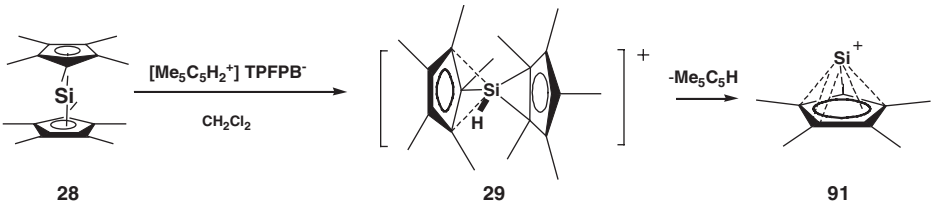

SCHEME 20. Synthesis of η^5-Cp*Si$^+$.[194]

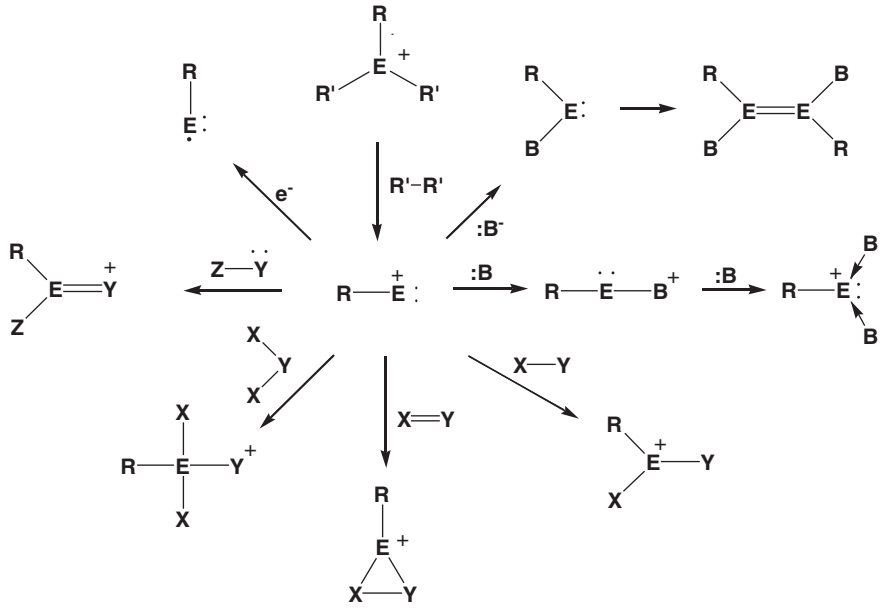

SCHEME 21. Generation of four-valence-electron, singly coordinated organometallic group 14 cations by a 1,1-elimination reaction from R_3E^+ cations and its potential reaction scheme.[195,196]

other examples have been reported so far (see Section III.A.1).[88,89,195,196] Computations[82,83] propose that this type of fragmentation of trivalent group 14 organometallic cations is preferred for the heavier elements of group 14 and with the toluene complex of the terphenyl-substituted plumbylidynium **41** the first example of this type of compounds has been recently synthesized.[90] Gaspar recently pointed out the synthetic potential of these novel low-valent reactive intermediates, which is summarized in Scheme 21.[195,196] The intermediate formation of these species gives access to novel highly intriguing compounds and opens new synthetic approaches to heavy carbene analogues, to E=E unsaturated compounds, to trivalent R_3E^+ cations and to neutral element(I) compounds. The synthesis of the disilene **93** from reaction of the cation η^5-Cp*Si$^+$, **91**, with bis(trimethylsilyl)amide shows in principle the applicability of the suggested reactivity scheme.[194] Clearly, the chemistry of organometallic group 14 cations is only at its beginning and there is still much to investigate!

LIST OF ABBREVIATIONS

bco	bicyclooctyl
Cp	cyclopentadienyl
Cp*	pentamethylcyclopentadienyl
Cy	cyclohexyl
Dur	2, 3, 5, 6 tetramethylphenyl
DMPU	1,3-dimethyl,2-4,5,6-tetrahydro-2(1H)-pyrimidone
DMSO	dimethyl sulfoxide
FT ICR	Fourier Transform Ion Cyclotron Resonance
FT NMR	Fourier Transform Nuclear Magnetic Resonance
HMPA	hexamethylphosphoric triamide
IGLO	Individual Guage for Localized Orbitals
Mes	2, 4, 6-trimethylphenyl
Tip	2, 4, 6-triisopropylphenyl
TPN	1, 2, 3, 4-tetraphenylnaphthalene
$TPFPB^-$	tetrakis(pentafluorophenyl)borate
$TFPB^-$	tetrakis[3, 5-bis(trifluoromethyl)phenyl]borate
$TSFPB^-$	tetrakis[4-{tert-butyl(dimethyl)silyl}-2,3,5,6-tetrafluorophenyl]borate
TPB^-	Tetraphenylborate
Tol	Tolyl
WCA^-	weakly coordinating anion

Acknowledgements

Our contributions to the chemistry of organometallic cations of group 14 chemistry were supported by the Deutsche Forschungsgemeinschaft (DFG) and the German Israeli Foundation for Scientific Research and Development (GIF). The author wishes to thank the Professors C. A. Reed, A. Sekiguchi, J. Michl and K. Jurkschat for kindly supplying information prior to publication.

References

(1) (a) Sekiguchi, A.; Kinjo, R.; Ichinohe, M. *Science* **2004**, *305*, 1755. (b) Wiberg, N.; Niedermayer, W.; Fischer, G.; Nöth, H.; Suter, M. *Eur. J. Inorg. Chem.* **2002**, 1066. (c) Wiberg, N.; Vasisht, S. K.; Fischer, G.; Mayer, P. *Z. Anorg. Allg. Chem.* **2004**, *630*, 1823. (d) Stender, M.; Phillips, A. D.; Wright, R. J.; Power, P. P. *Angew Chem. Int. Ed.* **2002**, *41*, 1785. (e) Phillips, A. D.; Wright, R. J.; Olmstead, M. M.; Power, P. P. *J. Am. Chem. Soc.* **2002**, *124*, 5930. (f) Pu, L.; Twamley, B.; Power, P. P. *J. Am. Chem. Soc.* **2000**, *122*, 3524. (g) Power, P. P. *J. Chem. Soc. Chem. Commun.* **2003**, 2091.
(2) Olah, G. A. *J. Org. Chem.* **2001**, *66*, 5943.
(3) (a) Norris, J. F. *Am. Chem. J.* **1901**, *25*, 117. (b) Kehrmann, F.; Wentzel, F. *Chem. Ber.* **1901**, *34*, 3815.
(4) Lambert, J. B.; Zhao, Y.; Wu, H.; Tse, W. C.; Kuhlmann, B. *J. Am. Chem. Soc.* **1999**, *121*, 5001.
(5) Lambert, J. B.; Zhao, Y. *Angew. Chem. Int. Edit. Engl.* **1997**, *36*, 400.
(6) Müller, T.; Lambert, J. B.; Zhao, Y. *Organometallics* **1998**, *17*, 278.
(7) Kraka, E.; Sosa, C. P.; Gräfenstein, J.; Cremer, D. *Chem. Phys. Lett.* **1997**, *279*, 9.
(8) Sekiguchi, A.; Matsuno, T.; Ichinohe, M. *J. Am. Chem. Soc.* **2000**, *122*, 11250.
(9) Sekiguchi, A.; Tsukamoto, M.; Ichinohe, M. *Science* **1997**, *275*, 60.

(10) Lickiss, P. D. (Z. Rappoport, Y. Apeloig, Eds.), *The Chemistry of Organic Silicon Compounds* Vol. 2, **1998**, Wiley & Sons, Chichester, p. 557.
(11) Reed, C. A. *Acc. Chem. Res.* **1998**, *31*, 325.
(12) Lambert, J. B.; Kania, L.; Zhang, S. *Chem. Rev.* **1998**, *95*, 1191.
(13) Maerker, C.; Schleyer, P. v. R. (Z. Rappoport, Y. Apeloig, Eds.), *The Chemistry of Organic Silicon Compounds* Vol. 2, **1998**, Wiley & Sons, Chichester, p. 513.
(14) Houk, K. N. *Chemtracts Org. Chem.* **1993**, *6*, 360.
(15) Schleyer, P. v. R. *Science* **1997**, *275*, 39.
(16) Belzner, J. *Angew. Chem. Int. Edit.* **1997**, *36*, 1277.
(17) Zharov, I.; Michl, J. (Z. Rappoport, Y. Apeloig, Eds.), *The Chemistry of Organic Germanium, Tin, and Lead Compounds* Vol. 2, **2002**, Wiley & Sons, Chichester, p. 633.
(18) Prakash, G. K. S., Schleyer, P. v. R., Eds., *Stable Carbocation Chemistry*, Wiley, New York, 1997.
(19) Olah, G. A.; Mo, Y. K. *J. Am. Chem. Soc.* **1971**, *93*, 4942.
(20) (a) Hensen, K.; Zengerley, T.; Pickel, P.; Klebe, G. *Angew. Chem. Int. Edit. Engl.* **1983**, *32*, 725. (b) Hensen, K.; Zengerley, T.; Pickel, P.; Klebe, G. *Angew. Chem. Suppl.* **1983**, 973.
(21) Ishida, Y.; Sekiguchi, A.; Kabe, Y. *J. Am. Chem. Soc.* **2003**, *125*, 11468.
(22) Bartlett, P. D.; Condon, F. E.; Schneider, A. *J. Am. Chem. Soc.* **1944**, *66*, 1531.
(23) Deno, N. C.; Peterson, H. J.; Gaines, G. S. *Chem. Rev.* **1960**, *60*, 7.
(24) Corey, J. Y. *J. Am. Chem. Soc.* **1975**, *97*, 3237.
(25) Lambert, J. B.; Kuhlmann, B. *J. Chem. Soc. Chem. Commun.* **1992**, 931.
(26) Lambert, J. B.; Ciro, S. M.; Stern, C. L. *J. Organomet. Chem.* **1995**, *499*, 49.
(27) Kira, M.; Oyamada, T.; Sakurai, H. *J. Organomet. Chem.* **1994**, *471*, C4.
(28) Blackwell, J. M.; Piers, W. E.; McDonald, R. *J. Am. Chem. Soc.* **2002**, *124*, 1295.
(29) Henderson, L. D.; Piers, W. E.; Irvine, G. J.; McDonald, R. *Organometallics* **2002**, *21*, 340.
(30) Mayr, H.; Basso, N.; Hagen, G. *J. Am. Chem. Soc.* **1992**, *114*, 3060.
(31) Apeloig, Y.; Merin-Aharoni, O.; Danovich, D.; Ioffe, A.; Shaik, S. *Isr. J. Chem.* **1993**, *33*, 387.
(32) Chojnowski, J.; Fortuniak, W.; Stanczyk, W. A. *J. Am. Chem. Soc.* **1987**, *101*, 7776.
(33) Nishinaga, T.; Izukawa, Y.; Komatsu, K. *J. Am. Chem. Soc.* **2000**, *122*, 9312.
(34) Nishinaga, T.; Izukawa, Y.; Komatsu, K. *Tetrahedron* **2001**, *57*, 3645.
(35) Lambert, J. B.; Zhang, S. *J. Chem. Soc. Chem. Commun.* **1993**, 383.
(36) Lambert, J. B.; Zhang, S.; Stern, C. L.; Huffman, J. C. *Science* **1993**, *260*, 1917.
(37) Lambert, J. B.; Zhang, S.; Ciro, S. M. *Organometallics* **1994**, *13*, 2430.
(38) Xie, Z.; Manning, J.; Reed, R. W.; Mathur, R.; Boyd, P. D. W.; Benesi, A.; Reed, C. A. *J. Am. Chem. Soc.* **1996**, *118*, 2922.
(39) Lambert, J. B.; Schilf, W. *Organometallics* **1988**, *7*, 1659.
(40) Müller, T.; Bauch, C.; Ostermeier, M.; Bolte, M.; Auner, N. *J. Am. Chem. Soc.* **2003**, *125*, 2158.
(41) Gillespie, R. J.; Robinson, E. A. *Proc. Chem. Soc.* **1957**, 147.
(42) Gillespie, R. J.; Kapoor, R.; Robinson, E. A. *Can. J. Chem.* **1966**, *44*, 1197.
(43) Birchall, T.; Manivannan, V. *J. Chem. Soc. Dalton Trans.* **1985**, 2671.
(44) Birchall, T.; Manivannan, V. *Can. J. Chem.* **1985**, *63*, 2211.
(45) Birchall, T.; Chan, P. K. H.; Pereira, A. R. *J. Chem. Soc. Dalton Trans.* **1974**, 2157.
(46) Arshadi, M.; Johnels, D.; Edlund, U. *J. Chem. Soc. Chem. Commun.* **1996**, 1279.
(47) Lambert, J. B.; Lin, L. *J. Org. Chem.* **2001**, *66*, 8537.
(48) Lambert, J. B.; Lin, L.; Keinan, S.; Müller, T. *J. Am. Chem. Soc.* **2003**, *125*, 6022.
(49) Kim, K.-C.; Reed, C. A.; Elliot, D. W.; Mueller, L. J.; Tham, F.; Lin, L.; Lambert, J. B. *Science* **2002**, *297*, 825.
(50) Uhlig, W. (N. Auner, J. Weis, Eds.), *Organosilicon Chemistry*, **1994**, VCH, Weinheim, Germany, p. 21.
(51) Shade, L.; Mayr, H. *Makromol. Chem. Rapid Commun.* **1988**, *9*, 477.
(52) Siehl, H.-U.; Kaufmann, F.-P. *J. Am. Chem. Soc.* **1992**, *114*, 4937. Siehl, H.-U.; Kaufmann, F.-P.; Hori, K. *J. Am. Chem. Soc.* **1992**, *114*, 9343.
(53) Müller, T.; Bauch, C.; Bolte, M.; Auner, N. *Chem. Eur. J.* **2003**, *9*, 1746.
(54) Jerkunica, J. M.; Traylor, T. G. *J. Am. Chem. Soc.* **1971**, *93*, 6278.
(55) MacLachlan, M. J.; Bourke, S. C.; Lough, A. J.; Manners, I. *J. Am. Chem. Soc.* **2000**, *122*, 2126.
(56) Fukuzumi, S.; Kitano, T.; Mochida, K. *J. Am. Chem. Soc.* **1990**, *112*, 3246.

(57) Lochynski, S.; Boduszek, B.; Shine, H. J. *J. Org. Chem.* **1991**, *56*, 914.
(58) Peloso, A. *J. Organomet. Chem.* **1974**, *67*, 423.
(59) Kochi, J. K. *Angew. Chem. Int. Edit. Engl.* **1988**, *27*, 1227.
(60) Mochida, K.; Itani, A.; Yokoyama, M.; Tsuchiya, T.; Worley, S.; Kochi, J. K. *Bull. Chem. Soc. Jpn.* **1985**, *58*, 2149.
(61) Tanaka, H.; Ogawa, H.; Suga, H.; Torii, S.; Jutand, A.; Aziz, S.; Suarez, A. G.; Armatore, C. *J. Org. Chem.* **1996**, *61*, 9402.
(62) Okano, M.; Mochida, K. *Chem. Lett.* **1991**, 819.
(63) Doretti, L.; Faleschini, S. *Gazz. Chim. Ital.* **1970**, *100*, 819.
(64) Ichinohe, M.; Fukaya, N.; Sekiguchi, A. *Chem. Lett.* **1998**, 1045.
(65) Sekiguchi, A.; Fukaya, N.; Ichinohe, M. *Phosphorous Sulfur Silicon* **1999**, *150–151*, 59.
(66) Sekiguchi, A.; Fukaya, N.; Ichinohe, M.; Ispida, Y. *Eur. J. Inorg. Chem.* **2000**, 1155.
(67) Ichinohe, M.; Fukui, H.; Sekiguchi, A. *Chem. Lett.* **2000**, 600.
(68) Zharov, I.; King, B. T.; Havlas, Z.; Pardi, A.; Michl, J. *J. Am. Chem. Soc.* **2000**, *122*, 10253.
(69) Zharov, I.; Weng, T.-C.; Orendt, A. M.; Barich, D. H.; Penner-Hahn, J.; Grant, D. M.; Havlas, Z.; Michl, J. *J. Am. Chem. Soc.* **2004**, *126*, 12033.
(70) Sekiguchi, A.; Fukawa, T.; Nakamoto, M.; Ya Lee, V.; Ichinohe, M. *J. Am. Chem. Soc.* **2002**, *124*, 9865.
(71) Sekiguchi, A.; Fukawa, T.; Ya Lee, V.; Nakamoto, M. *J. Am. Chem. Soc.* **2003**, *124*, 9250.
(72) Sekiguchi, A.; Fukawa, T.; Nakamoto, M.; Ya Lee, V.; Ichinohe, M. *Angew. Chem. Int. Edit. Engl.* **2003**, *42*, 1143.
(73) Nakamoto, M.; Fukawa, T.; Sekiguchi, A. *Chem. Lett.* **2004**, *33*, 38.
(74) Sekiguchi, A.; Matsuno, T.; Ichinohe, M. *J. Am. Chem. Soc.* **2001**, *123*, 12436.
(75) Matsuno, T.; Ichinohe, M.; Sekiguchi, A. *Angew. Chem. Int. Edit. Engl.* **2002**, *41*, 1575.
(76) Jutzi, P.; Bunte, A. E. *Angew. Chem. Int. Edit.* **1992**, *31*, 1605.
(77) Müller, T.; Jutzi, P.; Kühler, T. *Organometallics* **2001**, *20*, 5619.
(78) Schmidt, H.; Keitemeyer, S.; Neumann, B.; Stammler, H.-G.; Schoeller, W. W.; Jutzi, P. *Organometallics* **1998**, *17*, 2149.
(79) Jutzi, P.; Keitemeyer, S.; Neumann, B.; Stammler, H.-G. *Organometallics* **1999**, *18*, 4778.
(80) Ichinohe, M.; Hayata, Y.; Sekiguchi, A. *Chem. Lett.* **2002**, 1054.
(81) Walsh, A. D. *J. Chem. Soc.* **1953**, 2260, 2266, 2288, 2296, 2301, 2306.
(82) Das, K. K.; Balasubramanian, K. *J. Chem. Phys.* **1990**, *93*, 5883.
(83) Kapp, J.; Schreiner, P.; Schleyer, P. v. R. *J. Am. Chem. Soc.* **1996**, *118*, 12154.
(84) del Rio, E.; Menandez, M. I.; Lopez, R.; Sordo, T. L. *J. Chem. Soc. Chem. Comm.* **1997**, 1779.
(85) Nicolaides, A.; Radom, L. *J. Am. Chem. Soc.* **1996**, *118*, 10561.
(86) Nicolaides, A.; Radom, L. *J. Am. Chem. Soc.* **1997**, *119*, 11933.
(87) Nicolaides, A.; Radom, L. *J. Am. Chem. Soc.* **1994**, *116*, 9769.
(88) Jarek, R. L.; Shin, S. K. *J. Am. Chem. Soc.* **1997**, *119*, 6376.
(89) Schuppan, J.; Herrschaft, B.; Müller, T. *Organometallics* **2001**, *20*, 4584.
(90) Hino, S.; Brynda, M.; Phillips, A. D.; Power, P. P. *Angew. Chem.* **2004**, *116*, 2709.
(91) Basch, H.; Hoz, T. (S. Patai, Z. Rappoport, Eds.), *The Chemistry of Organic Germanium Tin and Lead Compounds* Vol. 1, **1995**, Wiley & Sons, Chichester, p. 1.
(92) Müller, T. Unpublished results.
(93) Frenking, G.; Fau, S.; Marchand, M.; Grützmacher, H. *J. Am. Chem. Soc.* **1997**, *119*, 6648.
(94) Karni, M.; Apeloig, Y.; Kapp, J.; Schleyer, P. v. R. (Z. Rappoport, Y. Apeloig, Eds.), *The Chemistry of Organic Silicon Compounds* Vol. 3, **2001**, Wiley & Sons, Chichester, p. 1.
(95) Basch, H. *Inorg. Chim. Acta* **1996**, *242*, 191.
(96) Kühler, T.; Jutzi, P. *Adv. Organomet. Chem.* **2003**, *49*, 1.
(97) Kira, M.; Ishida, S.; Iwamoto, T.; Kabuto, C. *J. Am. Chem. Soc.* **1999**, *212*, 9722.
(98) Olah, G. A.; Field, L. *Organometallics* **1982**, *1*, 1485.
(99) Maerker, C.; Kapp, J.; Schleyer, P. v. R. (N. Auner, J. Weis, Eds.), *Organosilicon Chemistry II*, Wiley-VCH, Weinheim, **1996**, p. 329.
(100) Pidun, U.; Stahl, M.; Frenking, G. *Chem. Eur. J.* **1996**, *2*, 869.
(101) Ottosson, C.-H.; Cremer, D. *Organometallics* **1996**, *15*, 5495.
(102) Ottoson, C.-H.; Szabó, K.; Cremer, D. *Organometallics* **1997**, *16*, 2377.

(103) (a) Atkins, P. W.; Friedman, R. S. *Molecular Quantum Mechanics*, 3rd Ed., Oxford University Press, Oxford, 1997. (b) Mason, J. (Ed.) *Multinuclear NMR*, Plenum Press, New York, 1987. (c) Kaupp, M.; Bühl, M.; Malkin, V. G. *Calculations of NMR and EPR Parameters*, Wiley-VCH, Weinheim, 2004.
(104) Müller, T. *J. Organomet. Chem.* **2003**, *686*, 251.
(105) Müller, T.; Hennegriff, T. *Organometallics* **2004** (submitted).
(106) Olsson, L.; Ottosson, C.-H.; Cremer, D. *J. Am. Chem. Soc.* **1995**, *117*, 7460.
(107) Olah, G. A.; Rasul, G.; Prakash, G. K. S. *J. Organomet. Chem.* **1996**, *521*, 271.
(108) Olah, G. A.; Rasul, G.; Buchholz, H. A.; Li, X.-Y.; Prakash, G. K. S. *Bull. Soc. Chim. Fr.* **1995**, *132*, 569.
(109) Kutzelnigg, W.; Fleischer, U.; Schindler, M. *NMR Basic Principles and Progress*, Vol. 23, Springer, Berlin, Heidelberg, **1990**, p. 165.
(110) Duncan, T. M. *A Compilation of Chemical Shift Anisotropies*, Farragut Press, Farragut, TN.
(111) Müller, T. Presented in part at the XXth North American Organosilicon Symposium, London, Ontario, May 1997 and at the 13th International Symposium on Organosilicon Chemistry, Guanojuato, GTO, Mexico, September 2002.
(112) Calculated at GIAO/B3LYP/6-311G(2d,p)//B3LYP/6-31G(d). (Me3Si)2(Me)Si-Si$^+$tBu2; E(B3LYP/6-31G(d) = −1752.92353H; r(Si$^+$Si) = 236.2 pm; r(Si$^+$C) = 191.8 pm, Σ°(Si+) = 360°. [92]
(113) Arshadi, M.; Johnels, D.; Edlund, U.; Ottoson, C.-H.; Cremer, D. *J. Am. Chem. Soc.* **1996**, *118*, 5120.
(114) Xie, Z.; Bau, R.; Benesi, A.; Reed, C. A. *Organometallics* **1995**, *14*, 3933.
(115) Bahr, S.; Boudjouk, P. *J. Am. Chem. Soc.* **1993**, *115*, 4514.
(116) Xie, Z.; Bau, R.; Reed, C. A. *J. Chem. Soc. Chem. Commun.* **1994**, 2519.
(117) Lambert, J. B. Personal communication to Frenking G. reported in ref.100. Chicago, 1990.
(118) Sekiguchi, A.; Muratami, A.; Fukaya, N.; Kabe, Y. *Chem. Lett.* **2004**, *33*, 530.
(119) (a) Panisch R. Diploma Thesis, University Frankurt, **2004**. (b) Panisch, R.; Müller, T. submitted for publication.
(120) Berger, S.; Braun, S.; Kalinowski, H.-O. NMR –Spektroskopie von Nichtmetallen, Stuttgart; New York Thieme: Bd. 4 ^{19}F NMR Spektroskopie.
(121) Müller, T. *Angew. Chem. Int. Edit. Engl.* **2001**, *40*, 3033.
(122) Takeuchi, Y.; Takayama, T. (Z. Rappoport, Y. Apeloig, Eds.), *The Chemistry of Organic Silicon Compounds* Vol. 2, **1998**, Wiley & Sons, Chichester, p. 267.
(123) Steinberger, H.-U.; Müller, T.; Auner, N.; Maerker, C.; Schleyer, P. v. R. *Angew. Chem. Int. Edit. Engl.* **1997**, *36*, 626.
(124) Kira, M.; Hino, T.; Sakurai, H. *J. Am. Chem. Soc.* **1992**, *114*, 6697.
(125) Olah, G. A.; Li, X.-Y.; Wang, Q.; Rasul, G.; Prakash, G. K. S. *J. Am. Chem. Soc.* **1995**, *117*, 8962.
(126) Driess, M.; Barmeyer, R.; Monsé, C.; Merz, K. *Angew. Chem. Int. Edit.* **2001**, *40*, 2308.
(127) Xie, Z.; Liston, D. L.; Jelinek, T.; Mitro, V.; Bau, R.; Reed, C. A. *J. Chem. Soc. Chem. Commun.* **1993**, 384.
(128) Olah, G. A.; Narang, S. C.; Gupta, B. G. B.; Malhotra, R. *J. Org. Chem.* **1979**, *44*, 1247.
(129) Kira, M.; Hino, T.; Sakurai, H. *Chem. Lett.* **1993**, 555.
(130) Johannsen, M.; Jørgensen, K. A.; Helmchen, G. *J. Am. Chem. Soc.* **1998**, *120*, 7637.
(131) Schleyer, P. v. R.; Buzek, P.; Müller, T.; Apeloig, Y.; Siehl, H.-U. *Angew. Chem. Int. Edit. Engl.* **1993**, *32*, 1471.
(132) Lambert, J. B.; Zhang, S. *Science* **1994**, *263*, 984.
(133) Reed, C. A.; Xie, Z. *Science* **1994**, *263*, 985.
(134) Olsson, L.; Cremer, D. *Chem. Phys. Lett.* **1993**, *6*, 360.
(135) Olah, G. A.; Rasul, G.; Buchholz, H. A.; Li, X. Y.; Sandford, G.; Prakash, G. K. S. *Science* **1994**, *263*, 983.
(136) Pauling, L. *Science* **1994**, *263*, 983.
(137) Ottosson, C.-H.; Cremer, D. *Organometallics* **1996**, *15*, 5495.
(138) Reed, C. A.; Xie, Z.; Bau, R.; Benesi, A. *Science* **1993**, *262*, 402.
(139) Stasko, D.; Reed, C. A. *J. Am. Chem. Soc.* **2002**, *124*, 1148.
(140) Reed, C. A. *Acc. Chem. Res.* **1998**, *31*, 133.

(141) Ivanov, S. I.; Rockwell, J. J.; Polykov, O. G.; Gaudinski, C. M.; Anderson, O. P.; Solntsev, K. A.; Strauss, S. H. *J. Am. Chem. Soc.* **1998**, *120*, 4224.
(142) Richardson, C.; Reed, C. A. *J. Chem. Soc. Chem. Commun.* **2004**, 706.
(143) Xie, Z.; Manning, J.; Reed, R. W.; Mathur, R.; Boyd, P. D. W.; Benesi, A.; Reed, C. A. *J. Am. Chem. Soc.* **1996**, *118*, 2922.
(144) Mathieu, B.; de Fays, L.; Ghosez, L. *Tetrahedron Lett.* **2000**, *41*, 9561.
(145) Tsang, C.-W.; Yang, Q.; Tung-Po, E.; Mak, T. C. W.; Chan, D. T. W.; Xie, Z. *Inorg. Chem.* **2000**, *39*, 5851.
(146) Setaka, W.; Sakamoto, K.; Kira, M.; Power, P. P. *Organometallics* **2001**, *20*, 4460.
(147) Jutzi, P.; Dickbreder, R. *J. Organomet. Chem.* **1989**, *373*, 301.
(148) (a) Nakatsuji, H.; Inoue, T.; Nakao, T. *Chem. Phys. Lett.* **1990**, *167*, 111. (b) Nakatsuji, H.; Inoue, T.; Nakao, T. *J. Phys. Chem.* **1992**, *96*, 7953. (c) Kaneko, H.; Hada, M.; Nakajiama, T.; Nakatsuji, H. *Chem. Phys. Lett.* **1996**, *261*, 1. (d) de Dios, A. C. *Magn. Res. Chem.* **1996**, *34*, 773. (e) Avalle, P.; Harris, R. K.; Karadakov, P. B.; Wilson, P. J. *Phys. Chem. Chem. Phys.* **2002**, *4*, 5925. (f) Vivas-Reyes, R.; De Proft, F.; Biesemans, M.; Willem, R.; Geerlings, P. *J. Phys. Chem. A.* **2002**, *106*, 2753. (g) Avalle, P.; Harris, R. K.; Fischer, R. D. *Phys. Chem. Chem. Phys.* **2002**, *4*, 3558.
(149) Mitchell, T. N. *J. Organomet. Chem.* **1983**, *255*, 279.
(150) Watkinson, P. J.; Mackay, K. M. *J. Organomet. Chem.* **1984**, *275*, 39.
(151) Cremer, D.; Olsson, L.; Reichel, F.; Kraka, E. *Isr. J. Chem.* **1994**, *33*, 369.
(152) Wrackmeyer, B.; Stader, C.; Horchler, K. *J. Magn. Reson.* **1989**, *83*, 601.
(153) Dillon, K. B.; Hewitson, G. F. *Polyhedron* **1984**, *3*, 957.
(154) Edlund, U.; Arshadi, M.; Johnels, D. *J. Organomet. Chem.* **1993**, *456*, 57.
(155) Nádvorník, M.; Holeček, J.; Handlíř, K.; Lička, A. *J. Organomet. Chem.* **1984**, *275*, 43.
(156) Holeček, J.; Nádvorník, M.; Handlíř, K.; Lička, A. *J. Organomet. Chem.* **1983**, *241*, 177.
(157) Wrackmeyer, B.; Kundler, S.; Milius, W.; Boese, R. *Chem. Ber.* **1994**, *127*, 333.
(158) Wrackmeyer, B.; Kundler, S.; Boese, R. *Chem. Ber.* **1993**, *126*, 1361.
(159) Rodriguez-Fortea, A.; Alemany, P.; Ziegler, T. *J. Phys. Chem. A* **1999**, *103*, 8244.
(160) Bauch, C. Ph. D. Thesis, Frankfurt/Main, FRG, **2003**.
(161) Wrackmeyer, B.; Horchler, K.; Boese, R. *Angew. Chem. Int. Edit. Engl.* **1989**, *28*, 1500.
(162) Meyer, R.; Werner, K.; Müller, T. *Chem. Eur. J.* **2002**, *8*, 1163.
(163) Olah, G. A.; Liang, G. *J. Am. Chem. Soc.* **1975**, *97*, 6803.
(164) Prakash, G. K. S.; Farnia, M.; Keyanian, S.; Olah, G. A.; Kuhn, H. J.; Schaffner, K. *J. Am. Chem. Soc.* **1987**, *109*, 911.
(165) Branch, G.; Walba, H. *J. Am. Chem. Soc.* **1954**, *76*, 1564.
(166) Lambert, J. B.; Lin, L.; Nowik, I.; Herber, R. H. *Inorg. Chem.* **2004**, *43*, 405.
(167) Mackay, K. M. (Z. Rappoport, Y. Apeloig, Eds.), *The Chemistry of Organic Germanium, Tin, and Lead Compounds* Vol. 1, **1995**, Wiley & Sons, Chichester, p. 97.
(168) Baines, K. M.; Stibbs, W. G. *Coord. Chem. Rev.* **1995**, *145*, 157.
(169) Jemmis, E. D.; Srinivas, G. N.; Leszczynski, J.; Kapp, J.; Korkin, A. A.; Schleyer, P. v. R. *J. Am. Chem. Soc.* **1995**, *117*, 11361.
(170) Ichinohe, M.; Igarashi, M.; Sauuki, K.; Sekiguchi, A. *J. Am. Chem. Soc.,* **2005**, ASAP, published on web 25.06.05.
(171) Ichinohe, M.; Matsuno, T.; Sekiguchi, A. *Angew. Chem. Int. Edit.* **1999**, *38*, 2194.
(172) Kaftory, M.; Kapon, M.; Botoshansky, M. (Z. Rappoport, Y. Apeloig, Eds.), *The Chemistry of Organic Silicon Compounds* Vol. 2, **1998**, Wiley & Sons, Chichester, p. 181.
(173) (a) Chuit, C.; Corriu, R. J. P.; Mehdi, A.; Reyé, C. *Angew. Chem. Int. Edit. Engl.* **1993**, *32*, 1311. (b) Belzner, J.; Schär, D.; Kneisel, B. O.; Herbst-Irmer, R. *Organometallics* **1995**, *14*, 1840. (c) Berlekamp, U.-H.; Jutzi, P.; Mix, A.; Neumann, B.; Stammler, H.-G.; Schoeller, W. W. *Angew. Chem. Int. Edit.* **1999**, *38*, 2048. (d) Schmidt, H.; Keitemeyer, S.; Neumann, B.; Stammler, H.-G.; Schoeller, W. W.; Jutzi, P. *Organometallics* **1998**, *17*, 2149. (e) Kalikhman, I.; Krivonos, S.; Lameyer, L.; Stalke, D.; Kost, D. *Organometallics* **2001**, *20*, 1053. (f) Kingston, V.; Gostevskii, B.; Kalikhman, I.; Kost, D. *Chem. Commun.* **2001**, 1272. (g) Kost, D.; Kingston, V.; Gostevskii, B.; Ellern, A.; Stalke, D.; Walfort, B.; Kalikhman, I. *Organometallics* **2002**, *21*, 2293. (h) Kalikhman, I.; Gostevskii, B.; Girshberg, O.; Krivonos, S.; Kost, D. *Organometallics* **2002**, *21*, 2551.

(i) Jurkschat, K.; Pieper, N.; Seemeyer, S.; Schürmann, M.; Biesemanns, M.; Verbruggen, I.; Willem, R. *Organometallics* **2001**, *20*, 868. (k) Ruzicka, A.; Jambor, R.; Cisarova, I.; Holecek, J. *Chem. Eur. J.* **2003**, *9*, 2411. (l) Mehring, M.; Löw, C.; Schürmann, M.; Jurkschat, K. *Eur. J. Inorg. Chem.* **1999**, 887. (m) Mehring, M.; Vrasidas, I.; Horn, D.; Schürmann, M.; Jurkschat, K. *Organometallics* **2001**, *20*, 4647. (n) Peveling, K.; Schürmann, M.; Ludwig, R.; Jurkschat, K. *Organometallics* **2001**, *20*, 4654. (o) Peveling, K.; Schürmann, M.; Jurkschat, K. Z. *Anorg. Allg. Chem.* **2002**, *628*, 2435. (p) Kasna, B.; Jambor, R.; Dostal, L.; Ruzicka, A.; Cisarova, I.; Holecek, J. *Organometallics* **2004**, *23*, 5300.

(174) Fukaya, N.; Ichinohe, M.; Sekiguchi, A. *Angew. Chem. Int. Edit.* **2000**, *39*, 3881.

(175) (a) Bondi, A. *J. Phys. Chem.* **1964**, *68*, 441. (b) Davies, A. G. *Organotin Chemistry*, VCH, Weinheim, 2003. (c) Batsanov, S. S. *Russ. J. Gen. Chem.* **1998**, *68*, 495.

(176) Riggs-Gelasco, P. J.; Mei, R.; Ghanotakis, D. F.; Yocum, C. F.; Penner-Hahn, J. E. *J. Am. Chem. Soc.* **1996**, *118*, 2400.

(177) Prakash, G. K. S.; Keyaniyan, S.; Aniszfeld, R.; Heiliger, L.; Olah, G. A.; Stevens, R. C.; Choi, H.-K.; Bau, R. *J. Am. Chem. Soc.* **1987**, *109*, 5123.

(178) Davies, A. G.; Goddard, J. P.; Hursthouse, M. B.; Walker, N. P. C. *J. Chem. Soc. Chem. Commun.* **1983**, 597.

(179) Nugent, W. A.; McKinney, R. J.; Harlow, R. L. *Organometallics* **1984**, *3*, 1315.

(180) Nitrile complexes of stannyl cations with a stoichiometry of stannyl cation/nitrile = 1:1 are described in the literature;[67] however no structural or spectroscopic data are given.

(181) (a) Lambert, J. B.; Zhao, Y. *J. Am. Chem. Soc.* **1996**, *118*, 7867. (b) Lambert, J. B.; Zhao, Y.; Wu, H. *J. Org. Chem.* **1999**, *64*, 2729. (c) Lambert, J. B.; Liu, C.; Kouliev, T. *J. Phys. Org. Chem.* **2002**, *15*, 667.

(182) (a) Müller, T.; Meyer, R.; Lennartz, D.; Siehl, H. U. *Angew. Chem. Int. Edit.* **2000**, *39*, 3074. (b) Müller, T.; Juhasz, M.; Reed, C. A. *Angew. Chem. Int. Edit.* **2004**, *43*, 1543.

(183) Driess, M.; Monsé, C.; Merz, K.; van Wüllen, C. *Angew. Chem. Int. Edit.* **2000**, *39*, 3684.

(184) Schormann, M.; Garratt, S.; Hughes, D. L.; Green, J. C.; Bochmann, M. *J. Am. Chem. Soc.* **2002**, *124*, 11266.

(185) Reed, C. A.; Kim, K.-C.; Bolskar, R. D.; Mueller, L. *Science* **2000**, *289*, 101.

(186) (a) Reed, C. A.; Fackler, N. L. P.; Kim, K.-C.; Stasko, D.; Evans, D. R.; Boyd, P. D. W.; Rickard, C. E. F. *J. Am. Chem. Soc.* **1999**, *121*, 6314. (b) Reed, C. A.; Kim, K.-C.; Stoyanov, E. S.; Stasko, D.; Tham, F. S.; Mueller, L. J.; Boyd, P. D. W. *J. Am. Chem. Soc.* **2003**, *125*, 1796.

(187) Juhasz, M.; Hoffmann, S.; Stoyanov, E.; Kim, K.-C.; Reed, C. A. *Angew. Chem. Int. Edit.* **2004**, *43*, 5352.

(188) Stasko, D.; Reed, C. A. *J. Am. Chem. Soc.* **2002**, *124*, 1148.

(189) Kato, T.; Reed, C. A. *Angew. Chem. Int. Edit.* **2004**, *43*, 2907.

(190) Auner, N. *Eur. Pat. Appl.* **1998**, EP 97-306480 19970826 .

(191) Steinberger, H.-U.; Bauch, C.; Müller, T.; Auner, N. *Can. J. Chem.* **2003**, *11*, 1223.

(192) Olah, G. A.; Rasul, G.; Prakash, G. K. S. *J. Am. Chem. Soc.* **1999**, *121*, 9615.

(193) Tanaka, M.; Hatanaka, Y. Presented at the XIIIth International Symposium on Organosilicon Chemistry, Guanajuato, GTO Mexico, Aug 2002, *Book of Abstracts C06*, p. 28.

(194) Jutzi, P.; Mix, A.; Rummel, B.; Schoeller, W. W.; Neumann, B.; Stammler, H. G. *Science* **2004**, *305*, 849.

(195) (a) Gaspar, P. P. Presented at the 2nd European Silicon Days, Munich, Germany, Sep 2003. (b) Gaspar, P. P. (N. Auner; J. Weis, Eds.), *Organosilicon Chemistry VI*, Wiley–VCH, Weinheim, 2005.

(196) Gaspar, P. P.; Read, D. Presented at the XIIIth International Symposium on Organosilicon Chemistry, Guanajuato, GTO Mexico, August 2002.